Approved and recommended for acceptance as a dissertation in partial fulfillment of the requirements for the degree of Doctor of Philosophy.

05/13/93
(Date)

Donald Rockwell
Professor in Charge

Accepted 05/13/93
(Date)

Special committee directing the doctoral work of Necati Mahir

~~Professor Antonios~~ Liakopoulos

Professor Jerzy Owczarek

Professor Sibel Pamukcu

Professor Charless R. Smith

ACKNOWLEDGMENTS

I am deeply grateful to Professor D. Rockwell for his interest and guidance during my research. I appreciate the support he provided as my academic advisor.

I would also like to thank my fellow inhabitants of the Fluids Lab. Thanks to Emerson Wagner and Frank Kluscik, without whom my experiment would not have been possible.

I wish to express my gratitude to Anadolu University of Turkey for their financial support during my study in Lehigh University.

NOMENCLATURE

A = Amplitude of cylinder oscillation

D = Diameter of cylinder

f_e = Frequency of excitation

f_i = Frequency of interest

f_m = Modulation frequency

f_n = Nyquist frequency

f_o^* = Natural vortex shedding frequency for stationary single cylinder

f_o^{**} = Natural vortex shedding frequency for stationary two-cylinder system

G = Distance between centers of cylinders in side-by-side arrangement

k_s = Stability(mass-damping) parameter $\equiv (2m_e\delta/\rho D^2)$

L = Cylinder length

m_e = Mass/unit length

n = Integer number

P = Distance between centers of two cylinders in tandem arrangement

Re = Reynolds number based on cylinder diameter $\equiv (UD/\nu)$

t = Time

T_e = Period of excitation.

T_m = Modulation period

u = Fluctuation component of velocity in streamwise direction

U = Freestream velocity

U_r = Reduced velocity $\equiv U/f_o^*D$

x = Streamwise coordinate

y = Transverse coordinate

ρ = Density of surrounding fluid

ϕ = Phase angle between cylinder oscillations

δ = Structural logarithmic decrement

Δ = Time interval

TABLE OF CONTENTS

ABSTRACT

The structure of the wake between and downstream of a two-cylinder system in tandem and side-by-side arrangements is investigated. The Reynolds number based on the cylinder diameter is 160. The control parameters are the excitation frequency and amplitude, as well as the phase angle between the oscillating cylinders. Flow visualization using the hydrogen bubble technique and point velocity measurements via Laser-Doppler anemometry allow characterization of the wake structure as a function of time.

Irrespective of the cylinder arrangement, the wake structure exhibits a number of common features. When the cylinders are stationary, the wake exhibits random, intermittent switching between states of vortex formation. When the cylinder system is subjected to forced oscillation, the wake response generally exhibits increased organization. A locked-in response, whereby the vortex formation is phase-locked to the motion of the cylinder system is attainable over a substantially wider range of excitation frequency than for the corresponding stationary cylinder. When the oscillation frequency is sufficiently close to the inherent vortex formation frequency of the two-cylinder system, the phase shift between the oscillating cylinders has an insignificant effect on the occurrence or non-occurrence of locked-in response, though the details of the vortex patterns are a function of phase shift. On the other hand, near the boundary of the locked in region of response, it is possible to manipulate the wake structure between locked-in and modulated states by variation of the phase shift between the oscillating

cylinders. Finally, outside the region of locked-in response, it is possible to generate modulated, ordered patterns of response, whereby the wake pattern repeats at a multiple of the period of the cylinder oscillation.

Each of these types of visualized response of the wake can be related to the spectrum of the velocity fluctuation in the wake. Locked-in response involves a sharp peak at the forcing frequency and its harmonics. On the other hand, modulated response involves coexistence of a number of peaks in the spectrum, each of which can be traced to the frequency of the oscillation cylinder, the inherent vortex formation frequency from the two-cylinder system, a modulation frequency, and their sum and difference components.

I. INTRODUCTION

Arrangements of two or more cylindrical structures occur in systems of transmission lines, chimney stacks, offshore structures, and heat exchanger tubes. The steady and unsteady loading on the cylindrical structures, convective heat transfer between the cylinders and the fluid, and the mixing process in the near-wakes of the cylinders are important practical considerations. Little is understood, however, of the detailed flow patterns, associated with these practical features.

Recent observations suggest that the process of vortex formation from a bluff body can be modified or enhanced by introducing a second bluff body at a finite distance of downstream of the first one, or by placing the second body outside the wake of, but sufficiently close to, the first one. Among other features, it is expected that resonance will occur when vortex shedding from the first body is in the phase with the disturbances created by second one.

In the following, a brief summary of related studies is provided. These studies, which involve various combinations of fixed, forced and elastic cylinders are reviewed to provide a basis for gaining insight into the flow structure in a two-cylinder system.

1. Vortex formation from a single cylinder

The instability of the wake behind a cylinder has been studied in recent years by, among others, Williamson and Roshko (1988), Öngören and Rockwell (1988), Sreenivasan (1985), and Van Atta and Gharib (1987).

Williamson and Roshko (1988) studied vortex interactions in the wake of an oscillating body. They found a series of synchronization regions in the amplitude-wavelength plane for excitation of the cylinder with an amplitude up to five diameters. In the fundamental synchronization region, acceleration of the cylinder induces the formation of two vortices during each half cycle of the cylinder motion and thereby four vortices during each cycle. Below the critical wavelength, a pair of like-sign vortices coalescence and a Karman vortex street develops in the wake. Beyond the critical wavelength, a vortex pair forms every half cycle.

Öngören and Rockwell (1988) examined the flow structure in the near-wake of an excited cylinder. The vortex formation is locked-in (phase-locked) with the cylinder oscillation when the excitation frequency is half the natural shedding frequency, corresponding to subharmonic synchronization, and when it is near the natural shedding frequency, corresponding to fundamental synchronization. In region of subharmonic synchronization, they observed vortex formation from the same side of the body irrespective of whether it moves towards to its maximum positive or negative position. In the fundamental synchronization region, the vortex forms from either side of the body. They also investigated the phase between the body motion and the

vortex formation. Drastic changes in the phase occurred between the cylinder motion and the initial vortex formation when the frequency of the body excitation was approximately equal to natural shedding frequency. This change involved a phase switch of the initial vortex shedding from the upper to the lower side of the cylinder or vice-versa. This switch occurs over a narrow range of the excitation frequency. They also reported that it is possible to avoid this switch if the cylinder has a sufficiently long afterbody length. This change in timing of the initially-formed vortex was first hypothesized by Zdravkovich (1982) and appears to occur over a wide range of Reynolds number. Öngören and Rockwell (1988) also observed a threshold value of body excitation frequency, above which the near-wake structure breaks into smaller vortices with shorter wavelength. They also observed recovery of near-wake vortex formation to a Karman mode having a frequency different from the natural shedding frequency.

The response of the near-wake behind a single cylinder has been studied in terms of chaotic response by Sreenivasan (1985) and Van Atta and Gharib (1987). In their experiments, they described the wake response using concepts of chaos. Sreenivasan (1985) studied the response of the wake from a stationary cylinder by considering Reynolds number as an external disturbance leading to chaotic response. He observed that vortex shedding behind a single cylinder occurs when the Reynolds number exceeds a value of 36. This vortex shedding is characterized in the response spectrum by a single peak at the natural shedding frequency. As the Reynolds number increases, the spectrum with the single peak at the natural shedding frequency is

replaced by an incommensurate frequency in addition to the basic natural shedding frequency. This, quasi-periodic response of the wake continues up to a value of the Reynolds number of 66. Beyond this value of Reynolds number, the response of the wake is characterized by a broadband peak, indicating the onset of the chaos. As the Reynolds number is increased to 76, a three-frequency, quasi-periodic response appears. When the Reynolds number is about 90, there is a broadened peak at the natural shedding frequency in the spectrum. Sreenivasan (1985) speculated that beyond this value of Reynolds number, quasi-periodic motion with four incommensurate frequencies exist. He also reported that the breaks in the variation of frequency with Reynolds number coincide with the existence of chaos at this Reynolds number.

Van Atta and Gharib (1987) studied the wake of a single cylinder by applying different degrees of tension to the ends of the cylinder. They recorded the cylinder and the wake oscillations simultaneously. By keeping the Reynolds number constant and changing the tension on the cylinder, they investigated the cylinder-wake interactions. When the cylinder was stationary, they observed only a single peak at the natural shedding frequency in the spectrum. When the cylinder was vibrating, the peaks in the spectrum appeared at the cylinder oscillation frequency, the natural shedding frequency and a modulation frequency, which is difference between cylinder oscillation frequency and natural shedding frequency, and their sum/difference combinations. For large values of tension, Van Atta and Gharib (1987) observed chaotic response in the wake with a broadened peak. They also

investigated the response of the wake by keeping the tension constant on a damped cylinder and changing the Reynolds number. They concluded that the regions of ordered response in all cases are due to aeroelastic coupling between vortex formation and elastic vibrations of the cylinder and not a result of pure hydrodynamic phenomena.

Karniadakis and Triantafyllou (1989a) have investigated the asymptotic states in the laminar wake of a circular cylinder at low Reynolds number. They concluded that, in unforced wakes, the frequency of the vortex street is determined by an absolute instability; however nonlinear effects determine the amplitude of the oscillation. In forced wakes, there is the potential for interaction between the naturally-produced waves and the forced waves. They observed two possible types of response in the forced wake of the cylinder. The first response is a lock-in state characterized by a dominant frequency in the wake. The second state is non-lock-in state, in which nonlinear interaction plays a secondary role. In this state, the absolute instability of the wake is the dominant factor in the frequency selection process. At the boundary of two regions, the competing wake patterns create a chaotic response, which appears only in the presence of external forcing. In this state, Karniadakis and Triantafyllou (1989b) observed a drastic increase in the instantaneous values of the Nusselt number.

2. Instabilities of/from tandem arrangement of two cylinders

The mean flow field and the vortex interaction between two cylinders, and in the region downstream of them, becomes very complex when either one or both cylinders oscillate. In the two-cylinder arrangement, the wake from the upstream cylinder strikes the downstream cylinder and causes a dynamic instability called wake-induced flutter. In addition to this type of fluid-elastic instability, the cylinder is also subjected to forces as a result of vortex shedding and turbulence in the incident flow. Various features of these types of steady and unsteady loading , have been addressed in recent years.

An overview of the flow regimes between two cylinders in tandem, side-by-side and staggered arrangements is presented by Chen (1985) and Zdravkovich (1985). Chen (1985) classified the instabilities of two-cylinder arrangement as wake-induced flutter and interference galloping. When the distance between the cylinders is large, and the wake from the upstream cylinder strikes the downstream cylinder, the instability is called wake-induced flutter. In this instability, a large amplitude oscillation of downstream cylinder is observed. On the other hand, the instability of a two cylinder system with a small pitch to diameter ratio is called " interference galloping ".

Zdravkovich (1987) observed three different flow regimes around two rigid, stationary cylinders in a tandem arrangement. When the distance between the cylinders is between 1 and 1.8, the shear layers separating from

the upstream cylinder do not attach to the downstream cylinder. The vortex street behind the downstream cylinder is formed from the shear layer separating from the upstream cylinder. For the value of the spacing between 1.8 and 3.4, the separated shear layer from the upstream cylinder reattaches to downstream one. There is no vortex formation between the cylinders; the vortex street forms only in the downstream region. When the spacing is between 3.4 and 6, the separated shear layer from upstream cylinder rolls up between two cylinders and vortices form in front of the downstream cylinder. The spacing over which vortex formation occurs between cylinders is called the critical spacing. The vortices formed from upstream cylinder and downstream cylinder are synchronized.

In order to understand fluctuating forces resulting from the vortex-cylinder interaction, the fluctuating pressure on the cylinder surface has been measured by Arie et al. (1983) and Moriya et al. (1986). They investigated the fluctuating surface pressure on cylinders in a tandem arrangement. Arie et al. (1983) report that the rms pressure distribution around the circumference of the upstream cylinder is much lower than that for a single cylinder when the distance between cylinders is smaller than critical spacing. The rms pressure distribution decreases as the spacing between the cylinders increases towards the critical spacing. When the spacing exceeds the critical value, there is vortex formation between the cylinders and the rms pressure sharply increases on the upstream cylinder to a value higher than that of a single cylinder. They observed a higher rms pressure distribution on the downstream cylinder than on the upstream one for all values of the spacing.

Finally, Arie et al. (1981) observed a sharp increase in pressure amplitude on the downstream cylinder similar to that on the upstream cylinder when a discontinuity in the flow pattern between the cylinders occurs.

3. Instabilities of/from tandem arrangement of flexible cylinders

The dynamic response of a tandem arrangement of cylinders has been studied by Jendrezejczky et al. (1979) and King and Johns (1976). Jendrezejczky et al. (1979) observed four natural modes of vibrations of two identical cylinders. They summarized these modes as: out-of-phase, in-plane motion; in-phase, in-plane motion; in-phase, out-of-plane motion; and out-of phase, out-of-plane motion. They reported that when two cylinders are identical, they oscillate at the same amplitude in each mode.

King and Johns (1976) studied the wake interaction from two flexible circular cylinders in a tandem arrangement. They changed the distance between cylinders, the flow velocity and the stability parameter of the cylinders. They reported that, the nature of the vibration of the cylinders is primarily a function of the gap between cylinders, the Strouhal number, the stability parameter and the Reynolds number. King and John (1976) observed that the amplitude of the downstream vibration is strongly influenced by the vortices shed from the upstream cylinder. They concluded that, if the gap between the cylinders is less than 1.75 diameters and the reduced velocity U_r is in the range $1.25 \leq U_r \leq 2.5$, the vortices are formed from both cylinders and the cylinders oscillate in the in-line direction for a

value of the stability parameter k_s less than 1.2. In their study, the reduced velocity is defined by:

$$U_r = U/f_o{}^*D$$

where, U is velocity, $f_o{}^*$ is natural shedding frequency, D is diameter of the cylinder; and the stability parameter defined by:

$$k_s = 2m_e\delta/\rho D^2$$

where, m_e is mass/unit length, δ is structural logarithmic decrement, and ρ is the density of the fluid. For a gap larger than 1.75 diameters and reduced velocity between 1.25 and 2.5, they observed large amplitude oscillation of the upstream cylinder in-line direction, while the downstream cylinder remained stationary. For a gap between 0.5 and 6 diameters, vortex formation from the upstream cylinder reinforced that from the downstream cylinder, when reduced velocity is between 2.7 and 3.8. For this spacing, the downstream cylinder oscillated with an amplitude larger than that of upstream cylinder. They reported that the vibration of cylinders in the cross-flow direction was less dependent on the distance between the cylinders when the gap was between 0.25 and 6 diameters.

Bokain and Geoola (1984) studied the fluid-elastic stability of the upstream cylinder of a two-cylinder arrangement. They applied quasi-steady theory to predict the instability of an upstream cylinder in the amplitude and frequency domain. They also carried out experiments by changing the distance between cylinders. The measured values of the lift and drag

coefficients on the upstream cylinder are used in the theoretical prediction of the instabilities. Their calculations also include the change of drag and lift coefficients with the distance between cylinders. Bokain and Geoola (1984) reported that, when the distance between cylinder in a tandem arrangement is smaller than two diameters, the downstream cylinder suppresses the formation of the vortex street in the gap. Bokain and Geoola (1984) observed negligible lift forces on the upstream cylinder in a tandem arrangement for a spacing between the cylinders of two diameters. They observed that vortex resonance occurred when the distance between cylinders is small. The downstream cylinder only has effect when it is in the near-wake of the upstream one. Bokain and Geoola (1984) also reported that in a tandem arrangement of two cylinders, the galloping instability begins at small flow velocities. The amplitude of the upstream cylinder attains a limit value at small velocities. The limit oscillation amplitude decreases and the frequency of vibration increases as the distance between cylinders increases. All these observations are valid only when the spacing between the cylinders remains sufficiently small. For a cylinder spacing larger than two diameters, the peak resonance amplitude, vortex resonance frequency and reduced velocity for onset of oscillation all decrease as the gap increases. Bokain and Geoola (1984) also studied the effect of cylinder aspect ratio on the instability of an upstream cylinder in the tandem arrangement. Upon increasing the aspect ratio, the amplitude of oscillation of the upstream cylinder changes, although its oscillation frequencies remain unchanged.

Zdravkovich (1985) classified the interference between cylinders depending on the arrangement of the cylinders and the space between them as: a coupled region; a wake-interference region; and a no-interference region. In the coupled region, the motion of either cylinder will affect the other. When the upstream cylinder has an effect on the one in its wake, the interference region is called the "wake interference" region. At relatively large spacing of the cylinders, the motion of either one will not effect the other. In this case, interference region is called as "no interference region". In this region, the flow around the cylinder is the same as that of a single cylinder in the flow field. The Strouhal frequency and the fluctuating drag and lift coefficients are also the same as those for a single cylinder. In the wake interference region, upstream cylinder effects the downstream one and the drag force on the downstream cylinder decreases as the gap between cylinders increases.

Tsui (1977) has studied the instability of a downstream cylinder in the wake of a fixed upstream cylinder. He assumed in his analysis there is no interaction between the wake generated by the upstream cylinder and that by the downstream one. He also employed measured drag and lift coefficients in to his analysis by assuming that these coefficients are independent of flow velocity.

In most of the foregoing research, the stability of two cylinder arrangement has been studied and the critical flow velocity determined by assuming harmonic oscillation of the cylinders. In theoretical studies, experimental data in the form of fluid force coefficients are required to

complete the analysis. These fluid force coefficients are obtained by employing a quasi-steady or quasi-static theory.

Kim and Conlisk (1990) employed point vortices to study the condition for the onset of cylinder vibration. They reported that nonlinear interaction between cylinders and vortices takes place when a vortex is close to each of the cylinders. They also reported that chaotic response may appears when four vortices are present. Kim and Conlisk's (1990) analysis did not include vortex shedding from the cylinders, although vortex formation existed between cylinders only when the gap between them is large enough.

4. Instabilities of/from side-by-side arrangement of two stationary cylinders

Most research efforts have focused on the tandem arrangement of two cylinders. Little attention has been given on parallel and staggered arrangements of two cylinder systems. Williamson (1985) studied the vortex interaction the region of two stationary cylinders in a side-by side arrangement by using a variety of flow visualization techniques. For Reynolds number of 200, he observed anti-phase vortex shedding from either cylinder over a range of spacing between 1 and 5 diameters. He also reported that it is possible for the flow pattern to switch from the antyphase mode to an in-phase mode and vice-versa. Either mode can continue for large number of cycles. For small spacing of cylinders, the flow downstream of them is asymmetric and the gap flow affects the frequency of vortex formation.

Bearman and Wadcock (1973) studied flows around two stationary cylinders in side-by-side arrangement. They also measured base pressure on the both cylinders in the range of spacing $1.1 < G < 2.0$. They observed that two cylinders experienced with different base pressure. Pressure changed from one steady value to another. Their hot film measurements showed higher frequency response close to cylinders than that in downstream region. Bearman and Wadcock (1973) carried out flow visualization experiments at $Re = 5*10^2$ when the spacings of the cylinder were three diameters and 1.85 diameter. They observed symmetric in-phase vortex formation when the distance between cylinder is three diameters. When the distance between cylinder was G/D = 1.85, they did not observe vortex structure in the wake, the flow between cylinders biased towards one of the cylinders and later, the flow swapped to the other side.

5. Instabilities of/from side-by-side arrangement of two flexible cylinders

The response of flexible cylinders in a side-by-side arrangement has been studied by Jendrzejzyk and et al.(1979) for close spacing of the cylinders. In their experiment, the gap between the cylinders had values of 0.5 and 0.75 diameters. They observed increase in the cylinder displacements in the drag direction towards a maximum value for the reduced velocities between 1.21 and 1.57. This amplitude was maximum when the reduced velocity was between 2.25 and 3.0. They concluded that the vortex shedding in the wake is controlled by cylinder motion for these values of the reduced velocity.

Chen (1985) summarized the interaction between cylinders for tandem and side-by-side arrangements of them. In the side-by-side arrangement, each cylinder vibrates as an isolated single cylinder when the distance between them is larger than two diameters. For small value of this gap, two modes were observed. At the lower value of the flow velocity, the cylinders oscillated out of phase; their oscillations were in phase for higher values of the velocity

6. Instabilities of/from arrays of cylinders

In some cases such as heat exchanger tubes, cylinders appear in closely-spaced arrays. When the cylinders in the array are subjected to sufficiently high flow velocity, they lose their stability and begin to oscillate. To estimate stability region of cylinder arrays, mathematical models have been developed. These models are based on quasi-static, quasi-steady and unsteady flow theories. These theories may allow prediction of the instability of cylinder arrays but require measured drag and lift coefficients in the analysis.

Leaver and Weaver (1982) have studied the instability of heat exchanger tubes by assuming that the instability mechanism is not dependent on the wake phenomena. From their experimental results for a triangular arrangement of cylinders, they concluded that the motion of the neighboring cylinders do not have essential effect on the onset of the instability. An insulated cylinder in a uniformly moving fluid does not exhibit a fluid-elastic instability. Vortex shedding from a single cylinder can be resonant with the

cylinder oscillation but can not cause the type of fluid-elastic instability of interest. The arrangement of cylinders in an array creates completely different flow field around any given cylinder, so that the instability mechanism of a cylinder in an array must consider flow field created by other cylinders. To calculate the unsteady forces on the cylinders, Leaver and Weaver (1982) considered the disturbances in the free-stream flow along either side of a single cylinder which goes a harmonic motion.

Paidoussis and Price (1988) based their analysis on a quasi-steady theory by assuming that the forces acting on an oscillating cylinder are the same as the static forces on the stationary cylinder at each point of the cycle of cylinder oscillation. They discussed two basic instability mechanisms. The first one is the negative damping mechanism which is similar to classical galloping and valid for low values of the mass-damping parameter. This instability involves one degree of freedom of a cylinder in a stationary cylinder array. This instability is closely connected with the time delay between cylinder motion and the resulting fluid forces, which produces flow induced damping forces on the cylinders. The second instability is similar to wake flutter. Instability is controlled by fluid-dynamic stiffness and becomes dominant for sufficiently high values of the mass damping parameter. This mechanism requires at least two degrees of freedom of a system.

Price and Valerio (1990) investigated the nonlinear instability of a cylinder array by employing a quasi-steady theory. In the analysis, they considered that only a single cylinder is free to move in the cross flow direction in an array of rigid cylinders. Their analysis also includes a time

delay between the cylinder motion and the resulting fluid forces on the cylinder which undergoes harmonic motion. Measured drag and lift coefficients on a static cylinder in the midst of an array of rigid cylinders were required as an input for the analysis.

7. Unresolved issues

The foregoing research on wakes from a system of two or more stationary or flexible cylinders suggests several flow regimes between downstream of the cylinders. In most cases, however, emphasis has been on the unsteady loading of the cylinders. Little emphasis has been given to the detailed flow structure which, in fact, dictates the unsteady loading.

Locked-in response. For the case of an isolated, single cylinder, it is well known that synchronization of the formation with the cylinder excitation occurs when the excitation frequency is near or at the natural shedding frequency. This phenomenon of "lock-in" involves phase-locking of the vortex formation with the cylinder motion. Occurrence of such lock-in for a system of two cylinders, either in a tandem or side-by-side arrangement has not been addressed. In analogy with the case of a single cylinder, the extent of the lock-in region is expected to depend on the amplitude and frequency of oscillation of the cylinders. In addition, the spacing between the cylinders is of obvious importance, since it determines the degree of interference or coupling of the flow patterns between and immediately downstream of the cylinders. Furthermore, the phase angle between two oscillating cylinders is

also expected to be important in determining the extent of the locked-in region. These aspects have been uninvestigated.

Non-locked-in response. Outside the region of phase-locked vortex formation from the two-cylinder system, it is expected that the flow pattern will undergo a variety of modulated oscillations. The nature of such modulations has not been addressed in any of the foregoing investigations. It is expected that excitation of the cylinder system at a frequency outside the region of locked-in response will give rise to wake fluctuations having spectral components at the excitation frequency, the inherent vortex formation frequency, and perhaps component corresponding to the sum and difference frequencies, the forced and inherent vortex formation frequencies. Which of these components occurs and their amplitudes relative to each other in relation to the time-varying flow patterns between and downstream of the cylinders has remained uninvestigated. Moreover, the effect of phase angle between the oscillating cylinders on the modulated flow patterns remains unclarified. It may be possible, for example, to promote a transition from locked-in to non-locked-in response of the flow structure, or vice versa, by altering the phase angle between the cylinders while maintaining the excitation frequency constant.

Discontinuous response. In the foregoing, it has been assumed that the phase-locked or modulated patterns of vortex formation are repeatable and persist over long periods of time. Yet it is known for the case of , for example, stationary cylinders in a side-by-side arrangement, that the pattern of vortex formation switches from an in-phase to an anti-phase mode, i.e.

symmetrical to antisymmetrical mode, without any external perturbations of the flow or cylinder. In the corresponding case of a cylinder system undergoing forced oscillations, the issue arises as to whether such discontinuous switching between modes occurs and, if so, how it can be controlled or eliminated.

Theoretical framework. The flow structure between and immediately downstream of a two-cylinder system involves highly nonlinear and unsteady phenomena that are difficult to relate to linear theories. Nevertheless, recently developed concepts of the near-wake instability from a single cylinder can provide a useful framework for formulating experiments. Recent description of the near-wake in terms of a global instability has received much attention and is reviewed in the work of Huerre and Monkewitz (1985). With regard to the present theme, the consequence of a linearly amplifying, globally-unstable flow is to eventually generate self-sustained oscillation of the near-wake from a single cylinder. That is, the wake oscillation may be viewed as a nonlinear oscillator. One expects that if the spacing between two cylinders is sufficiently large, then each of the wakes will exhibit self-sustained, nonlinear oscillations and it may be difficult to obtain a coupling between the wake flow structure unless both of the wake generators, i.e. cylinders, are forced at relatively high amplitude. On the other hand, when the cylinders are closely-spaced, for example in a tandem arrangement, the self-excited oscillation of the wake from the upstream cylinder will be attenuated and the gap region between the cylinders will no longer be globally-unstable. Instead, it will exhibit a convective-type instability, which

is very susceptible to applied disturbances. In this case, one expects that relatively small amplitude oscillations of cylinder system will have an effect on the flow structure in the region between them. In fact, the possible occurrence of either a global or convective instability in relation to the spacing of the cylinders has been used to guide the present experiments.

Another theoretical framework involves the possible occurrence of chaotic response in the region between or downstream of the oscillating cylinder system. This aspect has remained uninvestigated. It is well known that, in a closed system, chaotic response can occur, as described by Feigenbaum (1979). Gollub and Benson (1980) investigated the effect of boundary conditions on the sequence of transition to chaos in a Rayleigh-Bernard convection instability, which was driven by a temperature difference across a fluid layer. Concerning open flow systems, Sreenivasan (1985), Van Atta and Gharib (1987), and Karniadakis and Triantafyllou (1989) have addressed various aspects of the chaotic response of forced and unforced wakes from rigid and elastic cylinders. The possible occurrence of such chaotic behavior has not been addressed for a system of two or more cylinders.

8. Objectives of research

The overall goal of the present research program is to determine the variation of the flow structure with time in the region between and downstream of two cylinders subjected to controlled oscillation. In doing so, basic cylinder arrangements will be employed: a side-by-side arrangement and

a tandem arrangement irrespective of the particular configuration of two cylinders, the states of the flow structure from the system of stationary cylinders will be used to guide the investigation of the oscillating cylinders.

The objectives are defined in the following.

(1) The flow structure as a function of time as well as the time-averaged spectral content of the velocity fluctuations in the region between and downstream of two stationary cylinders, will be investigated. Particular emphasis will be given to the effect of cylinder spacing on attenuating self-excited oscillations of the near-wake.

(2) The nature of locked-in response, i.e. phase-locking of the flow structure to the cylinder motion, will be investigated as a function of frequency of excitation, relative to the natural vortex formation frequency. In addition, the effect of amplitude of, and the phase shift between, the cylinder oscillations will be considered.

(3) The nature of the modulated flow structure for excitation conditions lying outside the region of locked-in response will be characterized as a function of dimensionless frequency of excitation and phase shift between the oscillating cylinders. Time-averaged spectra of the velocity fluctuations in the gap and near-wake regions will be related to the instantaneous flow patterns in these regions.

II. EXPERIMENTAL SYSTEM

1. Test section and flow conditions

All experiments were performed in a free-surface, closed-loop water channel with a cross-section of 610 mm by 610 mm. The water depth in the channel was maintained at 520 mm, in order to keep a consistent relationship between the freestream velocity and the rpm of the pump. The freestream velocity U in the channel was U = 33 mm/sec, giving a Reynolds number Re = 160 based on cylinder diameter D = 4.7 mm. The test section of the water channel was made of Plexiglas to allow flow visualization and video recording.

2. Cylinder forcing system

As shown in Figure 1, the forcing and cylinder support mechanisms were mounted above the free surface of the water in order to allow an unobstructed view of the flow past the cylinders. The traverse tables were mounted such that the oscillation of the cylinders was always perpendicular to flow direction, irrespective of whether tandem or side-by-side cylinders were employed. One of the tables was also moved in the flow direction so that the distance between the cylinders could be adjusted. The cylinders were attached on to two separate, high-resolution Daedel traverse tables in order to obtain a defined phase shift between their synchronized motion. Each table was driven by a high-resolution Compumotor. These motors operated at about 10,000 steps per resolution. In turn, the Compumotors were driven by a micro-computer. Software developed in our laboratory by Magness and Troiano

(1991) was used to oscillate both cylinders simultaneously with desired amplitude and frequency. It also allowed application of a defined phase difference ϕ between the cylinder oscillations in the range of $0° \leq \phi \leq 360°$.

3. Flow visualization technique

The hydrogen bubble technique was used for flow visualization. Hydrogen bubbles were generated by a probe made of two brass tube prongs with a stretched platinum wire of diameter of 0.025 mm. The brass tube prongs were insulated by both heat shrink tubing and liquid insulating type to prevent localized hydrogen bubble formation, which decreased the intensity of the bubble lines. The probe was placed at the midspan of the cylinder extending from the water level to floor of the test section, in order to prevent end effects from the wall and free-surface effects. The platinum wire was energized by a bubble generator which produced a square wave voltage in the range 0-90 volts. During the experiments, the voltage was adjusted to a level which gave the best flow visualization. The frequency of generation of the bubble lines were adjustable within the range of 0-340 Hz. The condition of the water was observed to be an important factor in determining the quality of the flow visualization. Before beginning a flow visualization experiment, the water was filtered overnight using a one-micron filter. Water also was aged a sufficiently long time to get rid of the dissolved air. Chlorine was added periodically to prevent the growth of algae and to keep the water in good quality over a long time. A small amount of sodium sulfate was added to the water as an electrolyte. It was observed that the quality of hydrogen bubbles

changes after a few minutes of continuous operation. The bubble quality was improved by reversing the polarity of the platinum wire about every minute.

The record of flow visualization was obtained by using a camera, a monitor and VCR system. A Panasonic WV-BD 400 model video camera was placed under the channel to observe the unsteady flow between the cylinders and the downstream region of the flow as shown in Figure 2. The region of interest was illuminated by two high intensity lights having 1,000 watts and 650 watts power respectively. The lights were placed at both sides of the channel at an angle with respect to the channel wall in order to increase the brightness of the hydrogen bubble lines. Figure 2 illustrates the lighting system relative to the test section. The lower surfaces of the tables were covered by black paper to prevent light reflection from the metallic surfaces to the camera. The video camera had 580 lines of horizontal resolution. The flow visualization was recorded on a VHS tape by a AG-1960 model Panasonic video cassette recorder. The horizontal resolution of the recorder was more than 400 lines. A Sony PVM-122 black and white video monitor with a resolution of 950 horizontal lines was used to observe the region of interest. A hard copy of the flow visualization was obtained by taking black/white photos with a Nikon AF-8008 35 mm camera. In order to obtain the best contrast between the hydrogen bubble lines and the background Kodak, Technical Pan TP 135-36 film was used.

4. Cylinder systems

The experiments were carried out for a single cylinder and tandem and side-by-side arrangements of two cylinders. Figures 3 and 4 represent these arrangements. Each cylinder has a diameter D = 4.7 mm. and a length L = 514 mm. The geometrical aspect ratio of each cylinder was therefore L/D = 108.1. The aspect ratio of each cylinder based on the length of the submerged portion of the cylinder was 109.3. Experiments were performed at a Reynolds number Re = 160. With this high aspect ratio and small Reynolds number, the near-wake was assumed to be two-dimensional. There were no detectable end effects at the midspan of the cylinders, where the flow visualization and velocity measurements were performed.

4.1 Tandem arrangement of two cylinders

The experiments were performed at two different spacings of the cylinders in the tandem arrangement as shown in Figure 3. The spacing was selected by considering the vortex formation between the cylinders. When the distance between cylinders is small, as in Figure 3a, there is no vortex formation in the wake of upstream cylinder. A spacing of 2.5 diameters D between centers of the cylinders was selected to represent this case. When the distance between cylinders is large, as in Figure 3b, the separated shear layer rolls up in the wake of the upstream cylinder and vortices form between cylinders. A spacing of five diameters was selected to represent this case.

It was observed that the natural shedding frequency f_o^{**} from the two cylinder arrangement is different from that from a single cylinder denoted as

f_o^*. First, a single cylinder was placed in to flow field in order to determine the natural shedding frequency f_o^* of vortices in the downstream wake region. The value of f_o^* was measured as 1.33 Hertz at a location, referred as ξ_a in the Figures, from the center of the cylinder of 5 diameters D in the x direction and 1.8 diameters in the y direction. When a second cylinder was placed 2.5 diameters upstream of the first one, the natural shedding frequency f_o^{**} of the system was measured as 0.93 Hertz. For a distance of five diameters between centers of the cylinders in the tandem arrangement, the natural shedding frequency f_o^{**} was measured as 1.22 Hertz. At side-by-side arrangement of the cylinders, the natural shedding frequency f_o^{**} was measured as 1.39 Hertz at a location from center of the upper cylinder of 6 diameter D in the x direction and 1.8 diameter D in the y direction when the distance between cylinders G/D was three.

4.2 Side-by-side arrangement of two cylinders

Figures 4a and 4b represent the cases of stationary and oscillating cylinders in a side-by-side arrangement. Two spacing of the cylinders in the side-by-side arrangement were selected after considering the patterns of vortex formation in the downstream region. For close spacing of the two cylinders, a single wake forms in the downstream region and a gap flow, in the form of a jet, switches across the wake at irregular time intervals. When the distance between the cylinders is large, a separated vortex street forms downstream of the two cylinders. This vortex formation switches between symmetrical and antisymmetrical modes at irregular time intervals. As a representative case of the close spacing of the cylinders, distances G/D = 1.7 and 2 between cylinder

centers were selected. The cylinders were a distance G = 3D apart in order to study the case of relatively large spacing in the side-by-side arrangement.

5. Forcing of the cylinders in tandem and side-by-side arrangements

During the experiments, sinusoidal excitation was applied to both cylinders simultaneously. The amplitude A and the frequency f_e of the excitation were varied. A defined phase shift ϕ between the cylinders was also imposed.

Experiments were carried out at three different oscillation amplitudes. As representative of small amplitude oscillation of the cylinders, the ratio of excitation amplitude A to diameter D of A/D = 0.02 was selected. The ratio A/D = 0.2 was selected as a moderate value of amplitude. The ratio A/D = 0.5 was selected as representative of large-amplitude oscillations. For the single-cylinder experiments, the ratio of the excitation frequency f_e to natural shedding frequent f_o^* of the single cylinder was varied from 0.1 to 1.0. In the two-cylinder experiments, the ratio of the excitation frequency f_e to the natural shedding frequency f_o^{**} of the system was changed between 0.1 and 1. The phase shift ϕ between cylinder oscillations was varied from 0 to 180 degrees.

6. Velocity measurement and data sampling

Unsteady velocity measurements were carried out by employing a two-watt Argon-ion Laser-Doppler anemometer. This dual beam system LDA operates in the backscatter mode. Silver particles with 12 micron mean diameter and density of 2.6 gr/cm^3 were used to seed the flow. The analog

output of the LDA converter system was digitized and analogized by using a microcomputer system. The velocity measurements were carried out at the midspan of the test section, as illustrated in Figure 1. This location ensured that the flow structure was not affected by end effects. The LDA control volume was located between and downstream of the two cylinders in the tandem arrangement. Figure 3b and 4a represent the coordinates for the velocity measurements.

The velocity measurement locations were as follows:

Tandem arrangement of the cylinders;

Distance between cylinders	Locations
5D	x/D = -2.5, y/D = 0.6
	x/D = 5, y/D = 1.8
2.5D	x/D = -1.25, y/D = 0.6
	x/D = 5, y/D = 1.8

Side-by-side arrangement of the cylinders;

Distance between cylinders	Locations
3D	x/D = 6, y/D = 1.8
	x/D = 6, y/D = -1.5
1.7D	x/D = 6, y/D = 1.8
	x/D = 6, y/D = -0.85

The velocity signal (in volts) was transformed to digital format. The sampling interval between data points is dictated by the Nyquist frequency. Selection of the Nyquist frequency is important for ensuring accuracy of the data analysis. If the frequency of interest is not less than the Nyquist frequency, aliasing occurs. The frequency of interest is determined as follows. If the phenomenon repeats at approximately a period T_e, we may say that the frequency of interest is $f_e = 1/T_e$, however we are not only interested in primary frequency of the phenomena but also other frequencies. The highest value of the these frequencies may be selected as the frequency f_i of the interest. In the experiments the fourth harmonic of the natural shedding frequency of the single cylinder is selected as the frequency of interest. The Nyquist frequency is selected as $f_n = 2f_i$ in order to avoid aliasing effects. The time interval Δ of the sampled data is

$\Delta = 1/2f_n$.

This time interval corresponded to 0.04 seconds.

A trial of 5120 data points were taken for each sample. Data points were separated into five sets of 1024 points for processing. The Fast Fourier Transform (FFT) the digital data was taken in order to determine the power spectral density (PSDu) i.e. spectrum of the velocity signals u. An ensemble average of five sets of spectra was performed in order to eliminate random noise.

In order to determine the boundary between the locked-in and non-locked-in regions in the wake of a single or two-cylinder system, velocity

measurements were carried out in the near-wake. Spectra were determined from the time history of the velocity signal over a wide range of f_e/f_o^{**} at the dimensionless excitation amplitudes A/D = 0.2 and 0.5. Additional spectra were taken near the boundary of locked-in regions for a number of other amplitudes by using the locked-in boundaries at the amplitudes A/D = 0.2 and 0.5 as a guide. Figure 5 represents the average boundary of, and the uncertainty(error bars) at the boundary of, locked-in regions corresponding to a single isolated cylinder. Similar considerations hold for the two-cylinder system. Furthermore, table 1 represents typical peaks in the response and the categories of response of the wake of a single cylinder and two cylinders in a tandem arrangement for a cylinder spacing of P/D = 2.5 and a phase shift between them of $\phi = 0°$. The uncertainty of the boundary of locked-in regions is of the order of 5% of the dimensionless excitation frequency f_e/f_o^{**}.

III: WAKE RESPONSE FROM TANDEM ARRANGEMENT OF TWO CYLINDERS

1. OVERVIEW OF LOCKED-IN RESPONSE OF WAKE

1.1 Region of locked-in response of wake from largely-spaced cylinders

When the spacing between the stationary cylinders is sufficiently large, self-excited vortex formation occurs in the gap between the cylinders, i.e. the global (absolute) instability of the wake from the upstream cylinder is operative. The locked-in response of the wakes from this two cylinder system, relative to the wake from a single cylinder, is of interest. Locked-in response corresponds to occurrence of repetitive, phase-locked flow structure from cycle to cycle of the cylinder oscillations. The technique employed here to distinguish locked-in response is dominance of the peak at the forcing frequency in the spectrum of the velocity fluctuation in the near-wake (see spectra of Figure 10).

An overview of the regions of locked-in response for a system of oscillating cylinders, relative to a single cylinder, is given in Figure 6. In general, lock-in occurs when the excitation frequency f_e of the two-cylinder system is in the vicinity of the natural shedding frequency f_o^{**} from the two-cylinder system, as shown in Figure 6. The width of the lock-in region is a function of the normalized excitation amplitude A/D and the distance between the cylinders P/D. The locked-in response of the wake of a single

cylinder is illustrated by the shaded region. Both of the extreme phase angles $\phi = 0°$ and $180°$ produce locked-in response. The region of locked-in response at $\phi = 180°$ is shifted to the left of that at $\phi = 0°$; moreover, the lock-in region is narrower. In general, however, there is little difference between the responses of the single and two-cylinder systems. Regarding the minimum dimensionless amplitude A/D for occurrence of lock-in, the threshold value is at A/D = 0.1 for both the two- and single-cylinder systems.

1.2 Region of locked-in response of wake from cylinders with close spacing

When the cylinders are sufficiently close together, self-excited vortex formation is precluded in the gap between them, i.e. the system is convectively unstable, and highly responsive to small-amplitude disturbances induced by the cylinder motion. Moreover, at large amplitude, the mutually-induced flow in the gap region will promote coherent patterns of flow structure. Figure 7 shows the locked-in regions in the wakes of the single- and two-cylinder systems. The shaded region represents the lock-in region of the single cylinder. For both extreme phase angles, $\phi = 0°$ and $180°$, the locked-in region is substantially broader than that of the single cylinder. Furthermore, the locked-in region for $\phi = 180°$ is shifted to the left of that for $\phi = 0°$. Regarding the minimum dimensionless amplitude for lock-in to occur, the lowest threshold value of A/D = 0.05 occurs at $\phi = 0°$. The threshold value at $\phi = 180°$ is attained at A/D = 0.08, while the corresponding value for the single cylinder is A/D = 0.10. We therefore conclude that substantial reductions in threshold amplitude are attainable in the two-cylinder system.

Figures 8 and 9 represent typical spectrums taken in the locked-in and outside the locked-in regions in the wake of a single cylinder and two closely-spaced cylinder system with phase angle $\phi = 0°$. Locked-in response contains peaks at the excitation frequency and the other peaks its higher harmonics. Non-locked-in region contains at least one peak which is not higher harmonics of excitation frequency, such as peaks at the natural shedding frequency f_o^{**} or at the modulation frequency f_m.

1.3 Transformation from non-locked-in to locked-in response of wake

As shown in Figures 6 and 7, locked-in response occurs in a defined range of frequency in the vicinity of the natural shedding frequency f_o^{**} of the two-cylinder system. It is of interest to determine the spectra in the wake, starting from very low values of excitation frequency f_e and extending through the perfectly synchronized condition $f_e/f_o^{**} = 1$.

First, we address the case of the closely-spaced cylinders. The spectra in the left column of Figure 10 correspond to location ξ_a in the gap region, and those in the right column to location ξ_b in the near-wake region. In the gap region, the spectra are dominated by the forcing component f_e for all values of f_e/f_o^{**}; this behavior is what one would expect of a convectively-unstable system. However, the substantial amplitudes of the f_e component over such a wide frequency range suggests that the contribution to the velocity fluctuation induced by the motion of the cylinder at f_e plays a significant, if not dominant, role. The contribution of the component at the

self-excited wake frequency f_o^{**} is small, but detectable, for the lower values of excitation frequency.

In the near-wake region downstream of the cylinders, represented by the spectra in the right column of Figure 10, excitation at a frequency ratio $f_e/f_o^{**} = 0.1$ produces a broadened peak at the natural vortex formation frequency f_o^{**}, and there is no response at the excitation frequency f_e. When the excitation frequency is increased to $f_e/f_o^{**} = 0.3$, the broadened peak at f_o^{**} is replaced by two pronounced peaks, one is at the natural shedding frequency f_o^{**} and the other is at the modulation frequency f_m, which corresponds to the difference between the natural vortex formation frequency f_o^{**} and excitation frequency f_e. At a higher value of excitation frequency $f_e/f_o^{**} = 0.4$, the peaks at the excitation frequency and the natural shedding frequency become dominant. At a still higher value of excitation frequency $f_e/f_o^{**} = 0.5$, the peaks at the excitation frequency f_e and natural shedding frequency f_o^{**} are still dominant. At $f_e/f_o^{**} = 0.6$ and 0.7 there is an additional peak at the modulation frequency. When $f_e/f_o^{**} = 0.8$, a large number of discrete peaks occur. They correspond to the excitation frequency f_e, modulation frequency f_m, the natural vortex formation frequency f_o^{**} and their sum and difference components $f_e - f_m$, $f_e + f_m$, and $2f_e - f_m$. At the next highest value of the excitation frequency, $f_e/f_o^{**} = 0.9$, this multiple-peak spectrum has collapsed to a spectrum typical of classical lock-in. It is characterized by a dominant peak at the excitation frequency f_e and its first harmonic $2f_e$. Regarding the amplitudes of the spectral peaks, for small f_e/f_o^{**}, the amplitude of the natural shedding component f_o^{**} is

relatively low and its peak is relatively broad. As the excitation frequency reaches the region of classical locked-in response, the amplitude of the peak at the excitation frequency f_o^{**} increases.

For large spacing of the cylinders, as shown in Figures 11 and 12, generally similar modifications of the spectra are obtained. At such large spacing, peaks at the natural shedding frequency f_o^{**} are narrower in comparison with those corresponding to close spacing of the cylinders in Figure 10. Locked-in response occurs at smaller values of f_e/f_o^{**} than for the closely-spaced cylinders. As the oscillation amplitude of the cylinder system increases, the amplitudes of the peaks in the spectrum increase, as shown by comparison of Figures 11 and 12, representing A/D = 0.2 and 0.5 respectively.

2. WAKE STRUCTURE FROM SYSTEM OF CYLINDERS WITH LARGE SPACING

Depending on the excitation frequency and amplitude of the oscillating cylinders, and the phase angle between them, a variety of modulated and locked-in patterns of response can be generated. In the following, these possible regimes are categorized systematically starting with the case of a stationary cylinder, followed by oscillating cylinders with a defined phase angle ϕ between them.

2.1 Modulated wake response of system of stationary cylinders

Representative states of the wake system of two stationary cylinders in a tandem arrangement are indicated in Figure 13. These photos were extracted from video recordings over a large number of cycles of the near-wake vortex formation. The first photo is arbitrarily designated as N = 1. The pure form of the mode remains broken through N = 17 and 22. At N = 32, the classical mode of vortex formation reappears. It is evident that this pattern of vortex formation from the stationary cylinders involves modulation at frequencies substantially lower than the natural vortex formation frequency f_0^{**}. Corresponding spectra taken between and downstream of the cylinders are shown at the bottom of Figure 13. Both spectra indicate a relatively broad spectral peak at f_0^{**} and no contribution associated with low frequency modulation.

2.2 Overview of regimes of wake response for oscillating cylinders

Figure 14 represents overview of the regions of response on the plane of phase angle ϕ versus excitation frequency f_e/f_0^{**} for the excited, and cylinder system at large spacing. Regions I and III represent modulated responses and region II corresponds to locked-in response.

2.3 Modulated wake response for excitation of cylinder system at frequency lower than that of locked-in state

As shown in Figure 15, excitation of the system of two cylinders at a dimensionless frequency $f_e/f_o^{**} = 0.61$ with dimensionless amplitude A/D = 0.5, corresponding to a location just outside of the locked-in region in Figure 6, produces a modulated response of the wake. This response is very repetitive. It repeats every four cycles of the cylinder excitation frequency f_e, in contrast to the disordered type of modulated response of the wake from the stationary cylinders shown in Figure 13. Irrespective of the phase angle ϕ, the patterns of Figure 15 are the same at N = 1 and N = 4. The qualitative form of the wake patterns is not dependent on the value of ϕ, as is evident from comparison of photos at a given value of N for the three values of phase angle $\phi = 0°$, 80° and 180°.

Representative spectra taken between the cylinders and in the near-wake region are given in Figure 16. The predominant peaks are at the vortex formation frequency f_o^{**}, the excitation frequency f_e and modulation frequency $f_m = (f_o^{**} - f_e)$; other peaks are at $(f_e - f_m)$, $(f_e + f_m)$, $(2f_e + f_m)$. In fact, as shown in Figure 16, this same general form of the spectrum is obtained not only between the cylinders and in the near-wake region, but also for three values of the phase angle $\phi = 0°$, 80° and 180°. Although the relative amplitudes of the spectral peak vary, the dominance of the components f_m, f_o^{**}, f_e persists.

2.4 Locked-in wake response for excitation of cylinder system near synchronization condition

As illustrated in Figure 17, excitation of the cylinder system at dimensionless frequency $f_e/f_o^{**} = 0.86$ produces locked-in patterns of vortex formation. These patterns are insensitive to the phase angle between the cylinders. In contrast to the case of the stationary cylinders shown in Figure 13, there is no discrete vortex formation between the cylinders. Regarding the spectra, they have a form characteristic of locked-in response; there are peaks at the excitation frequency f_e and its harmonics $2f_e$ and $3f_e$, as shown in Figure 18.

2.5 Modulated wake response for excitation of cylinder system at frequency higher than that of locked-in state

Excitation of the cylinder system at a dimensionless frequency $f_e/f_o^{**} = 1.56$, i.e. at a frequency higher than the synchronization condition $f_e/f_o^{*} = 1$, results in a modulated response. As shown in Figure 19, the wake structure repeats every sixth cycle of the cylinder oscillation f_e. Corresponding spectra taken between and downstream of the cylinders are shown in Figure 20. The left column of Figure 20 presents the spectra taken between cylinders at phase angles of $\phi = 0°$, 80° and 180°. In these spectra, the dominant peak is at the modulation frequency f_m where $f_m = 3/5\ f_e$. The excitation frequency and the natural shedding frequency are suppressed by the modulation frequency. The right column of Figure 20 gives the spectra taken in the downstream region. When the phase angle $\phi = 0°$ and 80°, the

dominant peak is at the modulation frequency f_m. For all values of phase angle ϕ, detectable peaks occur at f_e, $f_e - f_m$, and $2f_m - f_e$.

This modulated response involving dominance of the modulation component f_m is distinctly different from the spectral response of Figure 16 represents excitation of cylinder system at frequency lower than corresponding locked-in state. In that case, f_m appears as a relatively low-amplitude component.

3. WAKE STRUCTURE FROM SYSTEM OF CYLINDERS WITH SMALL SPACING

3.1 Wake from system of stationary cylinders

The wake patterns shown in Figure 21 for small spacing between the stationary cylinders are distinctly different from these arising from large cylinder spacing, as shown in Figure 13. In Figure 21, there is no vortex formation between the cylinders and the initially-formed vortex from the system of cylinders occurs well downstream. The left and right columns of photos in Figure 21 show respectively close-up and far views of the flow. Regarding the spectrum shown at the bottom of Figure 21, there is a broad but clearly detectable peak at the natural shedding frequency f_o^{**} of the two cylinder system.

3.2 Overview of wake response for system of oscillating cylinders

Figure 22 gives an overview of the regimes of response of the excited cylinder system on the plane of phase angle ϕ versus excitation frequency f_e/f_o^{**}. The response in regimes I and III, representing modulated and locked-in response, is independent of ϕ. In regime II, however, variation of angle ϕ can generate transition from modulated to locked-in response. Comparison of Figure 22 with Figure 14 shows that the response for the former is more sensitive to ϕ than the latter.

3.3 Transformation from modulated to locked-in wake response for excitation of cylinder system at frequency lower than that of locked-in state

Figure 23 shows that when the excitation frequency is $f_e/f_o^{**} = 0.75$, the structure of the vortex formation between the cylinders transforms from modulated to locked-in states as the phase angle changes from $\phi = 0°$ to $\phi = 180°$.

The corresponding spectra are shown in Figure 23. The predominant peaks are at the natural vortex formation frequency f_o^{**} and the excitation frequency f_e. In fact, these two peaks have approximately the same amplitudes. These peaks in the spectra can be changed to a strongly resonant response at the excitation frequency by changing the phase angle from small

values, i.e. $\phi = 0°$, to large values, i.e. $\phi = 180°$ as shown in Figure 23. At larger phase angle ϕ, the peak at the inherent vortex formation frequency f_0^{**} is no longer detectable. The classical locked-in spectrum with a dominant component at f_e is evident. As shown in Figure 23, there is no separated vortex formation from the downstream cylinder. The separated shear layer from the upper cylinder rolls up behind the downstream cylinder.

This behavior of the wake shown in Figures 23 and 24 clearly shows the strong influence of the phase angle ϕ, provided the excitation frequency f_e/f_0^{**} is tuned to a stable value close to the boundary between the non-locked-in and locked-in response (compare Figure 7).

3.4. Locked-in wake response for excitation of cylinder system near synchronization condition

Excitation of closely spaced cylinders at a frequency ratio f_e/f_0^{**}= 1.0 produces locked-in patterns of vortex formation, as illustrated in Figure 25. The pattern of vortex formation between the cylinders is relatively insensitive to phase angle ϕ. Although there is no vortex formation between the corresponding system of stationary cylinders shown in Figure 21, forced excitation of the cylinder system induces rollup of the separated shear layer from the upstream cylinder and thereby vortex formation between the cylinders, as shown in Figure 25, Moreover, in contrast to the corresponding case of the stationary cylinders of Figure 21, vortex are formed immediately downstream of the oscillating cylinders, as shown in Figure 25.

IV. WAKE RESPONSE OF SIDE-BY-SIDE ARRANGEMENT OF TWO CYLINDERS

1. OVERVIEW OF LOCKED-IN RESPONSE OF WAKE

1.1 Region of locked-in response of wake

A well known feature of flow past an oscillating, single cylinder is the occurrence of locked-in vortex formation. Lock-in occurs when the flow pattern is phase-locked to the motion of the cylinder, i.e. it is repetitive at the same phase of the oscillation cycle of the cylinder, from one cycle to the next. This lock-in occurs over a narrow band of frequencies in the vicinity of the perfectly synchronized condition corresponding to $f_e/f_o^* = 1$, in which f_e is the frequency of controlled excitation of the cylinder and f_o^* is the natural vortex formation from the corresponding stationary cylinder. Moreover, the width of the lock-in region is, in general, a function of the amplitude A of oscillation normalized by the cylinder diameter D.

The domain of locked-in response for the case of a single cylinder is indicated by the cross-hatched region of Figure 26. A major issue is the degree to which a two-cylinder system exhibits locked-in response. The regions of locked-in response due to oscillations of two side-by-side cylinders, with phase angles $\phi = 0°$ and $180°$ between them, are illustrated in Figure 26. It is evident that both of these extreme values of phase angle can induce region of locked-in response of substantial width. Furthermore, both regions of locked-in response for the two-cylinder system are shifted to the

right of the lock-in region for the single cylinder. Regarding the lowest threshold value of amplitude A/D for which lock-in can be attained for the two cylinder system, it is of the order of 0.075 to 0.08, while that for single cylinder is attained at A/D = 0.10. It is interesting to note that at relatively high values of dimensionless amplitude A/D, i.e. for A/D greater than 0.57 lock-in is no longer attainable for the two-cylinder system at $\phi = 0°$. The two upper branches of the lock-in region converge; on the other hand, for $\phi =$ 180°, this large amplitude limiting condition does not occur.

1.2 Transformation from non-locked-in to locked-in response of wake

Since, as shown in Figure 26, lock-in occurs only over a narrow range of frequency, the issue arises as to the nature of the wake response outside the lock-in region. More specifically, it is of interest to determine the visualized flow patterns, as well as the spectra in the wake, starting at very low values of excitation frequency and proceeding to the perfectly synchronized condition $f_e/f_o^* = 1$ within the lock-in region.

First, the nature of the spectra is addressed. Figure 27 shows families of spectra for the two cylinder system at a value of phase angle $\phi = 0°$ in comparison with spectra corresponding to the single cylinder. For the case of the single cylinder, excitation at a relatively low frequency ratio $f_e/f_o^* = 0.1$ produces a broad peak at the natural vortex formation frequency f_o^* from the corresponding stationary cylinder; there is no pronounced contribution from the excitation frequency f_e. When the excitation frequency f_e is increased to values in the range 0.2 to 0.4, the broad peak at f_o^* is replaced by two

pronounced peaks, one at the natural vortex frequency f_o^* and the other at the modulation frequency f_m which is difference between natural shedding frequency f_o^* and excitation frequency f_e. That is, the excitation frequency is still not detectable in the spectra. Moreover, the value of f_m decreases as excitation frequency f_e increases. At higher values of excitation frequency f_e = 0.5, the peaks at f_m and f_o^* still dominate, but at f_e = 0.6, a large number of discrete peaks form. The detectable peaks at f_m and f_o^* are still evident, but there are additional sum and difference frequencies corresponding to f_m, f_e, f_o^*. At the next highest value of a excitation frequency f_e = 0.7, this multiple-peak spectrum collapses to a classical lock-in spectrum, involving dominance of the excitation frequency f_e component and its first harmonic component $2f_e$. This general form of the spectra is maintained for all larger values of dimensionless excitation frequency f_e until the perfectly synchronized condition $f_e/f_o^* = 1.0$ is attained.

For the two cylinder system, as shown in the second column of spectra in Figure 27, generally similar modification of the spectra are obtained for successively larger values of dimensionless excitation frequency f_e/f_o^{**}, where f_o^{**} is the frequency of natural vortex formation from the corresponding system of two cylinders. It is evident, however, that the amplitude of the peaks above the background level is substantially smaller over the entire range of dimensionless excitation frequency f_e/f_o^{**}. In fact, in the lock-in region of response, at $f_e/f_o^{**} = 1.0$, the peak amplitude of the fluctuation, normalized by the background level, is 0.2 for the two cylinder system, compared to a value of 1.2 for the single cylinder. It appears that an

important effect for the two-cylinder system, relative to the case of a single cylinder, is its inability to generate large amplitude spectral peaks in the wake response, not only in the locked-in region, but also well outside of it. Even at low values of excitation frequency f_e/f_o^{**}, say $f_e/f_o^{**} = 0.1$ and 0.2, the amplitude of the broadband peaks above the background level of the spectrum is small, relative to the case of the isolated cylinder. This effect is illustrated by a plot of the peak amplitude versus dimensionless excitation frequency f_e/f_o^{**} in Figure 28.

At lower amplitude of oscillations A/D = 0.2, represented by Figure 29, generally similar trends are observed as for Figure 27, except that the attainment of locked-in spectra occurs at higher f_e/f_o^{**}. Moreover, the differences between the peak amplitudes of the single and two-cylinder system are not as large.

2. WAKE STRUCTURE FROM SYSTEM OF CYLINDERS WITH LARGE SPACING

Depending upon the excitation frequency and the phase angle between the cylinders, a variety of modulated and locked-in patterns of response can be generated. In the following, an attempt is made to categorize systematically these possible regimes, starting with the case of the stationary cylinders, followed by oscillating cylinders with defined phase angle between them for successively higher values of excitation frequency f_e.

2.1 Modulated wake response of system of stationary cylinders

The succession of possible states of the wake from two stationary cylinders is indicated in Figure 30. Video recordings were made of the near-wake vortex formation over a large number of cycles. If we take the pattern of N = 1 as the starting point, then about 15 cycles of the near-wake vortex formation, i.e. N = 15, are required for the wake to evolve to an antisymmetrical mode of vortex formation. The pure form of this mode is temporarily broken at N = 17, there is a return to the antisymmetrical mode in N = 19, to a slightly different form of it in N = 33, and finally return to the nearly symmetrical pattern in N = 53. This pattern of vortex formation from the stationary cylinders involves modulations of the wake structure that should give rise to low frequency modulation components, substantially lower than the natural vortex formation frequency f_o^{**}. Corresponding spectra shown at the bottom of Figure 30 indicate only a relatively broad spectral peak at f_o^{**}. There are, however, and contributions to the energy at low frequencies, i.e. as zero frequency is approached, no doubt associated with the low frequency modulation shown in the flow visualization.

It should be noted that the experiments of Williamson (1985) show existence of either an out-of-phase (symmetrical) or in-phase (antisymmetrical) mode of vortex formation behind a system of stationary cylinders. He defines formation of a "binary-vortex" street when like-signed vortices from each cylinder pair up in the downstream region and form a large-scale wake. Williamson observed that the flow switched from in-phase

(antisymmetrical) to antiphase (symmetrical) vortex formation and vice-versa over a large number of cycles when the gap is between 1 and 5 diameter.

2.2. Overview of regimes of wake response for oscillating cylinders

When both cylinders oscillate at a given value of A/D, the crucial parameters are the excitation frequency f_e/f_o^{**} and the phase angle ϕ between them. Figure 31 is an overview of the regimes of response on the plane of ϕ versus f_e/f_o^{**}. The basic regimes are : locked-in response; subharmonic response; and modulated response. It should be emphasized that data were not obtained for sufficiently high or low f_e/f_o^{**} to generate possible additional regions of modulated response. The focus here is on regions of quasi-ordered, modulated response at modulation frequencies $f_m = f_e/n$, in which n is an integer. In the following, these regimes of Figure 31 are described in detail.

2.3 Modulated wake response for excitation of cylinder system at frequency lower than that of locked-in state

Excitation of the system of cylinders at a dimensionless frequency $f_e/f_o^{**} = 0.8$ lower than that of lock-in region (see Figures 26 and 31) generates wake patterns shown in Figure 32. The modulated response of the wake is an ordered repetitive one, repeating every fourth cycle of oscillation, in contrast to the variable frequency, disordered type of modulation of the wake from the stationary cylinder shown in Figure 30. For each value of the phase angle ϕ, the pattern is consistently the same at N = 1 and N = 4. The details of the patterns are, however, dependent on value of ϕ. The photos at

N = 1 exhibit varying degrees of symmetry for the three values of phase angle $\phi = 0°$, $\phi = 95°$ and $\phi = 180°$. In general, a nearly symmetrical pattern of vortex formation is attainable during part of each modulation cycle. However, the symmetry is not perfect, and this is the feature that requires it to continuously cycle through various states in a modulated fashion. A representative spectrum, taken for the $\phi = 0°$ series, is indicated at the bottom of Figure 32. The predominant peaks are the inherent vortex formation frequency f_e and the modulation frequency $f_m = f_o^{**} - f_e = f_e/3$.

In fact, as shown in Figure 33, this same general form of the spectrum is maintained not only for different locations in the wake, but also for the three values of phase angle $\phi = 0°$, $\phi = 95°$, and $\phi = 180°$. To be sure, the relative amplitudes of the spectral peaks do vary, but the dominance of the components f_m, f_o^{**}, and f_e does seem to persist.

2.4 Transformation from modulated to locked-in wake response for excitation of cylinder system at frequency lower than that of locked-in state

If the excitation frequency is increased to a value $f_e/f_o^{**} = 0.9$, and the period of the modulation decreases, as indicated in Figure 34a, the modulation period is twice, or the modulation frequency half, the period of the forced cylinder oscillation, i.e. $f_m = f_e/2$. In fact the photos N = 1 through 3 in the left column are quite similar. Close inspection reveals, however, that the central portion of the photo corresponding to N = 2 is discernibly different from that of N = 1 and N = 3. This small difference is amplified

further downstream in the wake, evident in the right photos. The formation of vortex pairs on the upper and lower sides of the wake is modulated. The corresponding spectrum, shown at the bottom of the Figure 34a, does not simply show a single peak at half the natural vortex formation frequency $f_e/2$. Rather, peaks at f_o^{**} and $f_o^{**} - f_e/2$ are also evident.

These peaks in the spectra can be removed, and a strongly resonant response at the excitation frequency can be generated, by changing the phase angle from the value $\phi = 0°$ in Figure 34a to either $\phi = 95°$ or $\phi = 180°$ in Figure 34b. In these cases, the peak at the inherent vortex formation frequency f_o^{**} is no longer detectable; the classical locked-in spectrum involving dominance of the component at f_e is evident. The corresponding near and far views of the locked-in patterns of vortex formation repeat, of course, for each successive cycle of the forced cylinder oscillation.

The behavior of the near-wake shown in Figures 34a and 34b clearly shows the strong effect of phase angle ϕ, provided the excitation frequency f_e is tuned to a marginally-stable value close to the boundary between the non-lock-in and the lock-in response (compare Figure 26).

2.5 Modes of locked-in response of wake via variation of phase angle between oscillating cylinders

Excitation of the cylinder system at dimensionless frequency $f_e/f_o^{**} = 1.0$, corresponding to the case of synchronized excitation, produces locked-in patterns of vortex formation, irrespective of the phase angle ϕ between the cylinders, as illustrated in Figure 35. Photos shown in the left column reveal

that, at $\phi = 0°$, the pattern of vortex formation is in a nearly purely antisymmetrical mode, transforming to a symmetrical mode for $\phi = 180°$. This transformation through values of phase angle $\phi = 40°$, 80°, and 120°, involves well-defined changes in the pattern of initially-formed vortices. In the right column of photos, it is evident that vortex pairs are always formed in the downstream region of the wake, irrespective of the value of phase angle ϕ. At all values of phase angle $0° \leq \phi \leq 120°$, however, there is a tendency for well-defined pairs to occur only on one side of the wake. Vortex pairs form consistently on both sides of the wake only for $\phi = 180°$. Regarding the spectra there is dominance of the peak at $f_e = f_o^{**}$ for all values of phase angle ϕ.

3. WAKE STRUCTURE FROM SYSTEM OF CYLINDERS WITH SMALL SPACING

The foregoing features of the wake are representative of wake structure for values of cylinder spacing in the range of $1.7 \leq G/D \leq 3$. When the spacing is decreased to a relatively small value, however, the mechanisms of response are fundamentally different, as shown in the following.

3.1 Modulated, broadband response of wake from stationary cylinders

Figure 36 shows that the vortex formation from closely-spaced cylinders is strongly influenced by the "jet-like" flow between them. It tends to exhibit a bistable behavior, switching from the top to the bottom side of the wake, strongly influencing the pattern of vortex formation, as shown in the left column of photos. In fact, only for the middle photo, for which the

jet is directed along the centerline of the wake, are there clearly-defined patterns of vortices, which tend to mimic the symmetrical mode of formation described in the foregoing for larger values of cylinder spacing. The right column of photos shows the corresponding structure of the wake in the downstream region of the wake. Although this visualization suggests occurrence of large-scale structures, the highly coherent vortex formation described in the previous section for larger spacing of the cylinders does not exist. As a consequence, the spectrum shows a very broadband character, with no discrete peaks.

Williamson (1985) has recently addressed the asymmetric flow pattern from two side-by-side cylinders with a small gap between them. He finds that the gap flow is deflected to one side, in agreement with the observations of Inshigai et al (1972), Bearman and Wadcock (1978), and Quadflieg (1977). Moreover, in his study, vortex pairs from the gap are squeezed together and coalesce with the dominant outer vortices. Both fundamental and harmonic peaks were detectable in the wake region, in contrast to the present results.

3.2 Transition from modulated, broadband wake response to organized vortex formation via variation of phase angle

Excitation of the closely-spaced cylinder system at a dimensionless frequency $f_e/f_o^{**} = 0.9$ and a phase angle $\phi = 0°$ produces the type of modulated response shown in Figure 37a. In this case, the pattern of large-scale vortex formation is not repetitive. Four successive cycles are shown in order to illustrate the complexity of the low frequency, modulated pattern.

The initially-formed vortices from the cylinder system are out of phase for cycles N = 1, 2, and 3; they are in-phase for N = 4. This symmetry rapidly degenerates into a disorganized mode of vortex formation further downstream in the wake. The lack of a clearly-defined modulated pattern is associated with a very broad-band spectrum, as shown at the upper right of Figure 37a.

If, however, the phase angle is altered to a value of $\phi = 180°$, the pattern of vortex formation takes on the modulated form shown in Figure 34b, whereby it repeats every other cycle of the cylinder oscillation. In this case, a discrete peak is detectable at the excitation frequency f_e, as well as a broadened one at the subharmonic $f_e/2$.

A distinguishing feature of this closely-spaced cylinder system is therefore that it is not possible to attain a highly coherent, locked-in pattern of vortex formation, even when dimensionless frequency of excitation $f_e/f_o^{**} = 1.0$.

V. CONCLUSIONS

This investigation has revealed new types of wake behavior occurring both between and downstream of a two-cylinder system in either a tandem or a side-by-side arrangement. Although the details are different for each arrangement, there are certain features generic to both the two-cylinder systems:

4.1. For the *stationary system of cylinders*, the near-wake exhibits a quasi-ordered pattern of vortices with a detectable instability frequency; this frequency can differ by as much as 70% from the instability frequency of the wake for a single cylinder. The pattern of vortex formation associated with this wake instability undergoes intermittent switching between identifiable states; a large number of oscillation cycles may be required for the wake to return to a given state of vortex formation. Due to this switching between states, the spectrum of the wake velocity fluctuation is relatively broad, in contrast to the sharp spectral peak associated with the wake from a single cylinder.

4.2. The wake for an *oscillating system of cylinders* can exhibit either a modulated state, a locked-in state, or a state of transition from modulated to locked-in response.

4.2.1. *Modulated response.* Excitation of a two-cylinder system at a dimensionless frequency below the locked-in region generates a modulated wake with highly-ordered patterns of vortices, which recur over with a modulation period that is a multiple of the period

of the cylinder oscillation. Although the form of the vortex pattern is dependent on the phase angle between the cylinders, the ratio of the modulation period to the period of cylinder oscillation is insensitive to the phase angle.

4.2.2. Locked-in response. When the cylinders are subjected to a controlled oscillation at or near the natural frequency of vortex formation, it is possible to generate locked-in patterns of vortex formation, whereby the vortices are phase-locked to the motion of the cylinders. In other words, the same vortex pattern repeats every oscillation cycle. This highly-ordered vortex formation is a global phenomenon occurring in both the gap region between and the region downstream of the cylinders. Such locked-in patterns of vortices are sustainable over a substantially wider range of excitation frequency than for a corresponding single cylinder. Moreover, it is possible to attain lock-in at significantly lower amplitudes than for the case of a single cylinder. The phase angle between the oscillating cylinders has a mild effect on the extent of the region of locked-in response when the cylinders are closely-spaced. On the other hand, the phase angle has a large effect when the cylinders are widely spaced.

Within this region of locked-in response, the near-wake pattern of vortex formation is sensitive to the phase angle between the oscillating cylinders. These patterns exhibit varying degrees of symmetry. In all cases, irrespective of the complexity of the pattern

of vortex formation, the pattern is highly repetitive from one cycle to the next.

4.2.3. Transitional response. Transition from modulated to locked-in response can be attained over limited bands of excitation frequency. Within these transition bands, the pattern of near-wake vortex formation is highly sensitive to the phase angle between the oscillating cylinders. For example, by holding all other excitation parameters constant, and varying only the phase angle, it is possible to transform the vortex pattern from a modulated to a locked-in state.

4.2.4. Spectra of states of response. The spectra of the velocity fluctuation in the wake of two oscillating cylinders fall into two basic classes. The first type of spectrum is present for the modulated state and displays a number of discrete peaks. These peaks are related to: (1) the cylinder oscillation frequency, (2) the inherent vortex formation frequency for the corresponding stationary, two-cylinder system; (3) a modulation frequency, and (4) sum and difference components of the foregoing frequencies. At excitation frequencies lower than that corresponding to locked-in response, all of the primary spectral components have substantial amplitudes; moreover, they are insensitive to the phase angle between cylinders. At excitation frequencies higher than that corresponding to locked-in response, the modulation component can dominate the spectrum. The second type of spectrum occurs in the locked-in state and exhibits a single predominant peak. The largest amplitude peak is at the

frequency of cylinder oscillation, while secondary peaks occur at its higher harmonics.

VI. PRACTICAL CONSEQUENCES AND RECOMMENDATIONS

The new observations of this investigation have important consequences for the areas of flow-induced vibration and noise generation, heat transfer and mixing. In the following, we interpret these observations of this study from the respective of these applications.

In the area of *flow induced vibration*, the direction of energy transfer between the fluid and the cylinder subjected to forced excitation indicates whether or not self-excited vibration of the corresponding elastically mounted system will occur. Within the locked-in region of vortex formation from a single cylinder, a change in timing of the vortex formation relative to the cylinder motion indicates a change in the direction of energy transfer. Although it was not intent of this investigation to address the possible change in timing occurring over a given range of excitation frequency, the extent of the region of locked-in response was addressed and, in some cases, found to be substantially larger than for the corresponding case of a single cylinder. We therefore expect self-excited, locked-in oscillations of elastically-mounted two-cylinder system, under certain conditions will occur, over a relatively wide range of frequency. On the other hand, outside the region of locked-in response, where the wake exhibits modulated oscillations, corresponding self-excited excitation of the elastically-mounted system is unlikely occur. In any case, additional information is needed on the unsteady lift and drag acting on the cylinder, in relation to the complex types of wake response revealed herein. In doing so, it is essential to characterize both the magnitude and the phase shift of the lift and drag on each cylinder, which in turn would

allow direct linkage to the concept of energy transfer between the fluid and the cylinder and the types of vortex patterns described here,

In the area of *convective heat transfer*, the types of locked-in and modulated response observed in this investigation no doubt influence the instantaneous and time averaged viscous layer about the cylinder. Correspondingly, it is expected that the effective heat transfer coefficient will be altered. In fact, the investigation of Karniadakis and Triantafyllou (1989b) suggests that the large amplitude fluctuations in Nusselt number are attainable at the boundary between locked-in and chaotic states of response. The fact that the extent of the region of locked-in response can be very substantially altered in the case of the two cylinder system, as well as the observation of strongly modulated response of the near-wake outside this locked-in region, suggests that the analogous phenomenon may occur for the two-cylinder system. It would be interesting to undertake a series of heat transfer studies, whereby the fluctuating and mean heat transfer coefficient would be related to the types of near-wake vortex patterns observed in this study.

Regarding the area of *mixing process*, one can envision a practical situation whereby species *a* in the freestream mixes with another species *b* bled from the surface of the cylinder. By imparting controlled perturbations of the cylinder, or perhaps oscillations of the freestream past stationary cylinder system, the effectiveness of the mixing of species *a* and *b* would be influenced by the time-dependent structure of the near-wake. In view of the fact that interesting types of locked-in and modulated response are attainable in the present investigation, it is likely that different rates of mixing in the

near-wake region are attainable as well. It would be fruitful to undertake an experimental study to examine this type of mixing, and relate it to the types of vortex patterns observed herein.

REFERENCES

Arie, M., Kiya, M., Moriya, M. and Mori, H. 1983 "Pressure Fluctuations on the Surface of Two Circular Cylinders in Tandem Arrangement", ASME *Journal of Fluids Engineering,* Vol. 105, pp. 161-167.

Bearman, P. W., Wadcock, A. J. 1973 "The Interaction beetween a Pair of Circular Cylinders Normal to a Stream", *Journal of Fluid Mechanics,* Vol. 61, part 3, pp. 491-511.

Bokaian, A. and Geoola, F. 1984 "Wake-Induced Galloping of Two Interfering Circular Cylinders", *Journal of Fluid Mechanics,* Vol. 146, pp. 383-415.

Chen, S. S. 1985 "A Review of Flow Induced Vibration of Two Circular Cylinders in Crossflow" Fluid-Structure Interaction and Aerodynamic Damping, ASME, New York (eds. E. H. Dowell and M. K. Au-Yang), pp. 133-157.

Feigenbaum, M. J. 1974 "The Onset Spectrum of Turbulence", *Physics Letters,* Vol. 74A, No. 6, pp. 375-378.

Gollub, J. P. and Benson, S. V. 1980 "Many Routes to Turbulent Convection", *Journal of Fluid Mechanics,* Vol. 100, part 3, pp. 449-470.

Huerre, P. and Monkewitz, P. A. 1985 "Absolute and Convective Instabilities in Free Shear Layers", *Journal of Fluid Mechanics,* Vol. 159, pp. 151-168.

Ishigai, S., Nishikawa, E., Nishimura, K. and Cho, K. 1972 "Experimental Study on Structure of Gas Flow in Tube Banks with Tube Axes Normal to Flow" *Bulletin of the Japan Society of Mechanical Engineers,* Vol. 15, No. 86, pp. 949-956.

Jendrzejczyk, J. A., Chen, S. S. and Wambsganss, M. W. 1979 "Dynamic Responses of a Pair of Circular Tubes Subjected to Liquid Cross Flow", *Journal of Sound and Vibration,* Vol. 67, No.2, pp. 263-273.

Karniadakis, G. Em and Triantafyllou, G. S. 1989a "Frequency Selection and Asymptotic States in Laminar Wakes", *Journal of Fluid Mechanics,* Vol. 199, pp. 441-469.

Karniadakis, G. Em and Triantafyllou, G. S. 1989b "The Crisis of Transport Measures in Chaotic Flow Past a Cylinder", *Physics of Fluids A,* Vol. 1, No.4, pp. 628-630.

Kim, C. M. and Conlisk, A. T. 1990 "Flow Induced Vibration and Noise by a Pair of Tandem Cylinders due to Buffeting", *Journal of Fluids and Structures,* Vol. 4, pp. 471-493.

King, R. and Johns, D. J. 1976 "Wake Interaction Experiments with Two Flexible Circular Cylinders in Flowing Water", *Journal of Sound and Vibration,* Vol. 45, No. 2, pp. 259-283.

Lever, J. H. and Weaver, D. S. 1982 "A Theoretical Model for Fluid-Elastic Instability in Heat Exchanger Tube Bandles", ASME *Journal of Pressure Vessel Technology,* Vol. 104, pp. 147-158.

Monkewitz, P. A. and Nguyen, L. N. 1987 "Absolute Instability in the Near-Wake of Two-Dimensional Bluff Bodies", *Journal of Fluids and Structures,* Vol. 1, pp. 165-184.

Moriya, M. and Sakamoto, H. 1986 "Effect of a Vibrating Upstream Cylinder on a Stationary Downstream Cylinder", ASME *Journal of Fluids Engineering,* Vol. 108, pp. 180-184.

Öngören, A. and Rockwell, D. 1988 "Flow Structure from an Oscillating Cylinder Part 1. Mechanisms of Phase Shift and Recovery in the near Wake", *Journal of Fluid Mechanics,* Vol. 191, pp. 197-223.

Païdoussis, M. P. and Price, S. J. 1988 " The Mechanisms Underlying Flow-Induced Instabilities of Cylinder Arrays in Crossflow", *Journal of Fluid Mechanics,* Vol. 187, pp. 45-59.

Price, S. J. 1975 "Wake-Induced Flutter of Power Transmission Conductors", *Journal of Sound and Vibration,* Vol. 38, No. 1, pp. 125-147.

Price, S. J. and Valerio, N. R. 1990 "A Non-linear Investigation of Single-Degree-of-Freedom Instability in Cylinder arrays Subject to Cross-Flow", *Journal Of Sound and Vibration,* Vol. 137, No.3, pp. 419-432.

Quadflieg, H. 1977 "Vortex Induced Load on the Cylinder Pair at high Re." *Forschung im Ingenieurwesen* Vol. 43, pp. 9-18.

Sreenivasan, K. R. 1985 "Transition and Turbulence in Fluid Flows and Low-Dimensional Chaos", Frontiers in Fluid Mechanics (eds. S. H. Davis and J. L. Lumley), pp. 41-67.

Tsui, Y. T. 1977 "On Wake-Induced Flutter of a Circular Cylinder in the Wake of Another", ASME *Journal of Applied Mechanics,* Vol. 44, pp. 194-200.

Van Atta, C. W. and Gharib, M. 1987 "Ordered and Chaotic Vortex Street behind Circular Cylinders at low Reynolds Numbers", *Journal of Fluid Mechanics,* Vol. 174, pp. 113-133.

Williamson, C. H. K. 1985 "Evalution of a Single Wake behind a Pair of Bluff Bodies", *Journal of Fluid Mechanics,* Vol. 159, pp. 1-18.

Williamson, C. H. K. and Roshko, A. 1988 "Vortex Formation in the Wake of an Oscillating Cylinder", *Journal of Fluids and Structures,* Vol. 2, pp. 355-381.

Zdravkovich, M. M. 1982 "Modification of Vortex Shedding in the Synchronization Range", Trans. ASME I : *Journal of Fluid Engineering,* Vol. 104, pp. 513-517.

Zdravkovich, M. M. 1985 "Flow Induced Oscillations of Two Interfering Circular Cylinders", *Journal of Sound and Vibration,* Vol. 101, No. 4, pp. 511-521.

Zdravkovich, M. M. 1987 "The Effects of Interference between Circular Cylinders in Cross Flow", *Journal of Fluids and Structures,* Vol. 1, pp. 239-261.

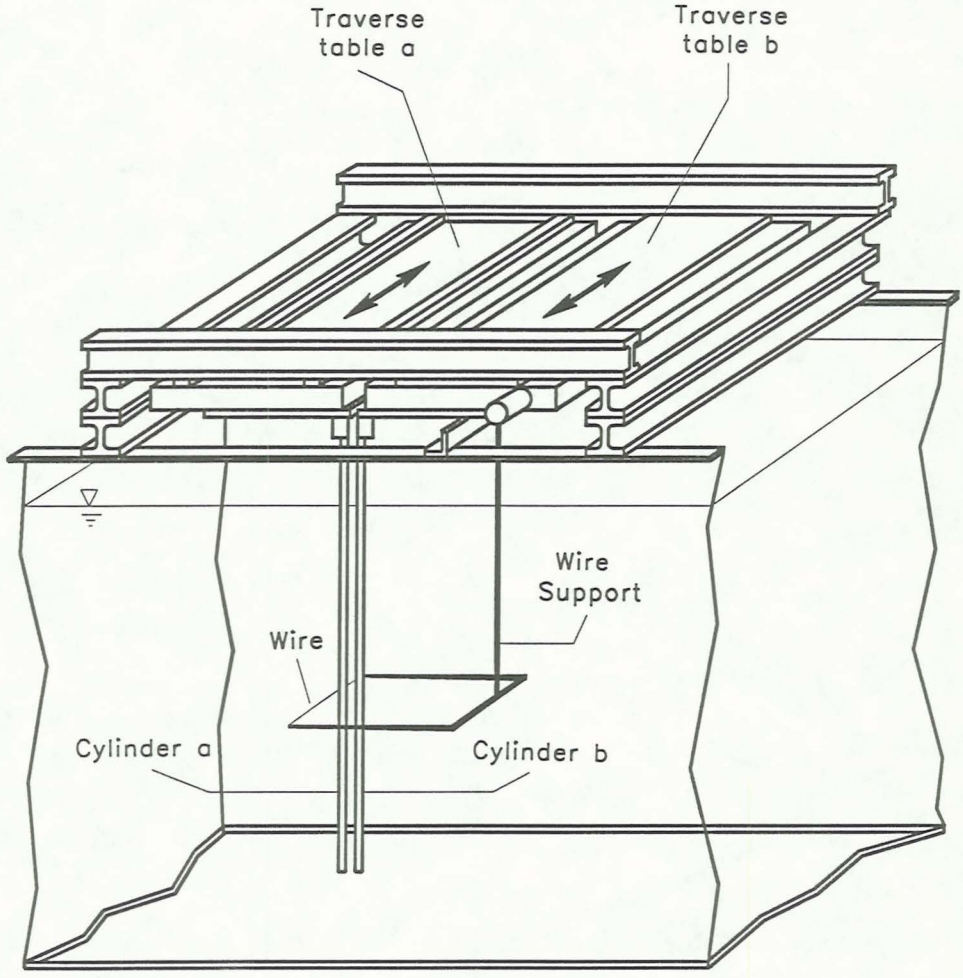

Figure 1: Overview of experimental system.

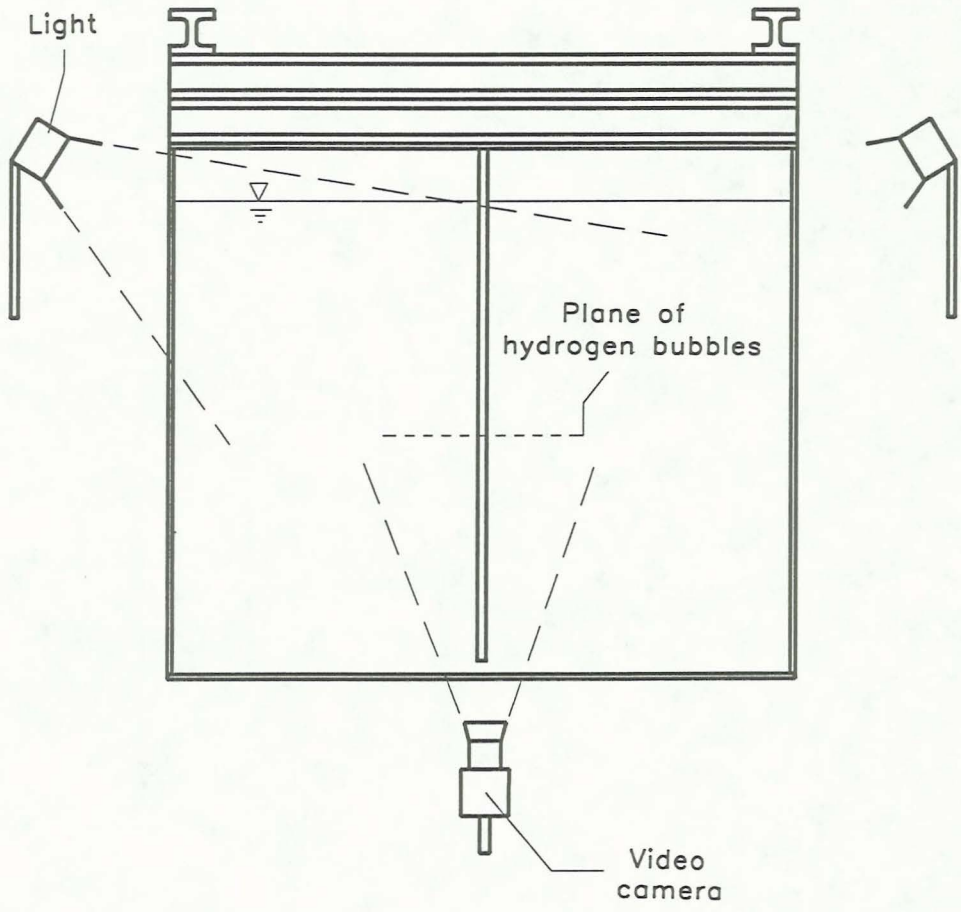

Figure 2: End view of experimental setup and lighting system.

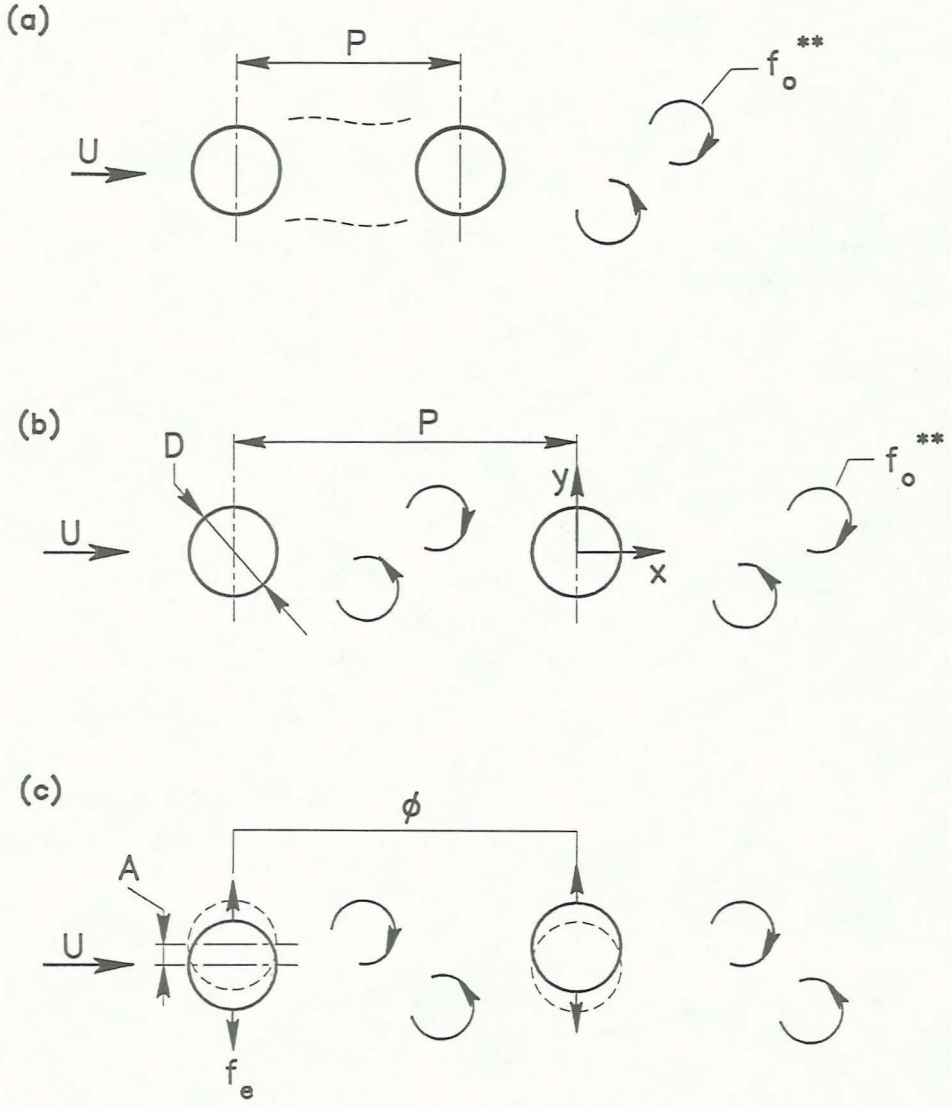

Figure 3: Tandem arrangement of cylinders.

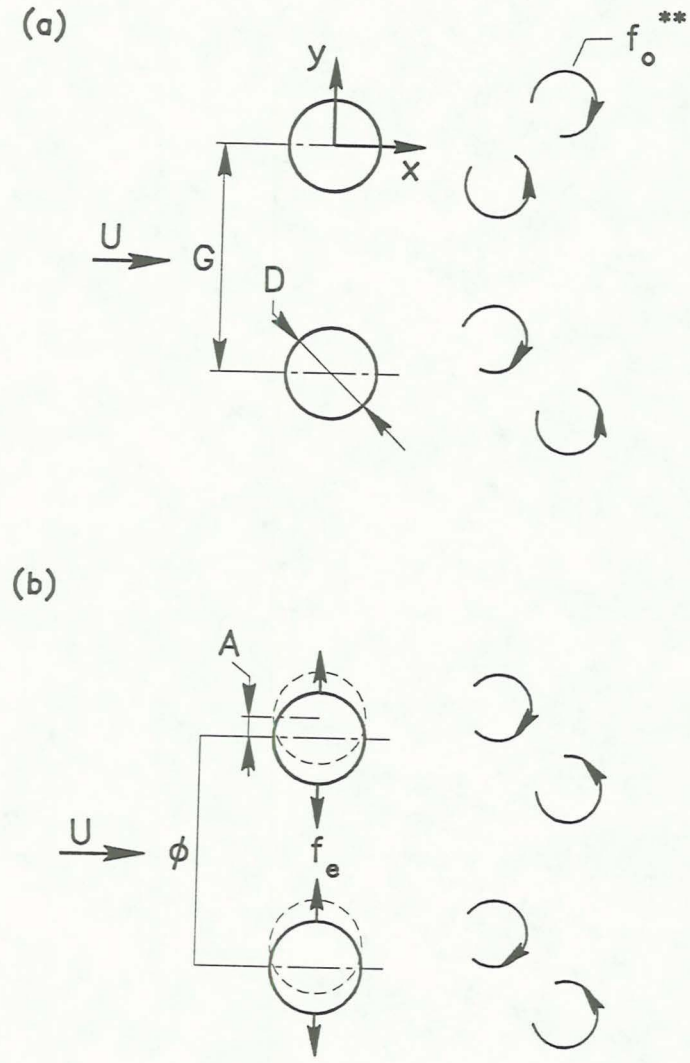

Figure 4: Side-by-side arrangement of cylinders.

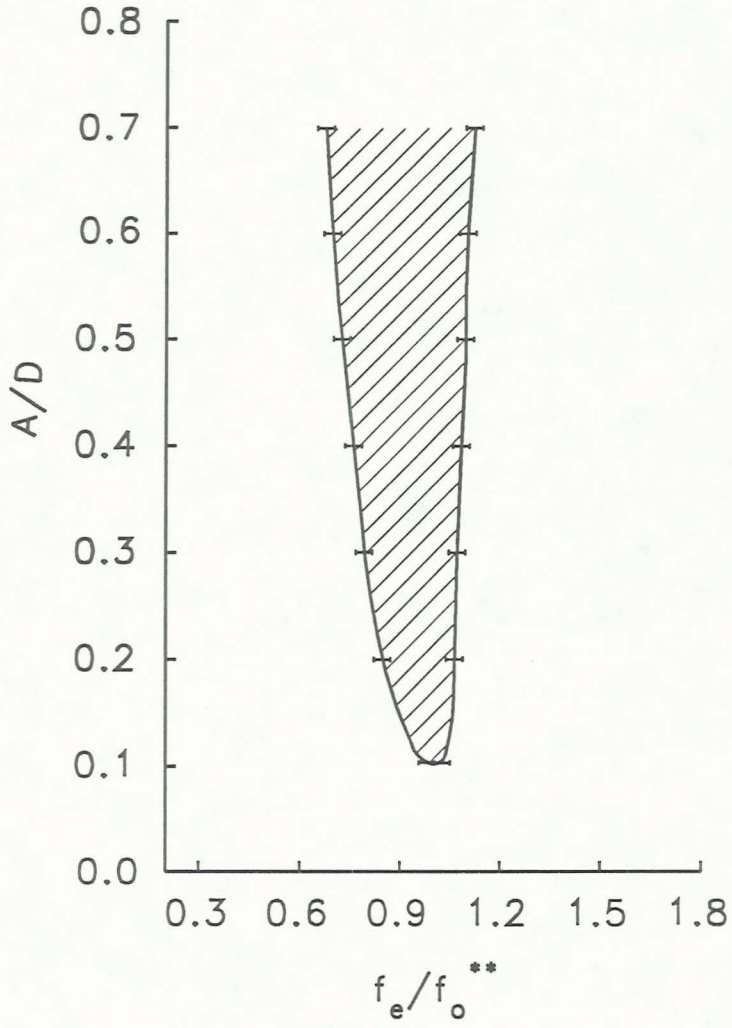

Figure 5: Illustration of uncertainty at the boundary of locked-in regions in the wake of a single cylinder.

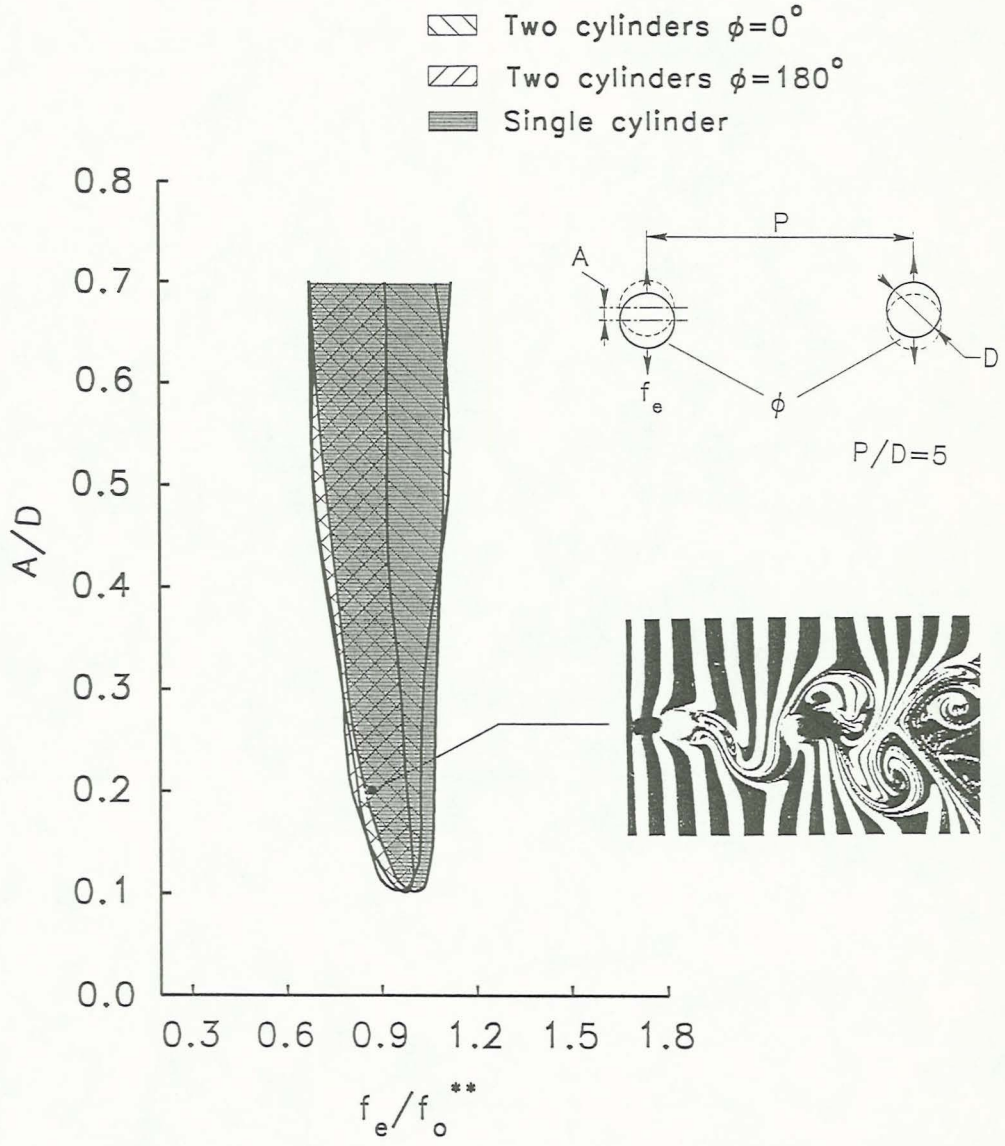

Figure 6: Illustration of regions of locked-in vortex formation as function of dimensionless oscillation frequency f_e/f_o^{**} and amplitude A/D of a single cylinder and two cylinders in tandem arrangement with spacing P/D = 5. Shaded region represents locked-in response wake of single cylinder.

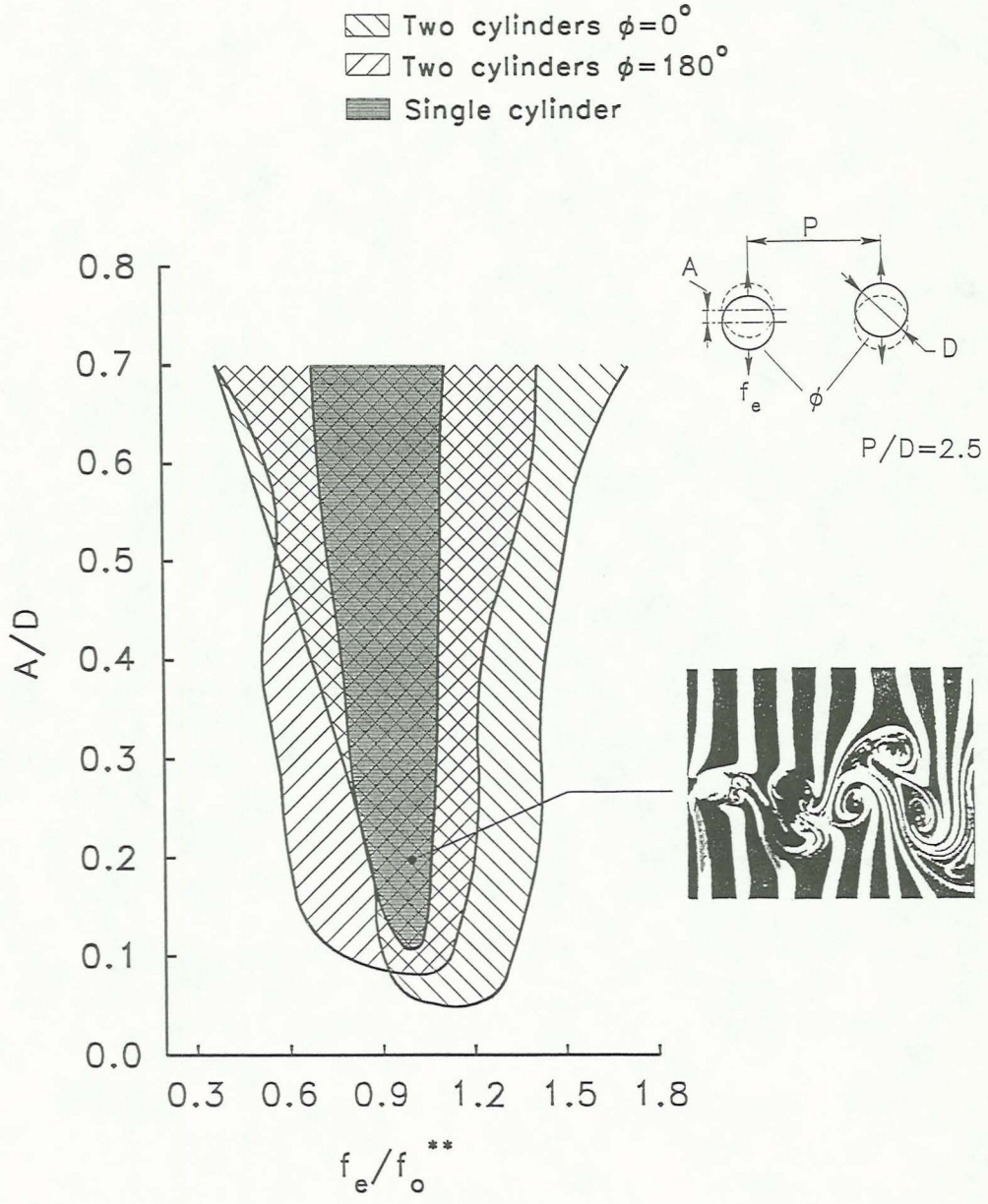

Figure 7: Illustration of region of locked-in vortex formation as function of dimensionless oscillation amplitude A/D and dimensionless frequency f_e/f_o^{**} of excited single cylinder and two cylinders in tandem arrangement with spacing P/D = 2.5. Shaded region corresponds to locked-in response of an isolated single cylinder.

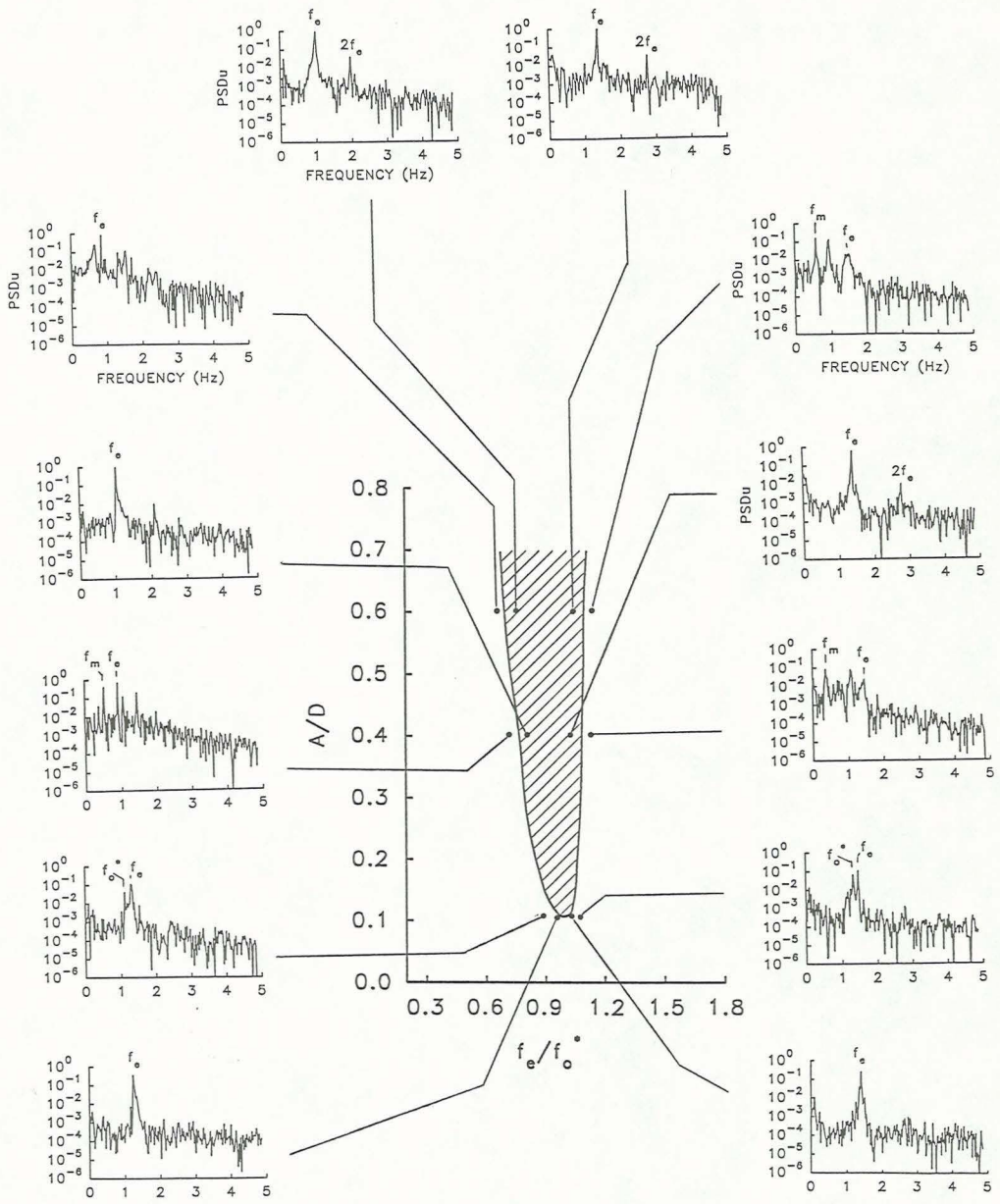

Figure 8: Spectral content of velocity fluctuations near boundary of locked-in regions in wake of a single cylinder.

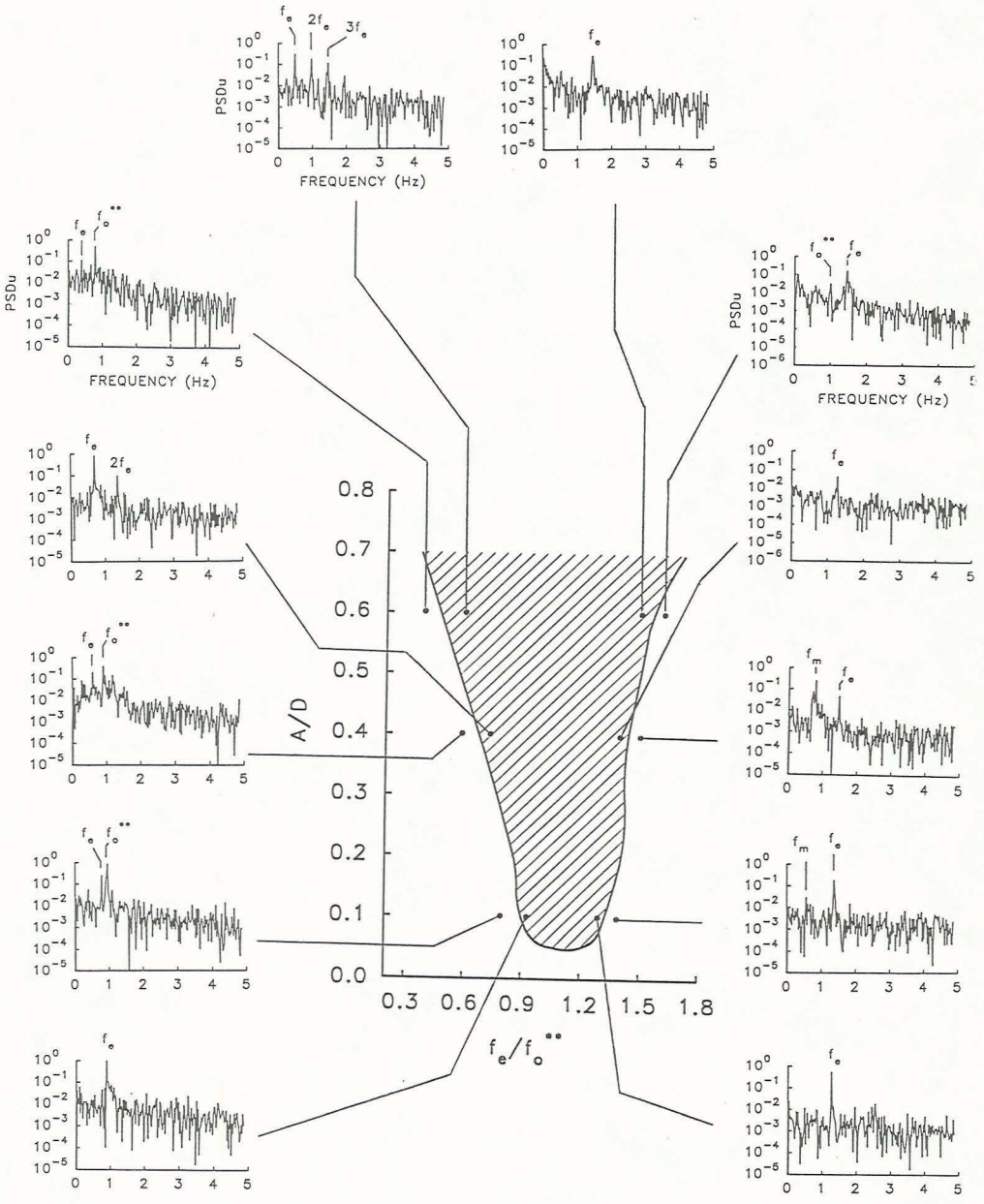

Figure 9: Spectral content of velocity fluctuations near boundary of locked-in regions in wake of two cylinders in tandem arrangement with spacing P/D = 2.5 and phase angle ϕ = 0°.

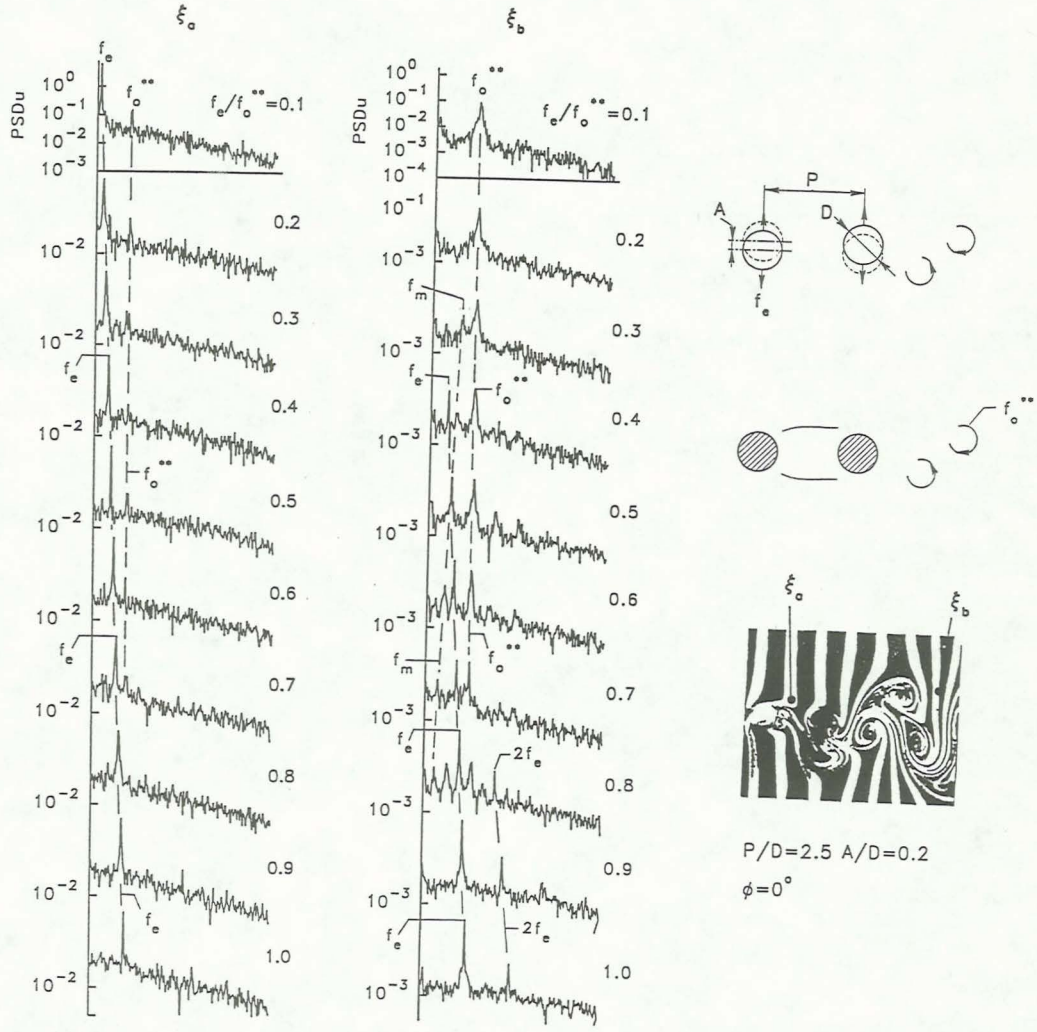

Figure 10: Spectral content of velocity fluctuation between cylinders and in near-wake region as function of dimensionless excitation frequency f_e/f_o^{**}. Dimensionless excitation amplitude A/D = 0.2; distance between cylinders P/D = 2.5. Spectra acquired at locations ξ_a and ξ_b.

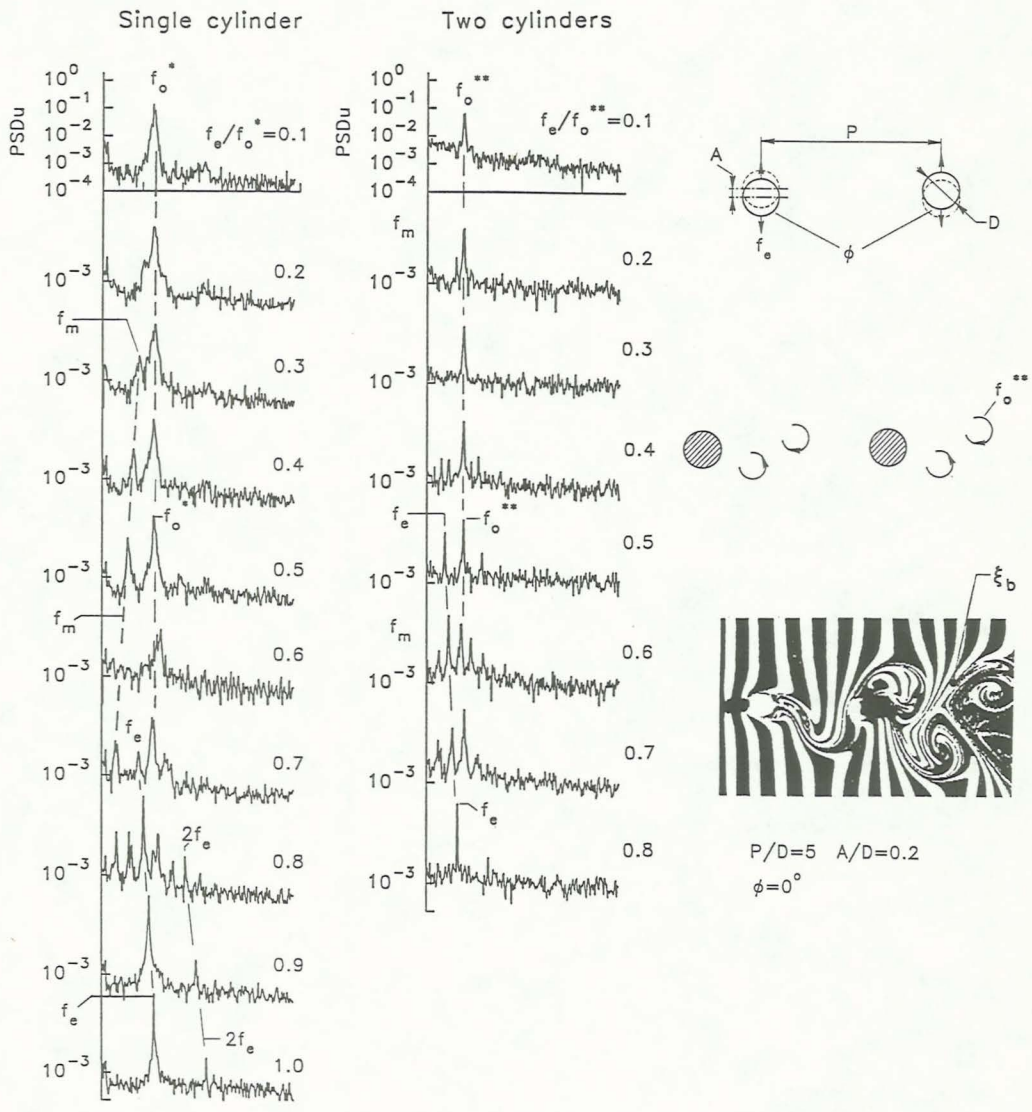

Figure 11: Spectral content of near-wake as function of excitation frequency f_e/f_o^{**}. Dimensionless excitation amplitude A/D = 0.2. Spectra in left column acquired in near-wake of isolated, single cylinder at location ξ_a. Spectra in right column acquired at location ξ_b downstream of two cylinders in tandem arrangement with spacing P/D = 5 and phase angle $\phi = 0°$.

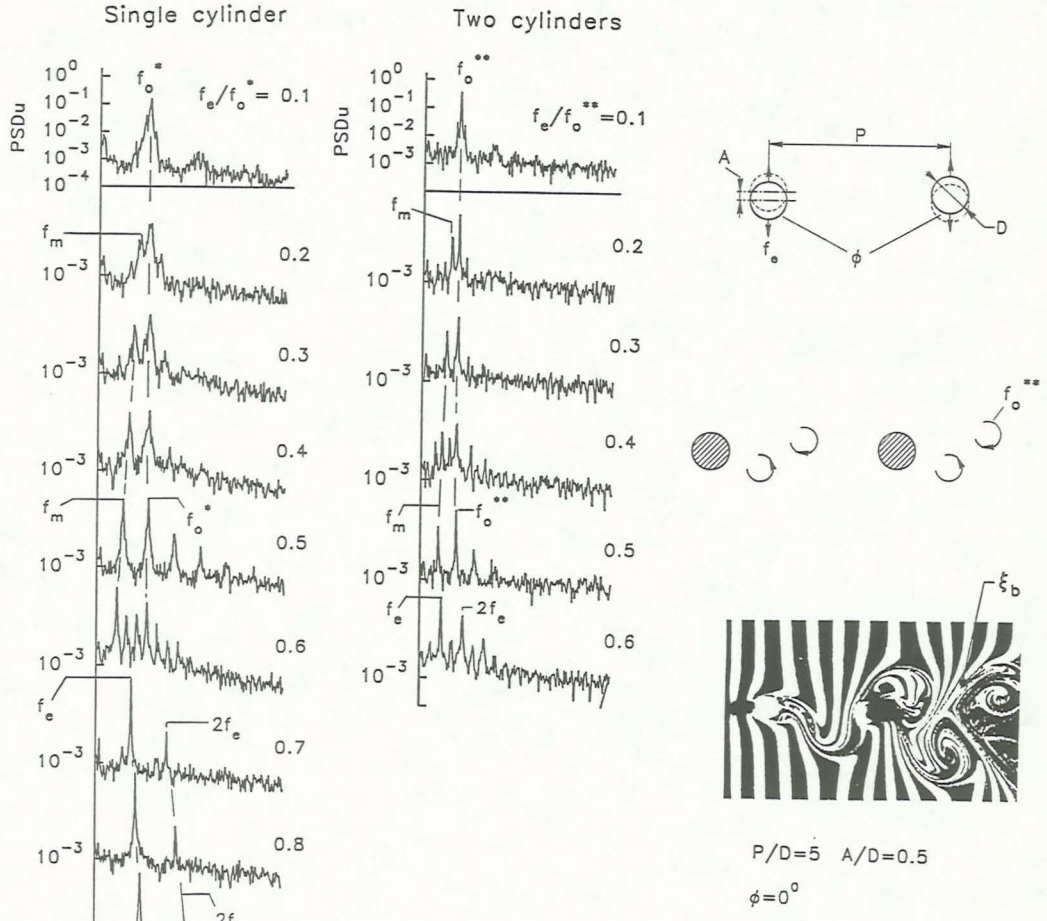

Figure 12: Spectral content of velocity fluctuation in near-wake as function of dimensionless excitation frequency f_e/f_o^{**}. Dimensionless excitation amplitude A/D = 0.5. Spectra in left column taken in near-wake of an isolated single cylinder at location ξ_a. Spectra in right column acquired at location ξ_b in wake of two cylinders in tandem arrangement with spacing P/D = 5 and phase angle $\phi = 0°$.

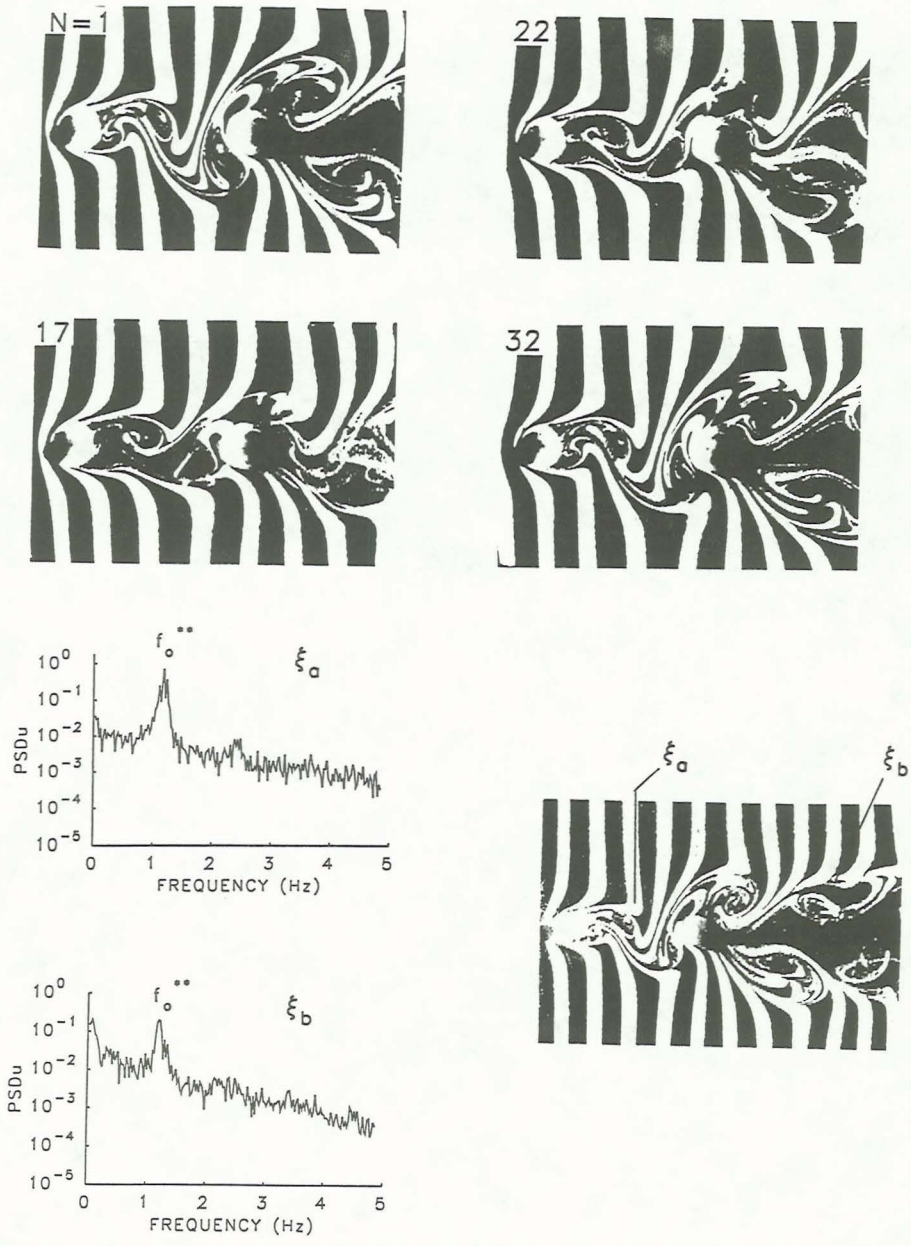

Figure 13: Flow structure and spectra of velocity fluctuation between and in near-wake of two stationary cylinders for N cycles self-excited oscillation. Spacing of cylinders P/D = 5. Spectra taken at locations ξ_a and ξ_b between and in the near-wake of cylinders respectively.

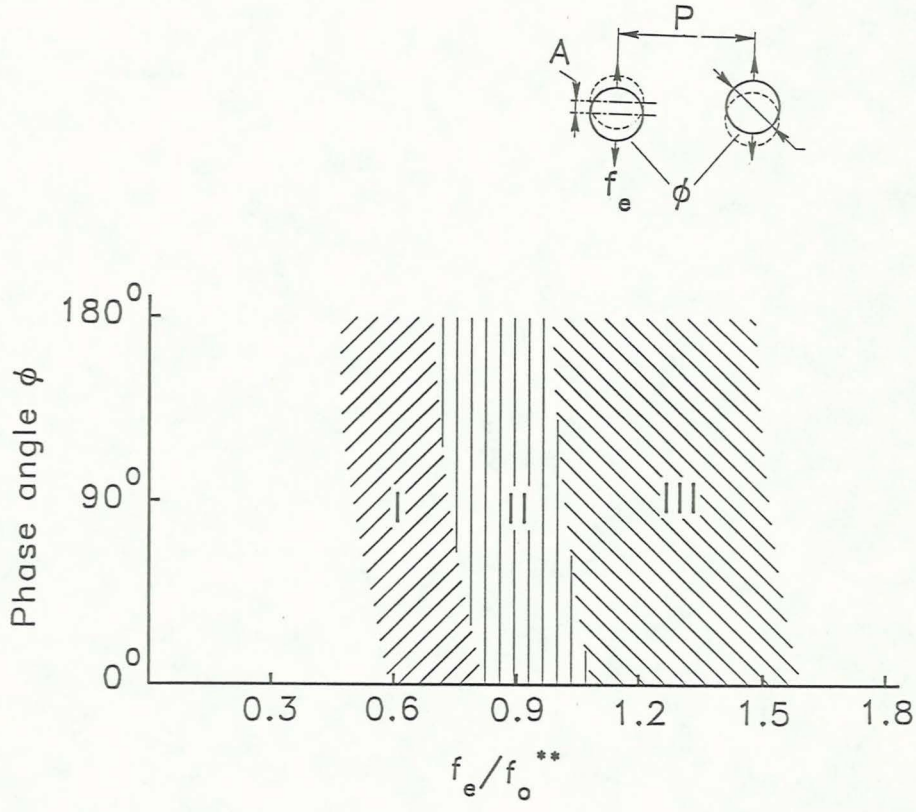

I, III Modulated response.
II Locked–in response.

Figure 14: Illustration of possible response regions on plane of phase angle ϕ versus frequency deviation f_e/f_o^{**}. Dimensionless excitation amplitude A/D = 0.5; spacing between cylinders P/D = 5. Region I represents modulated response, II represents transition from modulated response to locked-in response, and III corresponds to locked-in response.

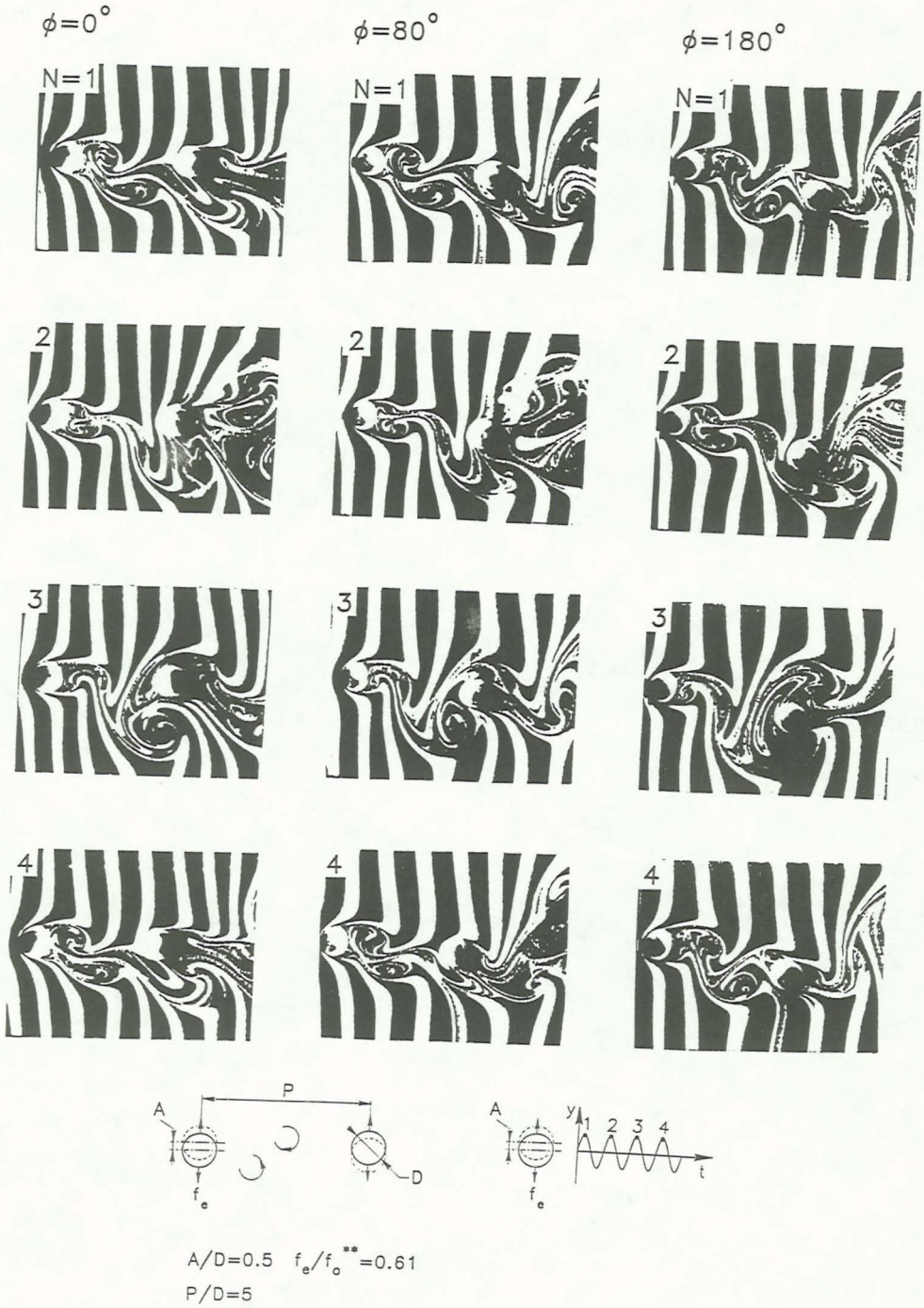

Figure 15: Flow structure corresponding to modulated response of wake, which repeats with period $T_m = 1/f_m$, for three values of phase angle $\phi = 0°$, 80° and 180°. All photos taken at same maximum displacement of upstream cylinder; N represents cycle number of forced oscillation at period $T_e = 1/f_e$. Spacing of cylinders P/D = 5; dimensionless excitation amplitude A/D = 0.5; and excitation frequency $f_e/f_o^{**} = 0.61$.

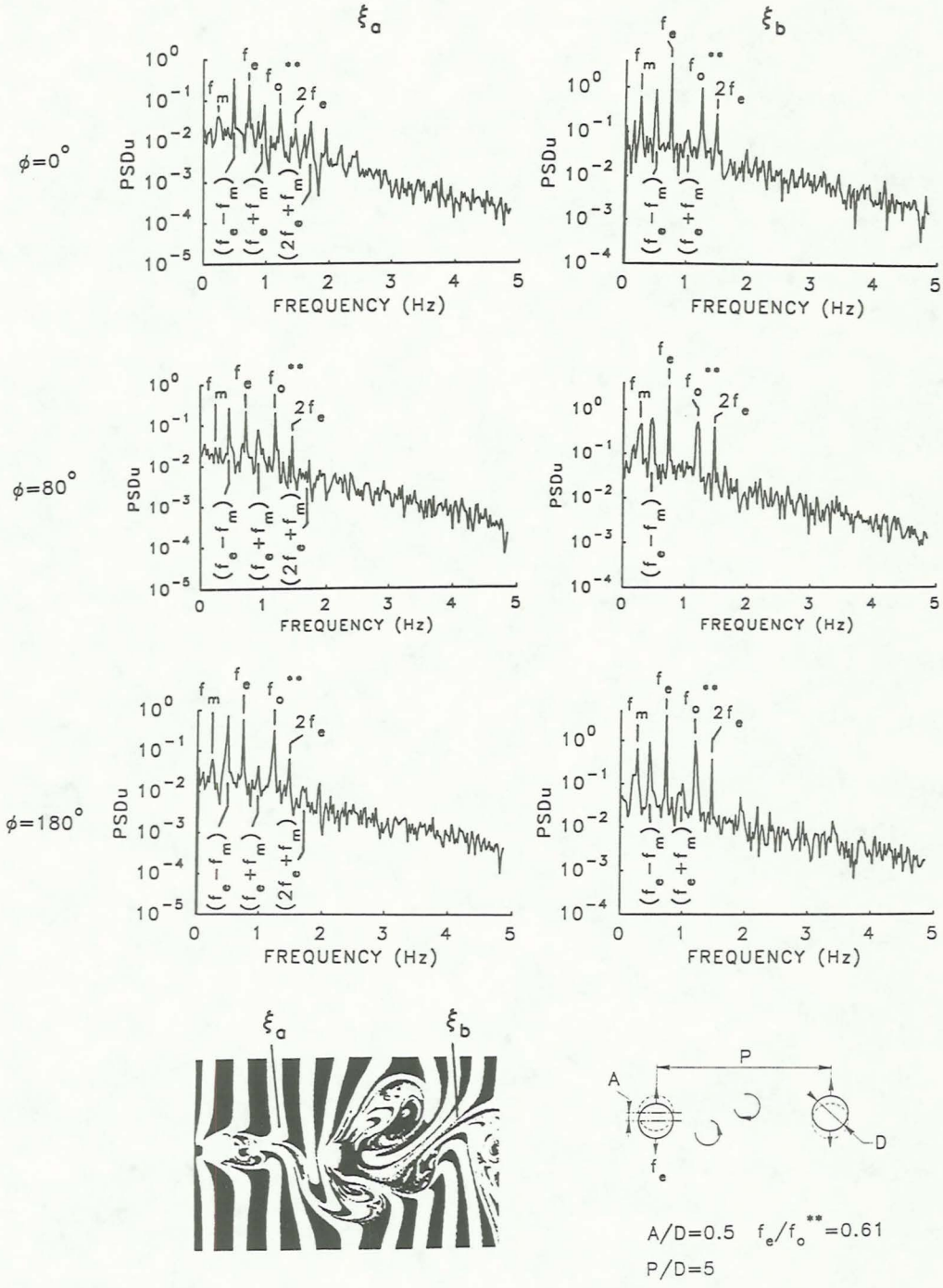

Figure 16: Spectra between cylinders (location ξ_a) and in near-wake region (location ξ_b) representing modulated response for values of phase angle ϕ = 0°, 80° and 180°. Spacing between cylinders P/D = 5; dimensionless amplitude A/D = 0.5; excitation frequency f_e/f_o^{**} = 0.61.

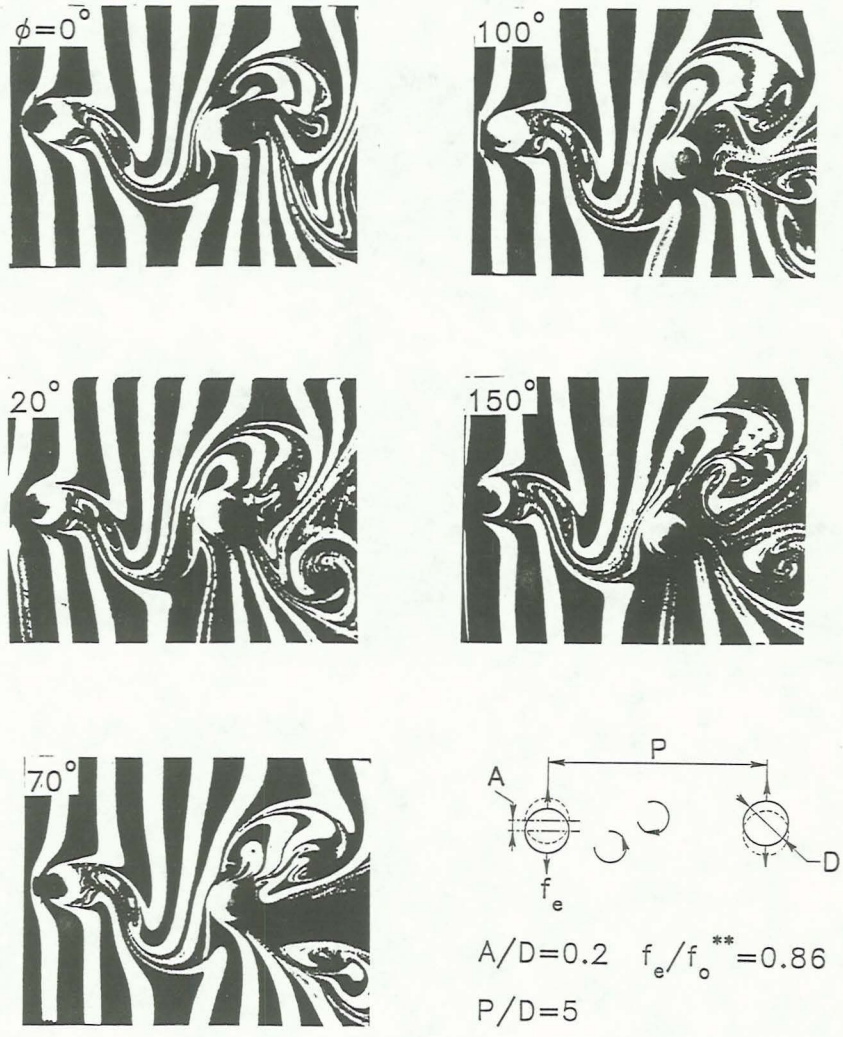

Figure 17: Flow structure corresponding to locked-in response for five different values of phase angle ϕ = 0°, 20°, 70°,100° and 150°. Spacing between cylinders P/D = 5, excitation amplitude A/D = 0.2, excitation frequency f_e/f_o^{**} = 0.86.

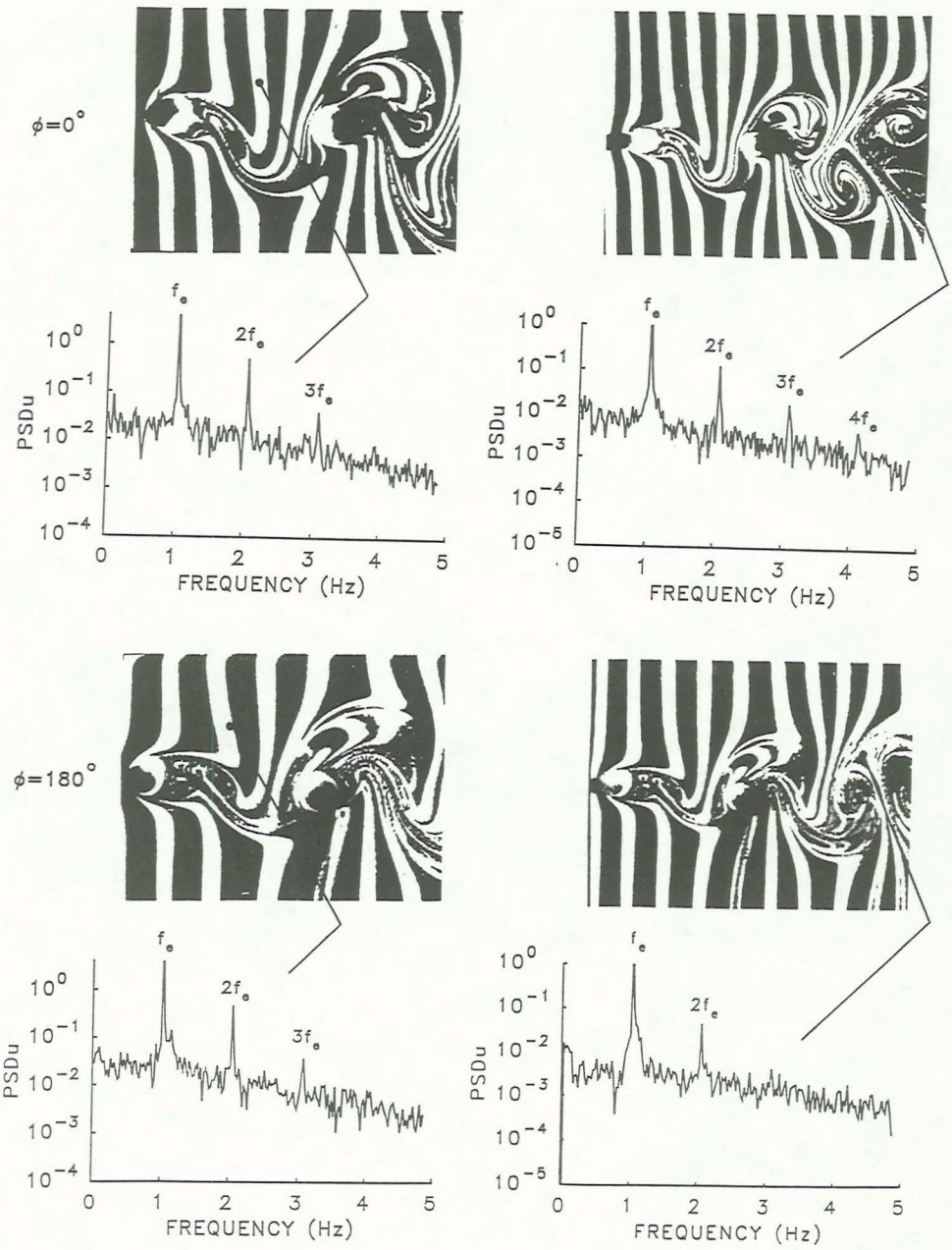

Figure 18: Spectra between and in near-wake of two cylinders corresponding to locked-in response for two values of phase angle ϕ = 0° and 180°. Spacing between cylinders P/D = 5; excitation amplitude A/D = 0.2; and excitation frequency f_e/f_o^{**} = 0.86.

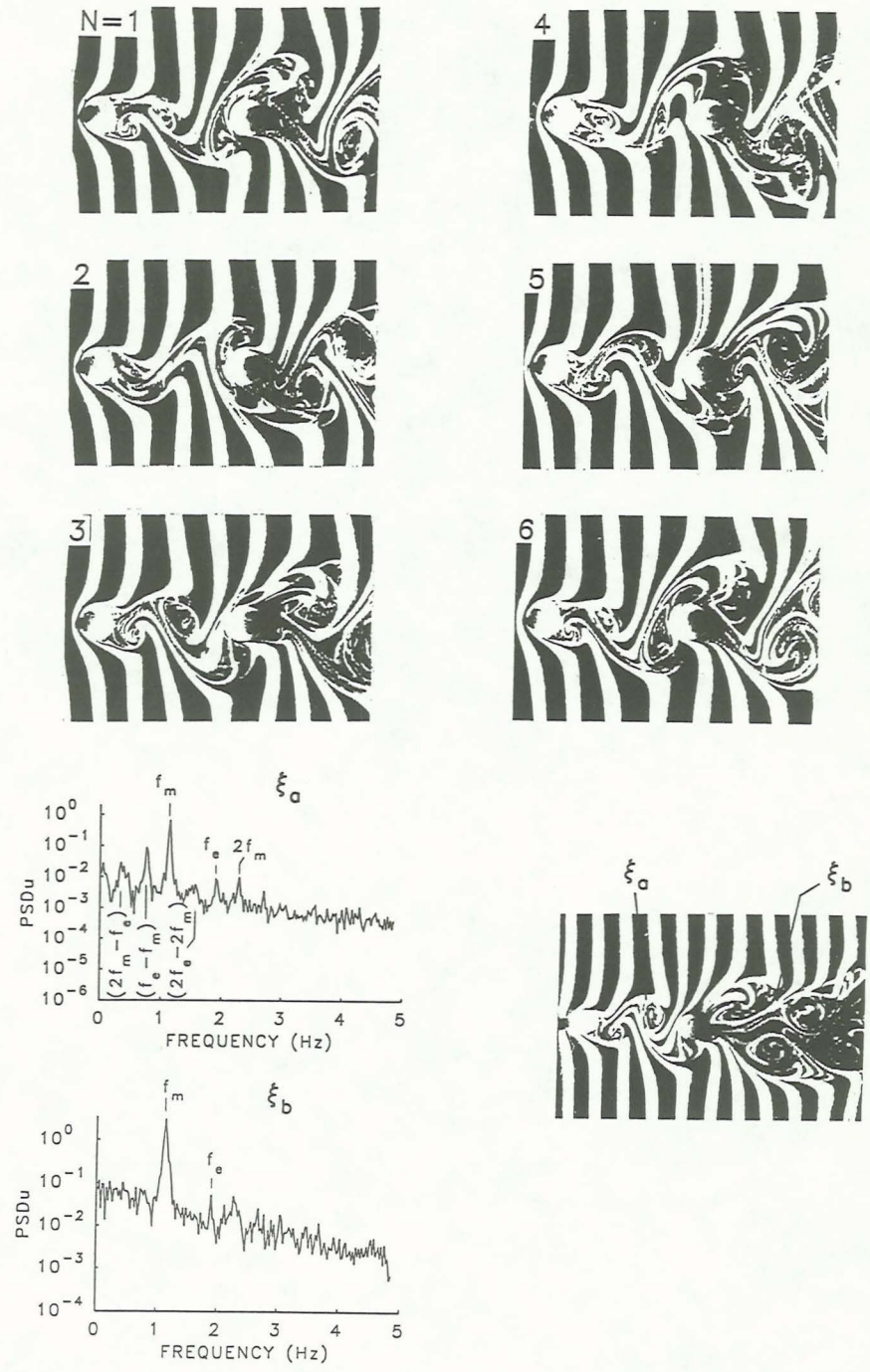

Figure 19: Flow structure and representative spectra at locations ξ_a and ξ_b between and in near-wake of two cylinders oscillating with phase angle $\phi = 0°$ between them. Spacing between cylinders P/D = 5, excitation amplitude A/D = 0.5, and excitation frequency $f_e/f_o^{**} = 1.56$.

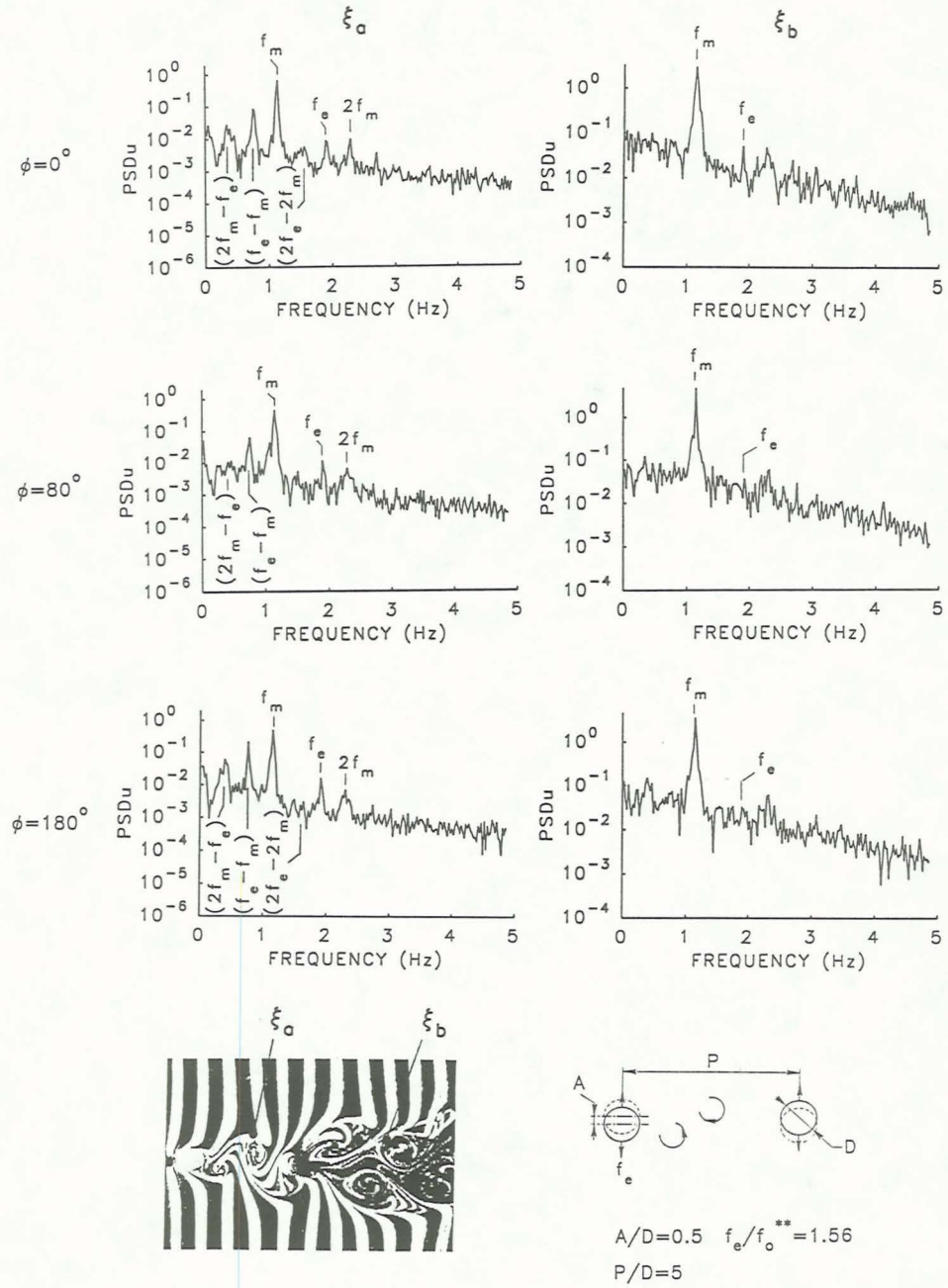

Figure 20: Spectra between cylinders (location ξ_a) and in near-wake region (location ξ_b) representing modulated response for values of phase angle ϕ = 0°, 80° and 180°. Spacing between cylinders P/D = 5; dimensionless amplitude A/D = 0.5; excitation frequency f_e/f_o^{**} = 1.56.

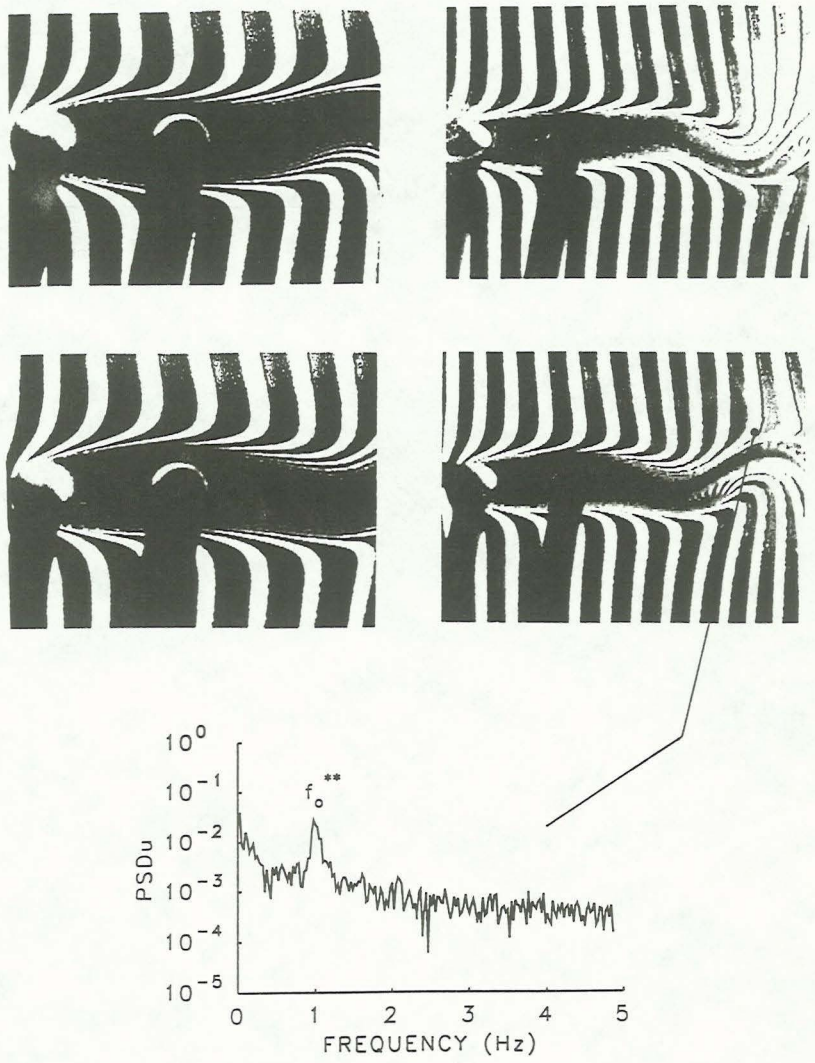

Figure 21: Flow structure and spectra of velocity fluctuation between and in near-wake of two stationary cylinders. Spacing between cylinders P/D = 2.5. Spectrum corresponds to near-wake region.

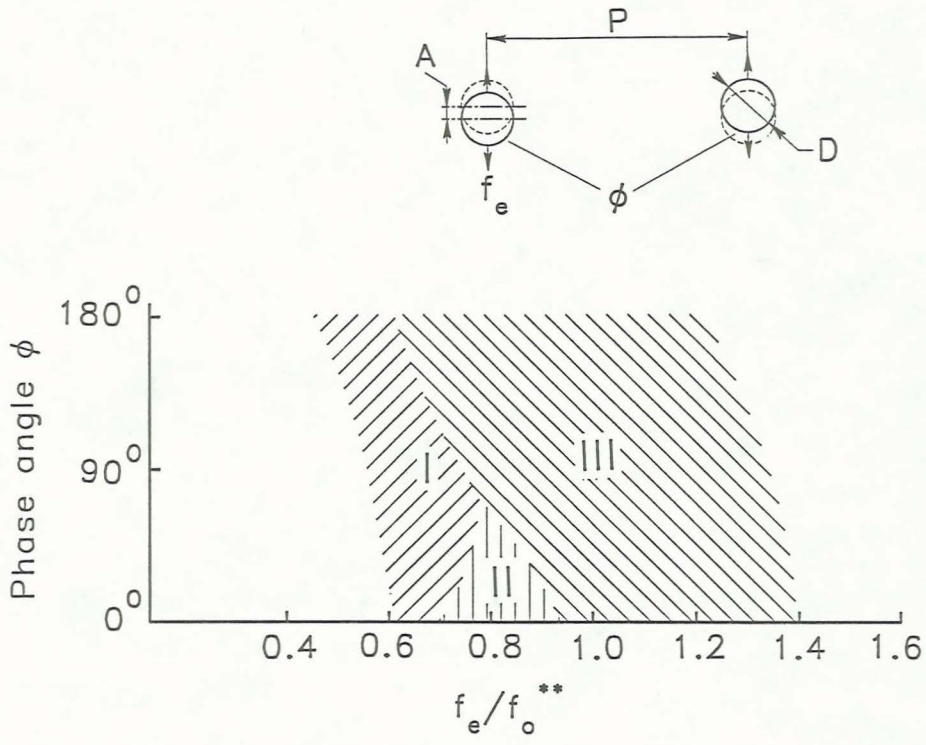

I Modulated response.

II Transition from modulated to locked-in response.

III Locked-in response.

Figure 22: Illustration of regions of response region on plane of phase angle ϕ versus dimensionless frequency of excitation f_e/f_o^{**}. Dimensionless excitation amplitude A/D = 0.2; spacing between cylinders P/D = 2.5. Regions I and III represent modulated response, region II corresponds to locked-in response.

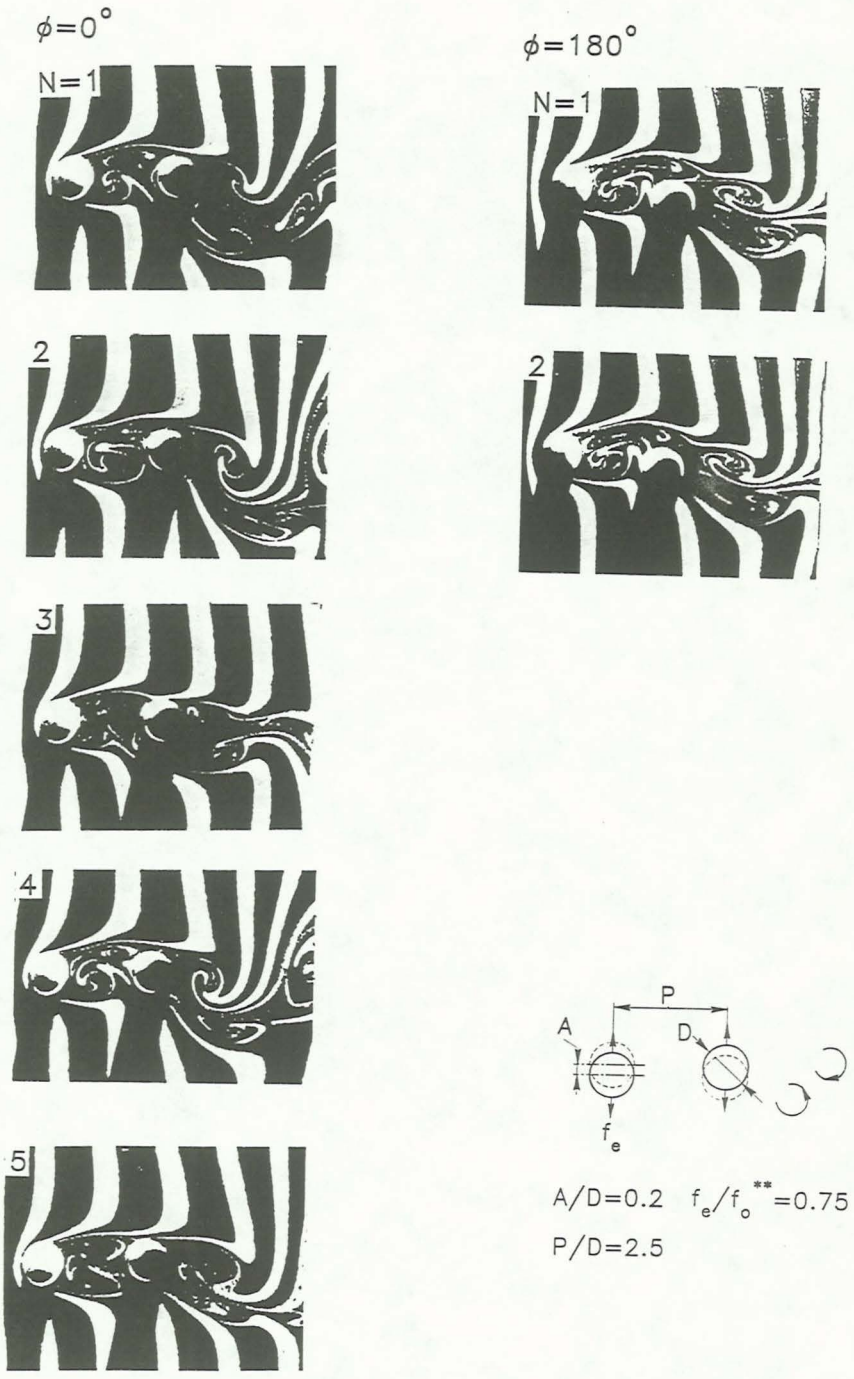

Figure 23: Flow structure between and in near-wake representing transformation from modulated to locked-in response via variation of phase angle. Photographs in left column correspond to phase angle $\phi = 0°$ and in right column correspond to phase angle $\phi = 180°$. All photos taken at same maximum displacement of cylinder. Spacing of the cylinders P/D = 2.5; excitation amplitude A/D = 0.2; and excitation frequency $f_e/f_o^{**} = 0.75$.

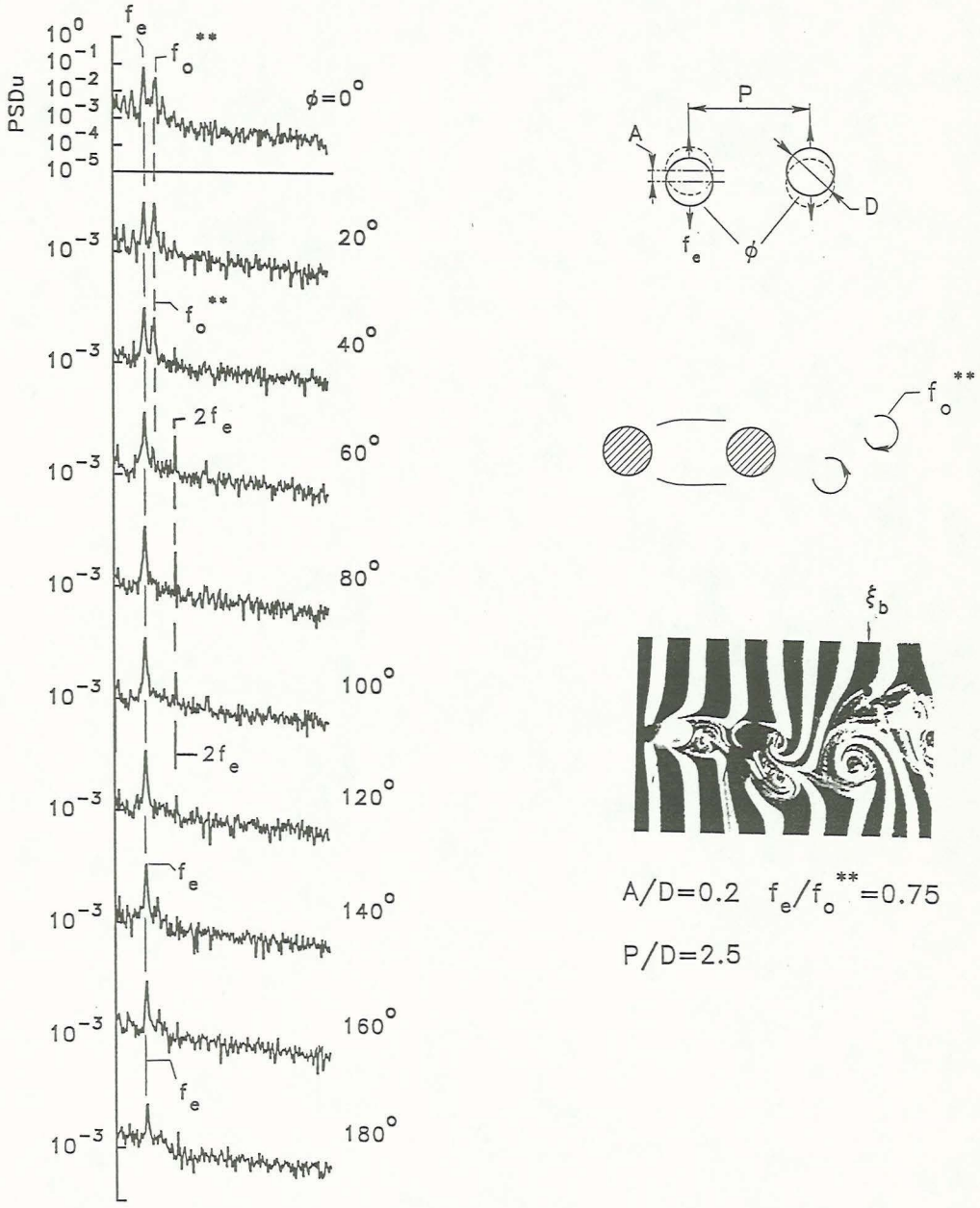

Figure 24: Spectra in near-wake region representing transformation from modulated to locked-in response via variation of phase angle. Spacing of the cylinders P/D = 2.5; excitation amplitude A/D = 0.2; and excitation frequency $f_e/f_o^{**} = 0.75$.

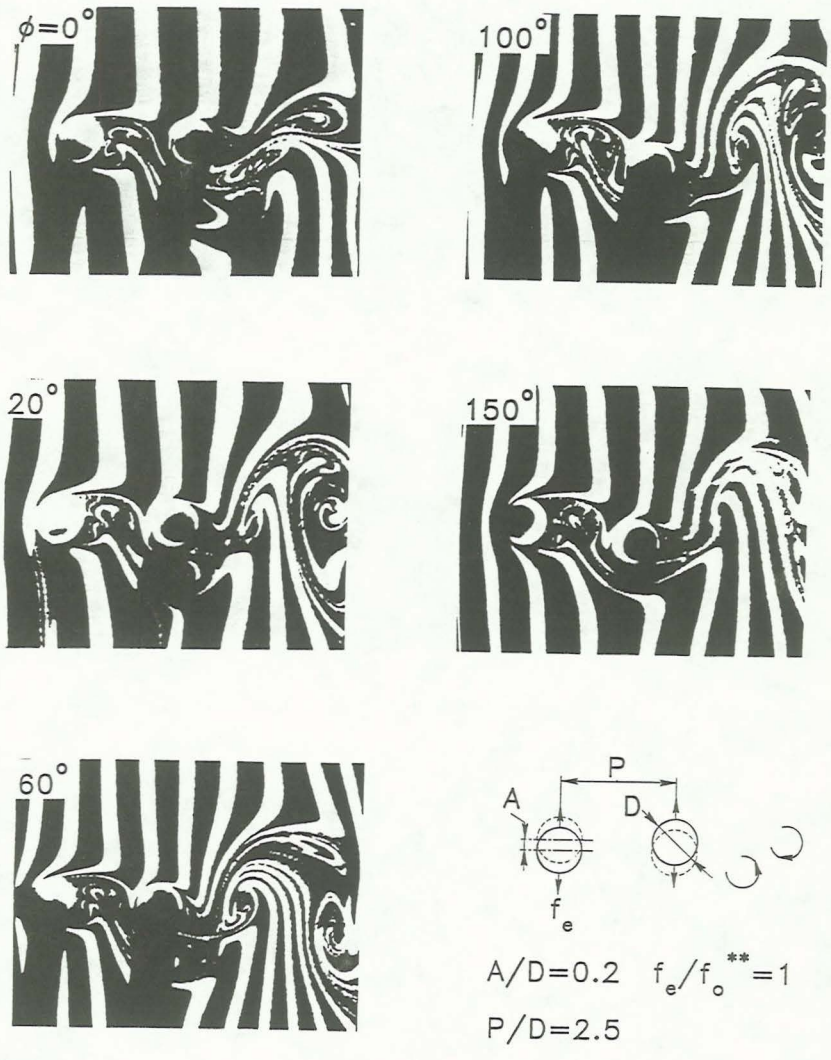

Figure 25: Flow structure corresponding to locked-in response for five different values of phase angles ϕ = 0°, 20°, 70°, 100° and 150°. Spacing between cylinders P/D = 2.5; excitation amplitude A/D = 0.2; excitation frequency f_e/f_o^{**} = 1.

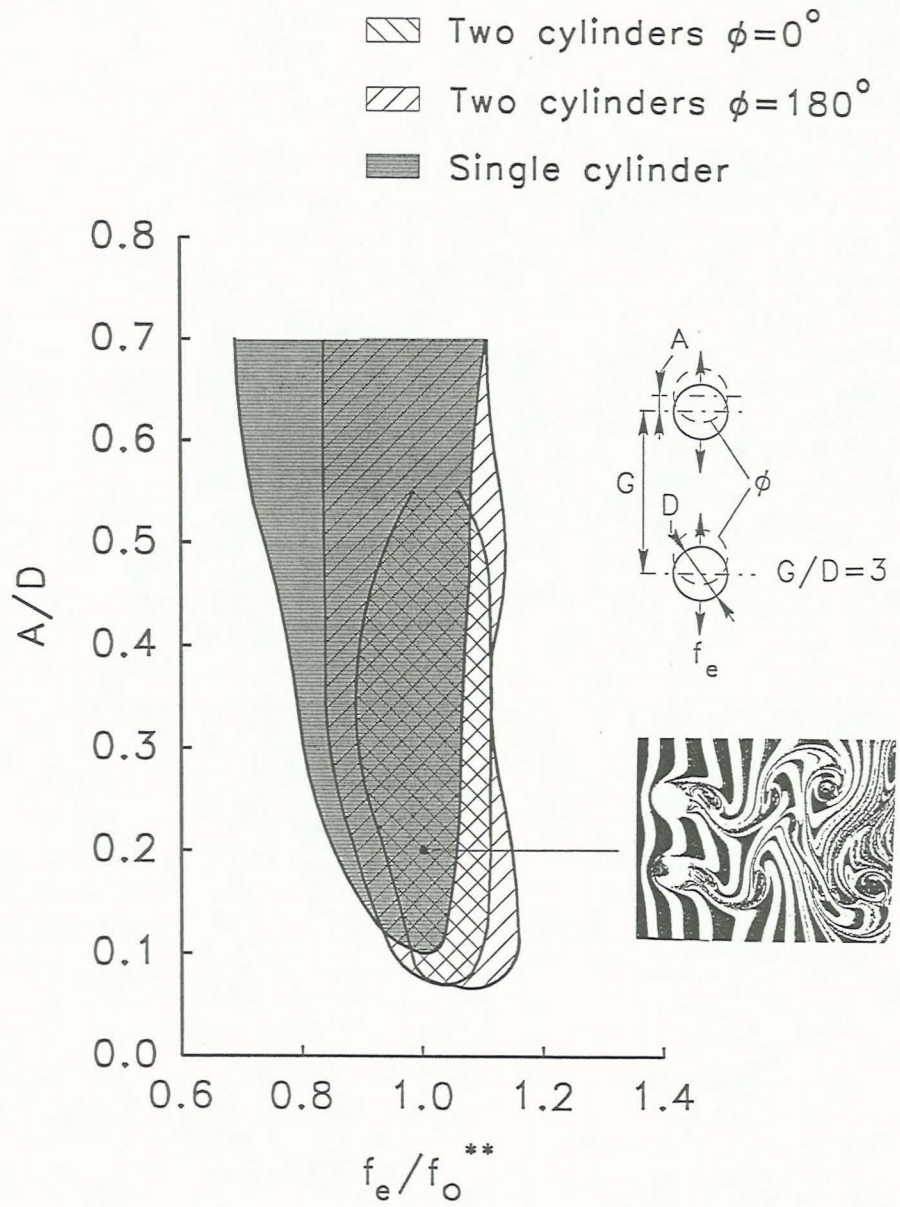

Figure 26: Illustration of regions of locked-in vortex formation as function of dimensionless oscillation frequency f_e/f_o^{**} and amplitude A/D of a single cylinder and two cylinders in side-by-side arrangement with spacing G/D = 3. Shaded region represents locked-in response of wake of single cylinder.

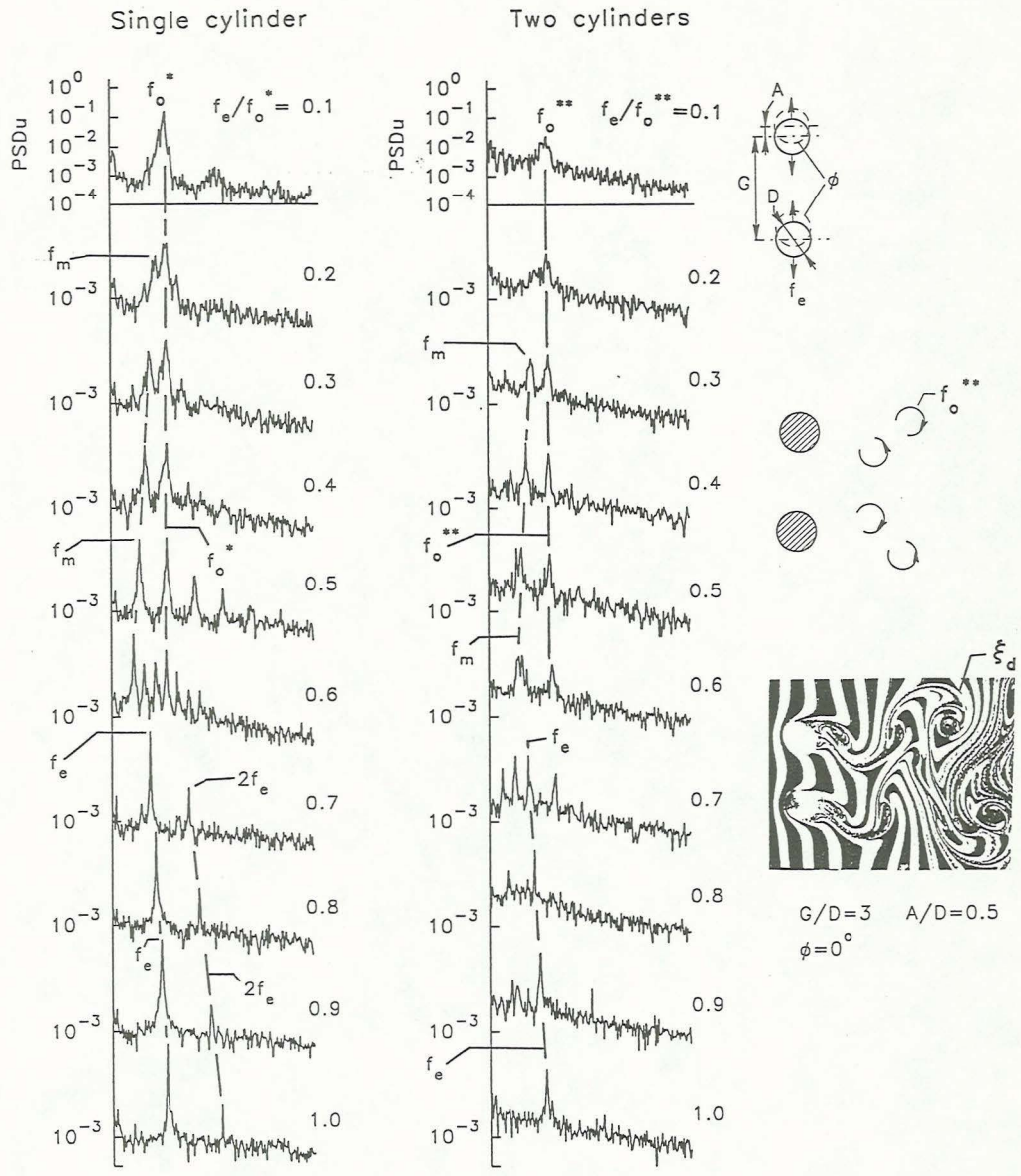

Figure 27: Spectral content of near-wake as function of excitation frequency f_e/f_o^{**}. Spectra in left column acquired in near-wake of isolated, single cylinder at location ξ_a. Spectra in right column acquired at location ξ_d downstream of two cylinders in side-by-side arrangement with spacing G/D = 3; dimensionless excitation amplitude A/D = 0.5; and phase angle $\phi = 0°$.

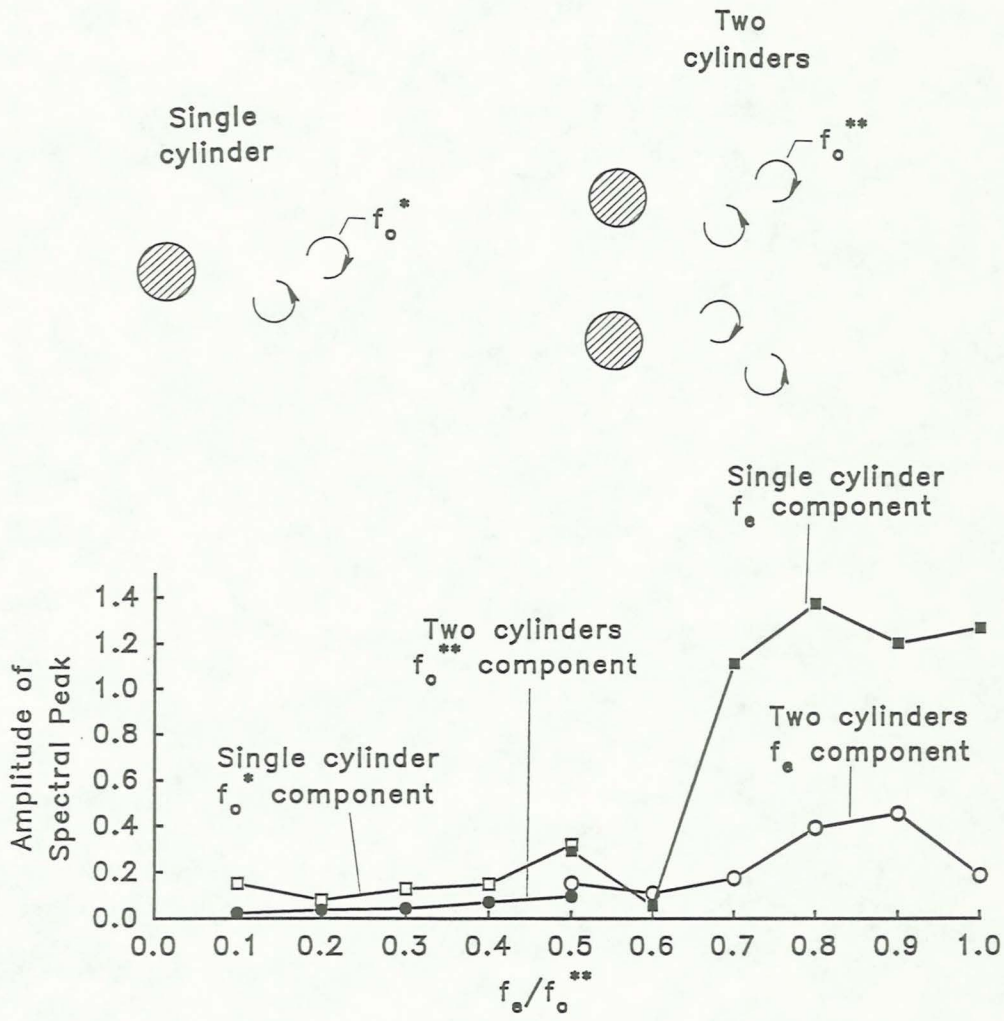

Figure 28: Illustration of amplitude of spectral peaks, acquired in near-wake of an isolated single cylinder and two cylinder system, as a function of frequency f_e/f_o^{**}. Excitation amplitude A/D = 0.5, G/D = 3 and $\phi = 0°$.

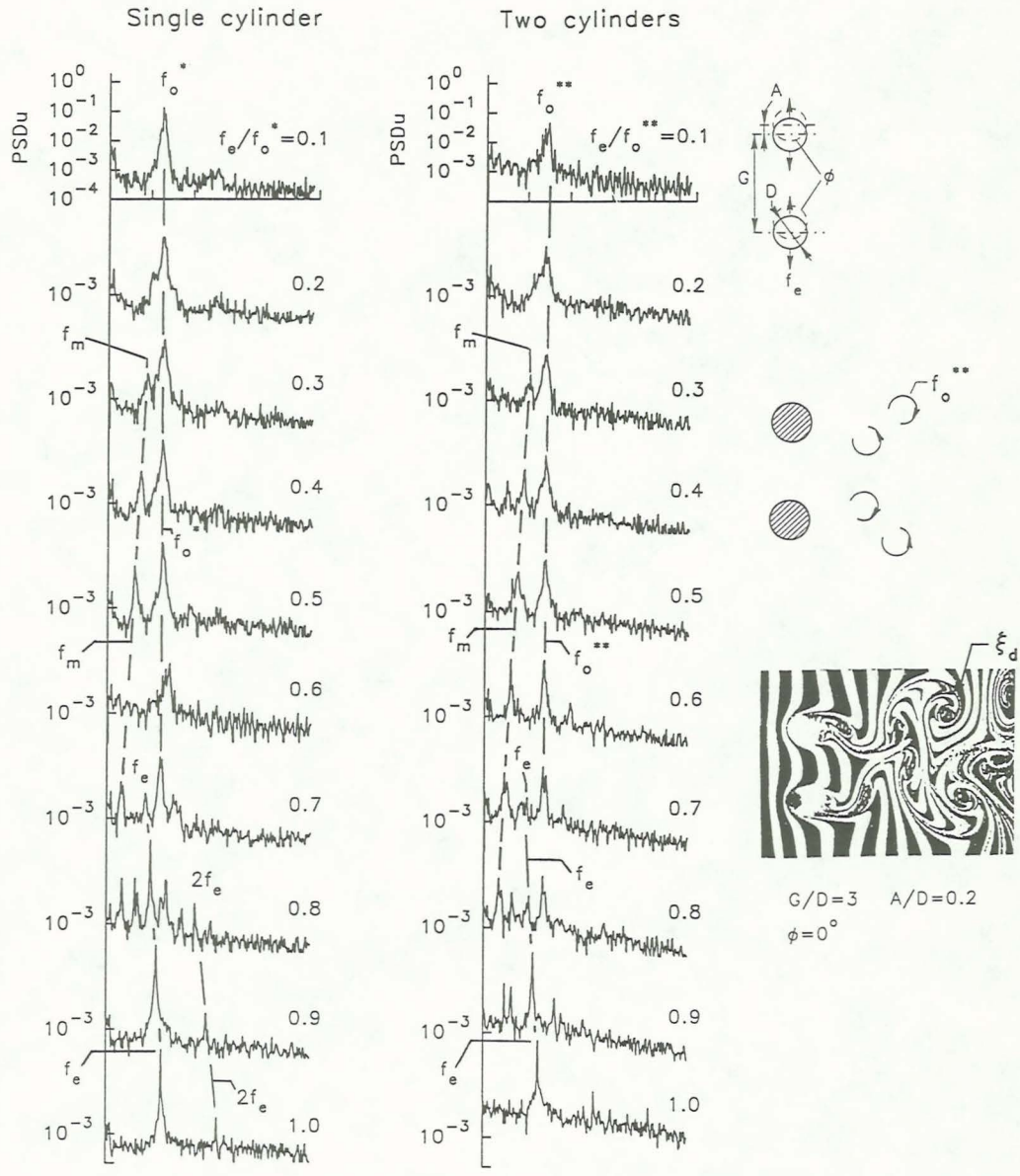

Figure 29: Spectral content of near-wake as a function of excitation frequency f_e/f_o^{**}. Dimensionless excitation amplitude A/D = 0.2. Spectra in left column acquired at location ξ_a in near-wake of isolated, single cylinder. Spectra in right column acquired at location ξ_d downstream of two cylinders in side-by-side arrangement with spacing G/D = 3 and phase angle $\phi = 0°$.

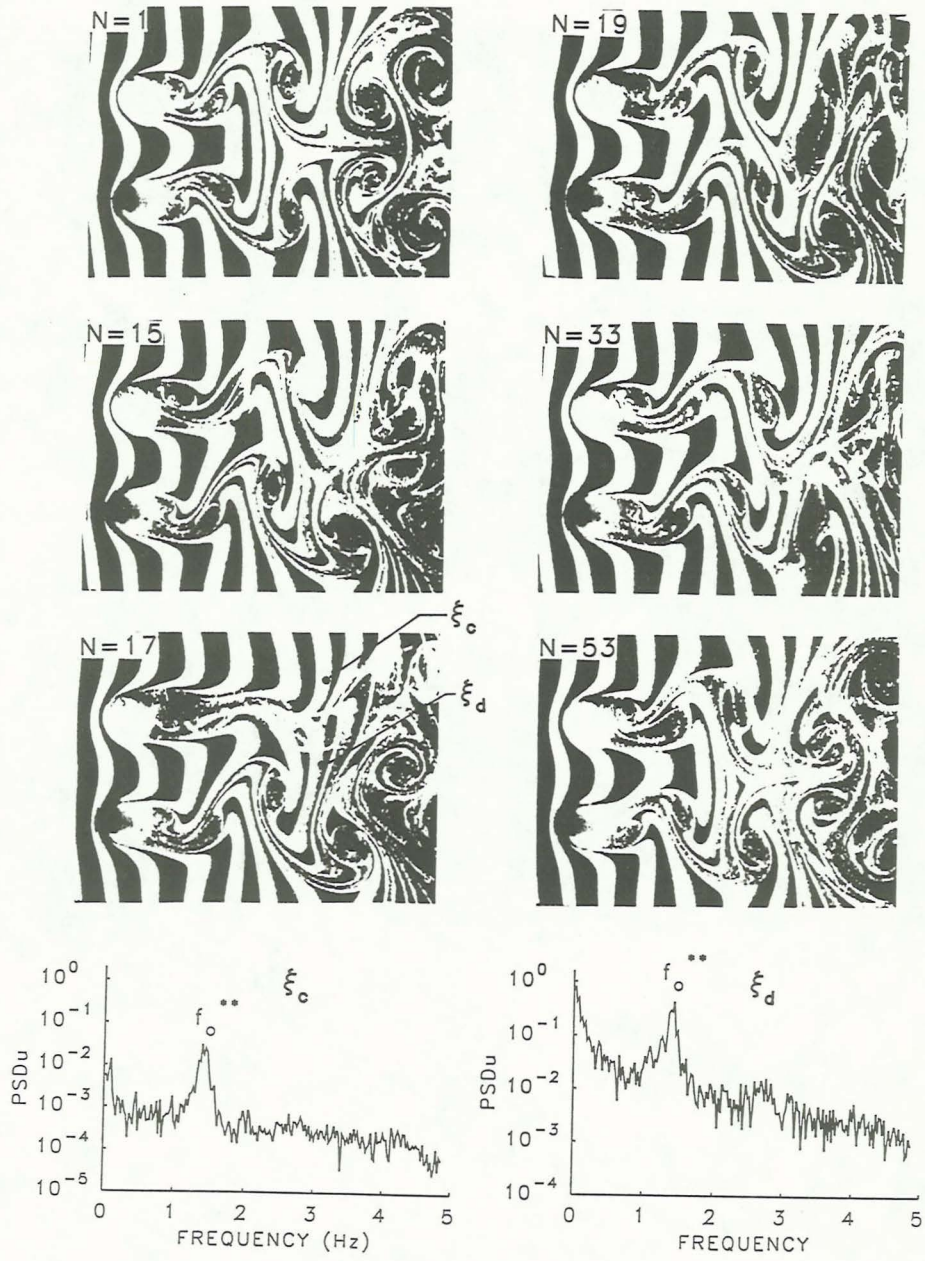

Figure 30: Flow structure and spectra of velocity fluctuation between and in near-wake of two stationary cylinders for N cycles self-excited oscillation. Spectra taken at locations ξ_c and ξ_d between and in near-wake of cylinders respectively. Spacing of cylinders G/D = 3.

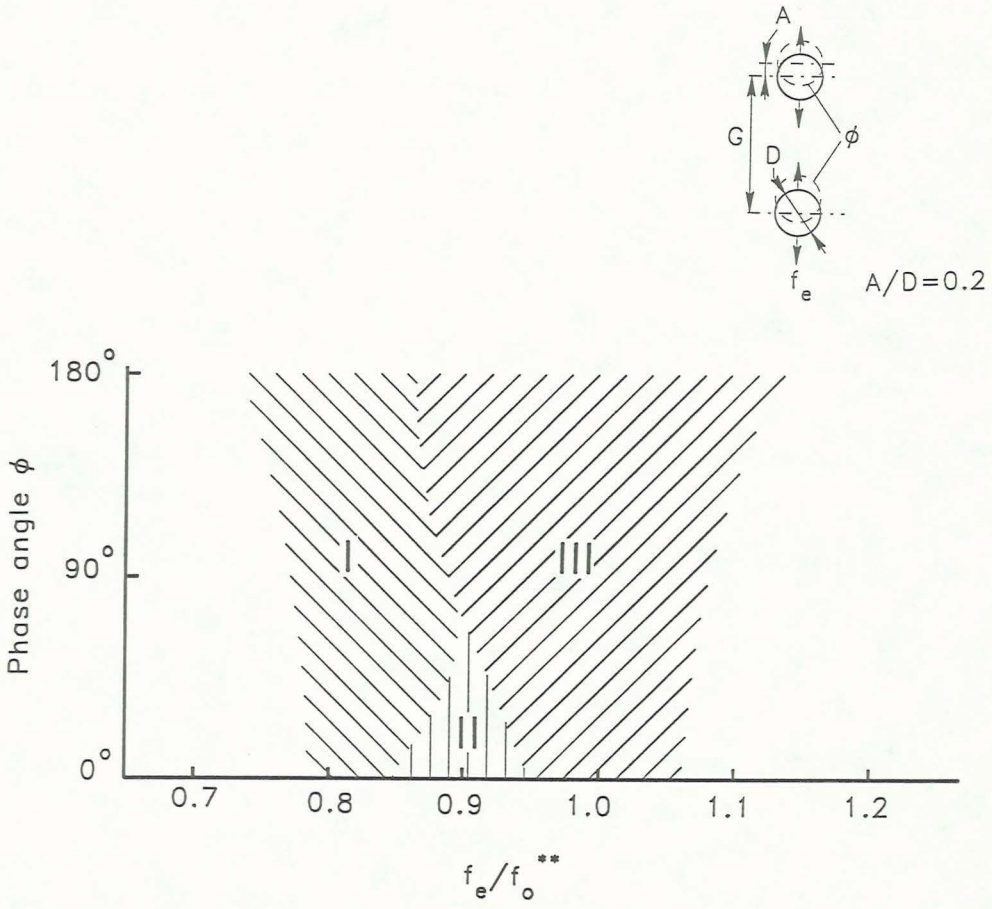

I Modulated response $f_m=f_e/3$.

II Subharmonic response $f_m= f_e/2$.

III Locked-in response. $_m=f_e/3$.

Figure 31: Illustration of possible response region on plane of phase angle ϕ versus frequency deviation f_e/f_o^{**}. Dimensionless excitation amplitude A/D = 0.2. Spacing of cylinders G/D = 3. Region I represents locked-in response, II represents subharmonic response with modulation frequency $f_m = f_e/2$, and region III corresponds to modulated response with modulation frequency $f_m = f_e/3$.

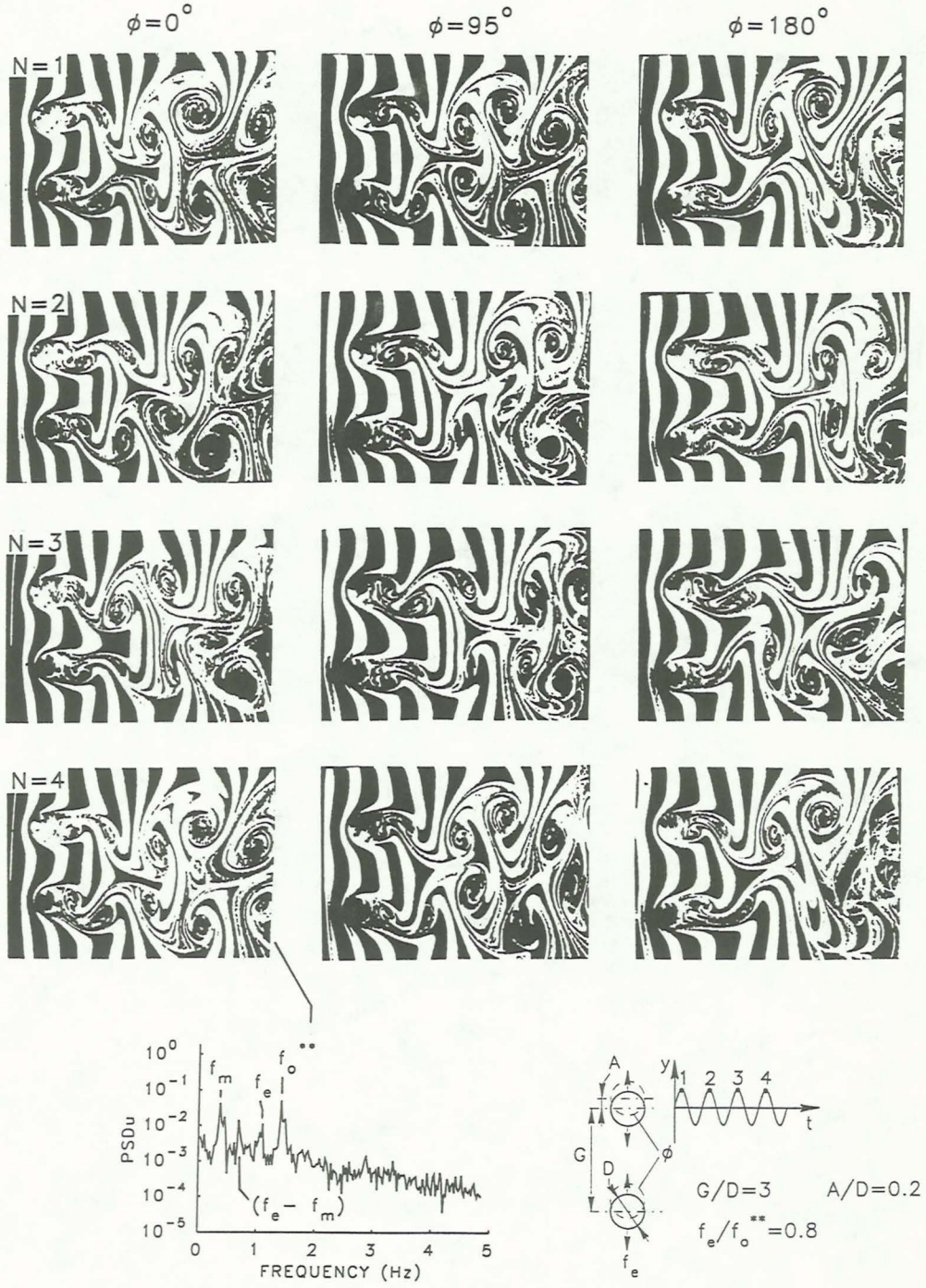

Figure 32: Flow structure corresponding to modulated response of wake which repeats with period $T_m = 1/f_m$, for three values of phase angle $\phi = 0°$, 95° and 180°. All photos taken at same maximum displacement of upper cylinder; N represents cycle number of forced oscillation at period $T_e = 1/f_e$. Spacing of the cylinders G/D = 3; dimensionless excitation amplitude A/D = 0.2; and excitation frequency $f_e/f_o^{**} = 0.8$.

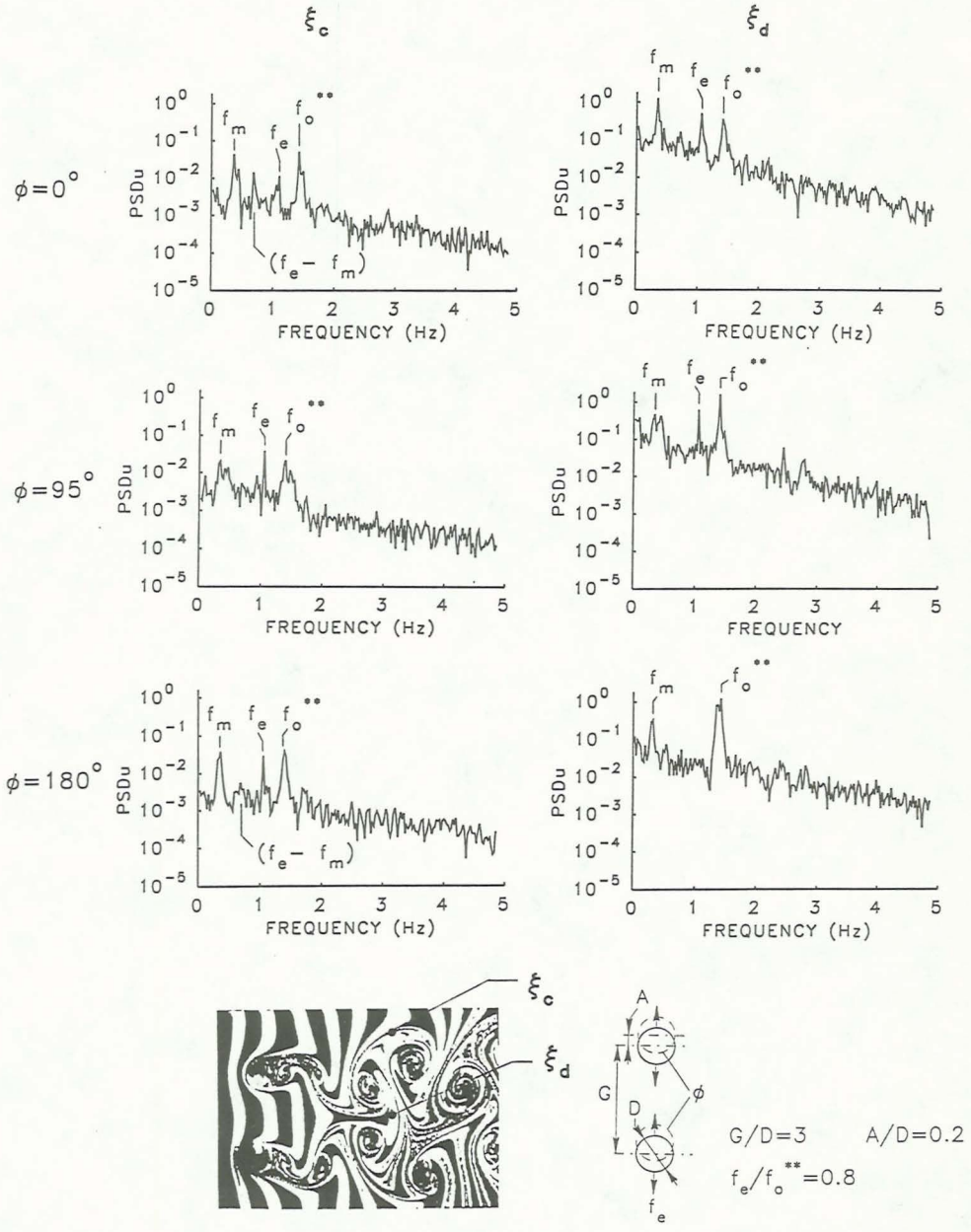

Figure 33: Spectra between cylinders (location ξ_c) and in near-wake region (location ξ_d) representing modulated response for values of phase angles ϕ = 0°, 95° and 180°. Spacing of cylinders G/D = 3; dimensionless amplitude A/D = 0.2; excitation frequency f_e/f_o^{**} = 0.8.

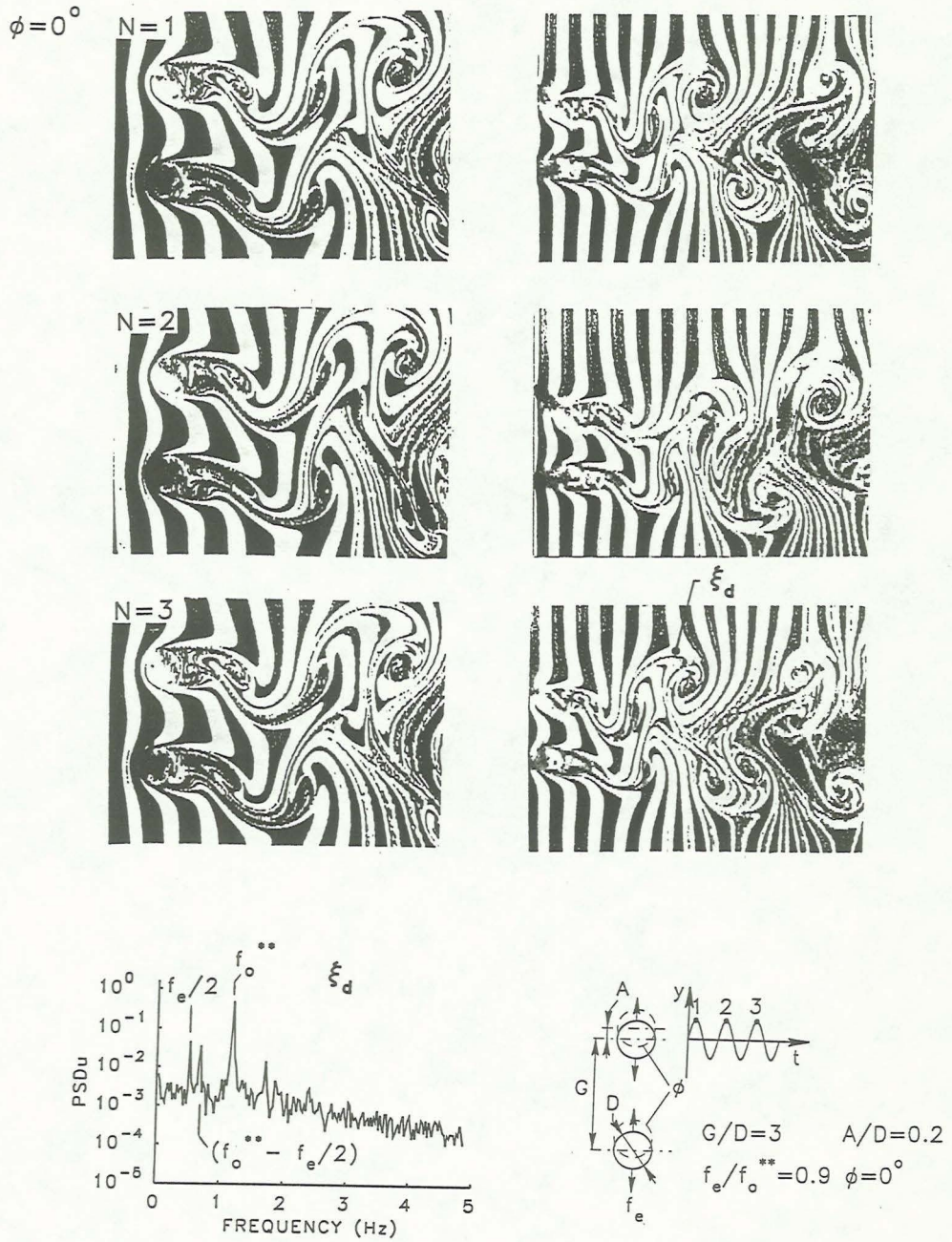

Figure 34a: Flow structure and spectra of velocity fluctuation between and in near-wake region representing transformation from modulated to locked-in response via variation of phase angle. All photos taken at same maximum displacement of upper cylinder. Spacing of cylinders G/D = 3; excitation amplitude A/D = 0.2; excitation frequency $f_e/f_o^{**} = 0.9$; and phase angle $\phi = 0°$. Spectra acquired at location ξ_d.

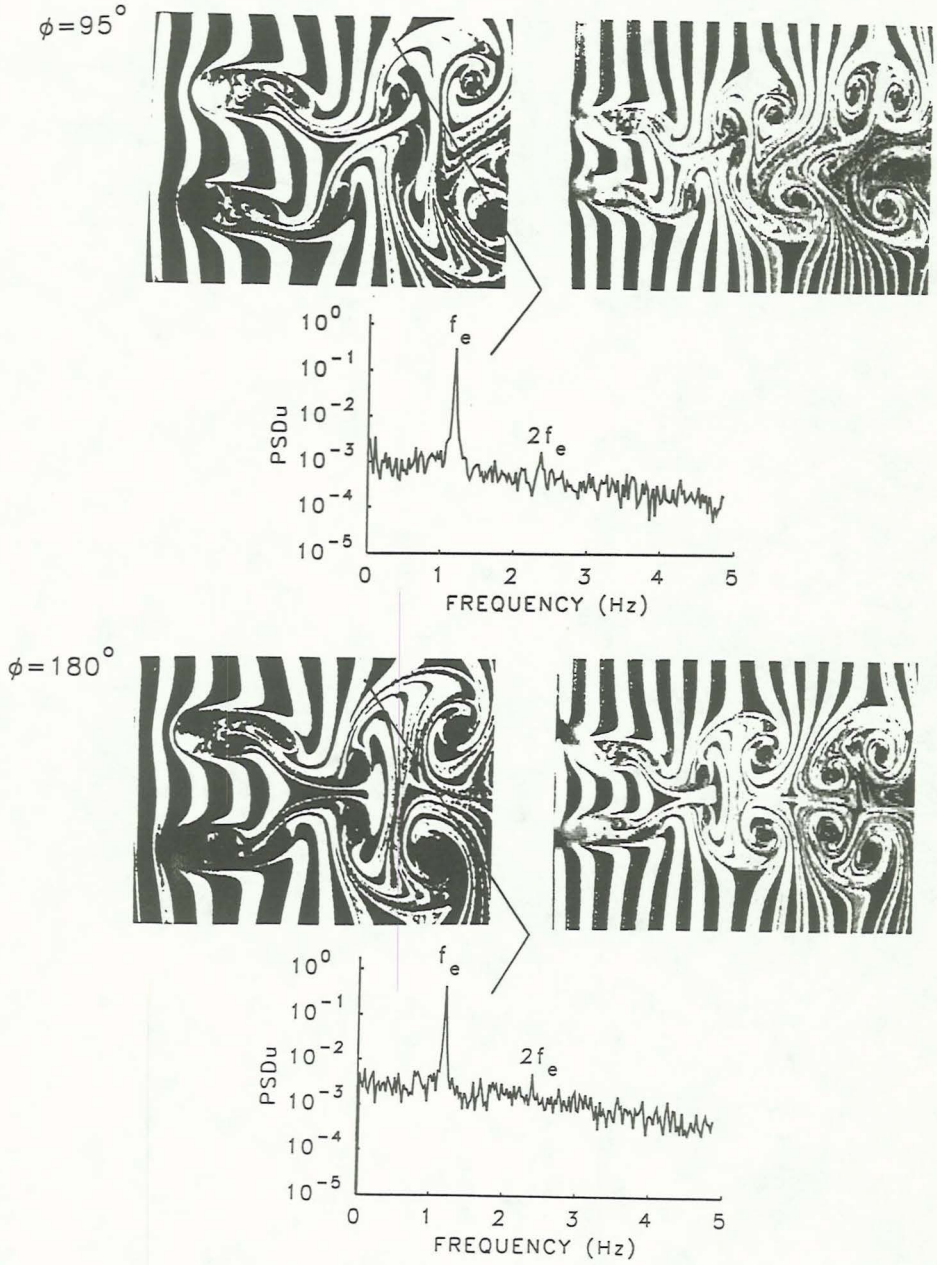

Figure 34b: Flow structure and spectra of velocity fluctuation between and in near-wake region representing transformation from modulated to locked-in response via variation of phase angle. All photos taken at same maximum displacement of upper cylinder. Spacing of cylinders G/D = 3; excitation amplitude A/D = 0.2; excitation frequency $f_e/f_o^{**} = 0.9$; and phase angles $\phi = 95°$ and 180°. Spectra acquired at location ξ_d.

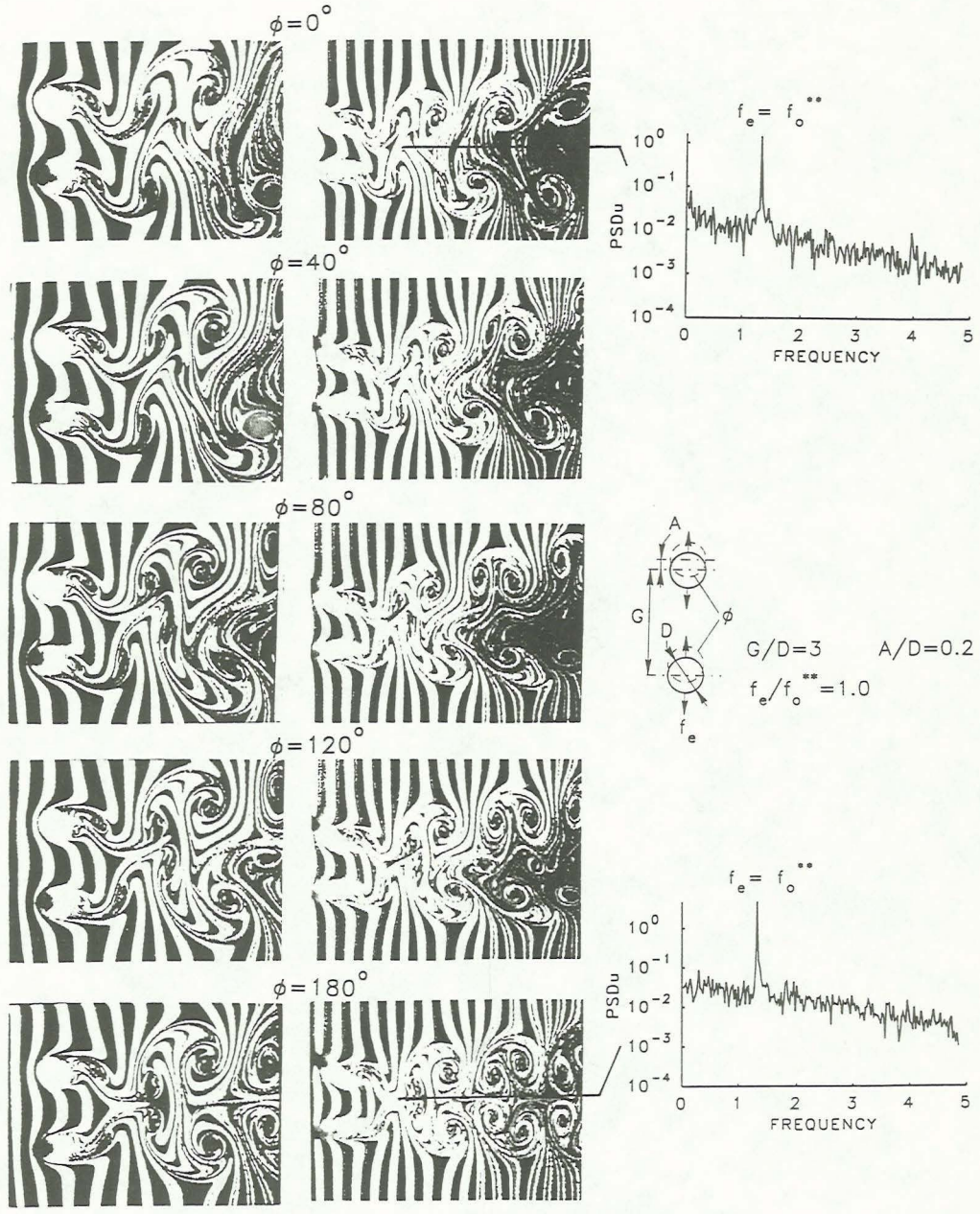

Figure 35: Flow structure and spectra of velocity fluctuation corresponding to locked-in response for five different values of phase angle ϕ = 0°, 40°, 80°, 120° and 180°. All photos taken at same maximum displacement of upper cylinder. Spacing between cylinders G/D = 3, excitation amplitude A/D = 0.2, excitation frequency f_e/f_o^{**} = 1.0. Spectrums in the left column correspond to ϕ = 0° and 180°.

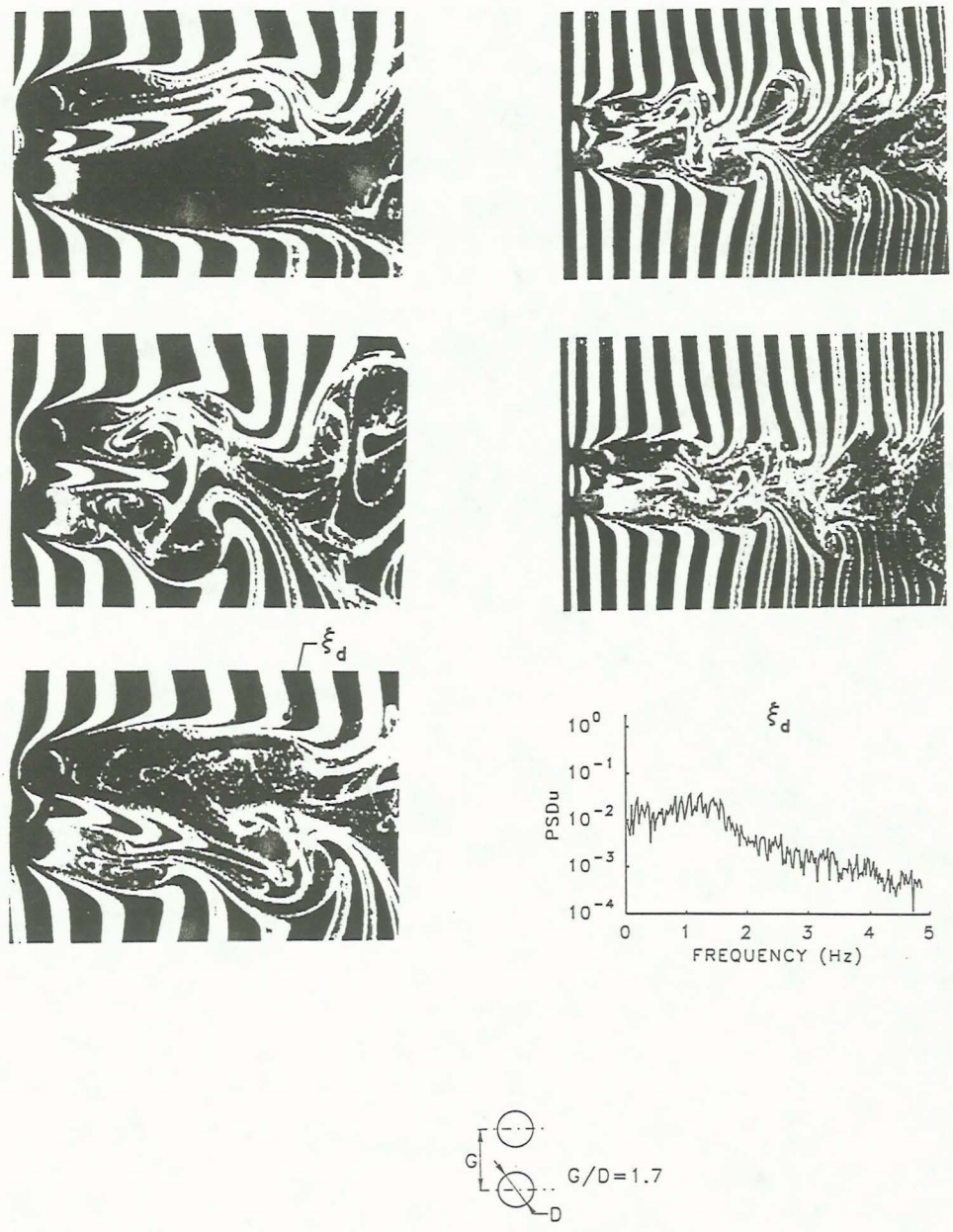

Figure 36: Flow structure and spectra of velocity fluctuation between and in near-wake of two stationary cylinders. Spacing of cylinders G/D = 1.85. Spectrum acquired at location ξ_d.

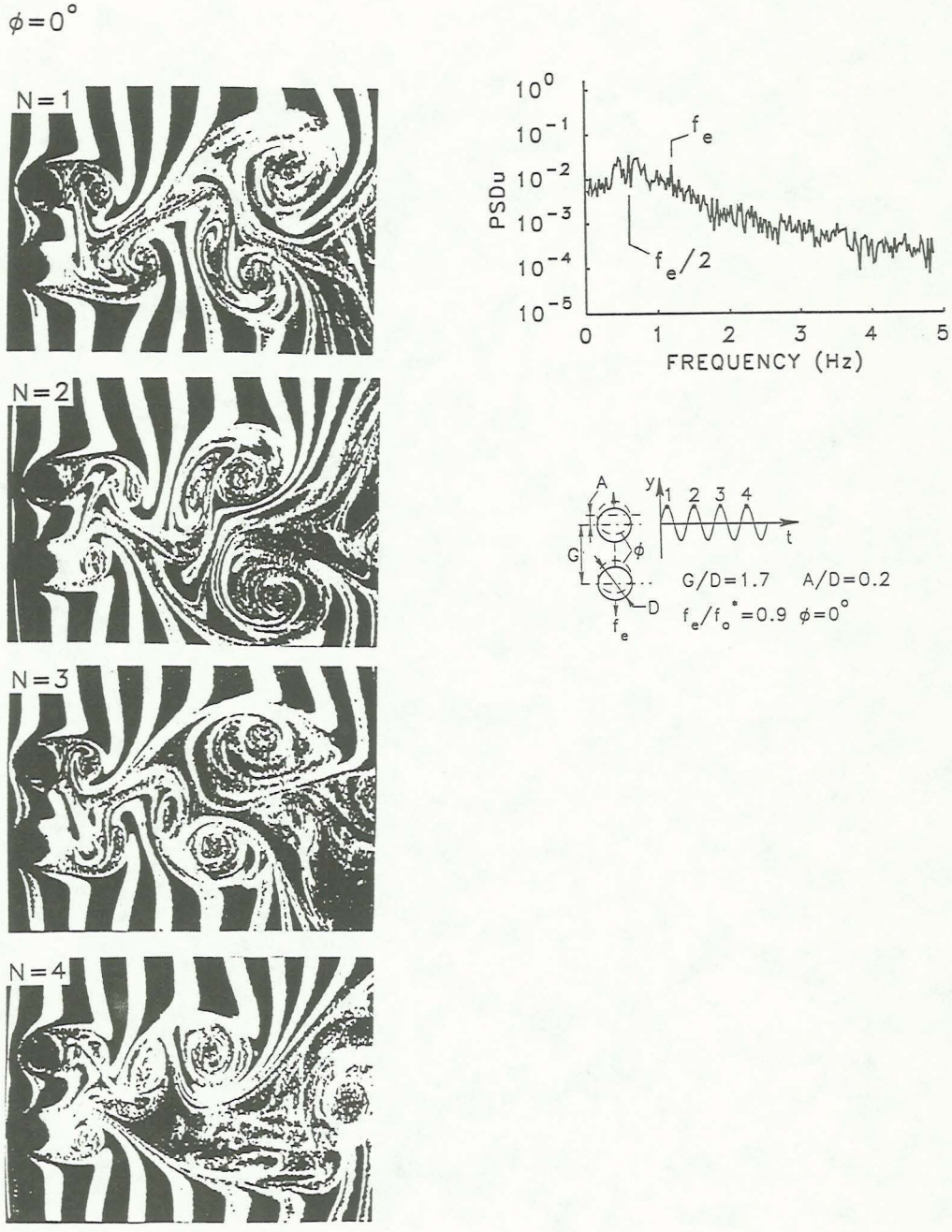

Figure 37a: Flow structure and spectra of velocity fluctuation in near-wake region of two cylinders representing transition to organized vortex formation via changes in phase angle. Spacing of cylinders G/D = 1.85; excitation amplitude A/D = 0.2; excitation frequency f_e/f_o^{**} = 0.9; and phase angle ϕ = 0°. Spectra acquired at location ξ_d.

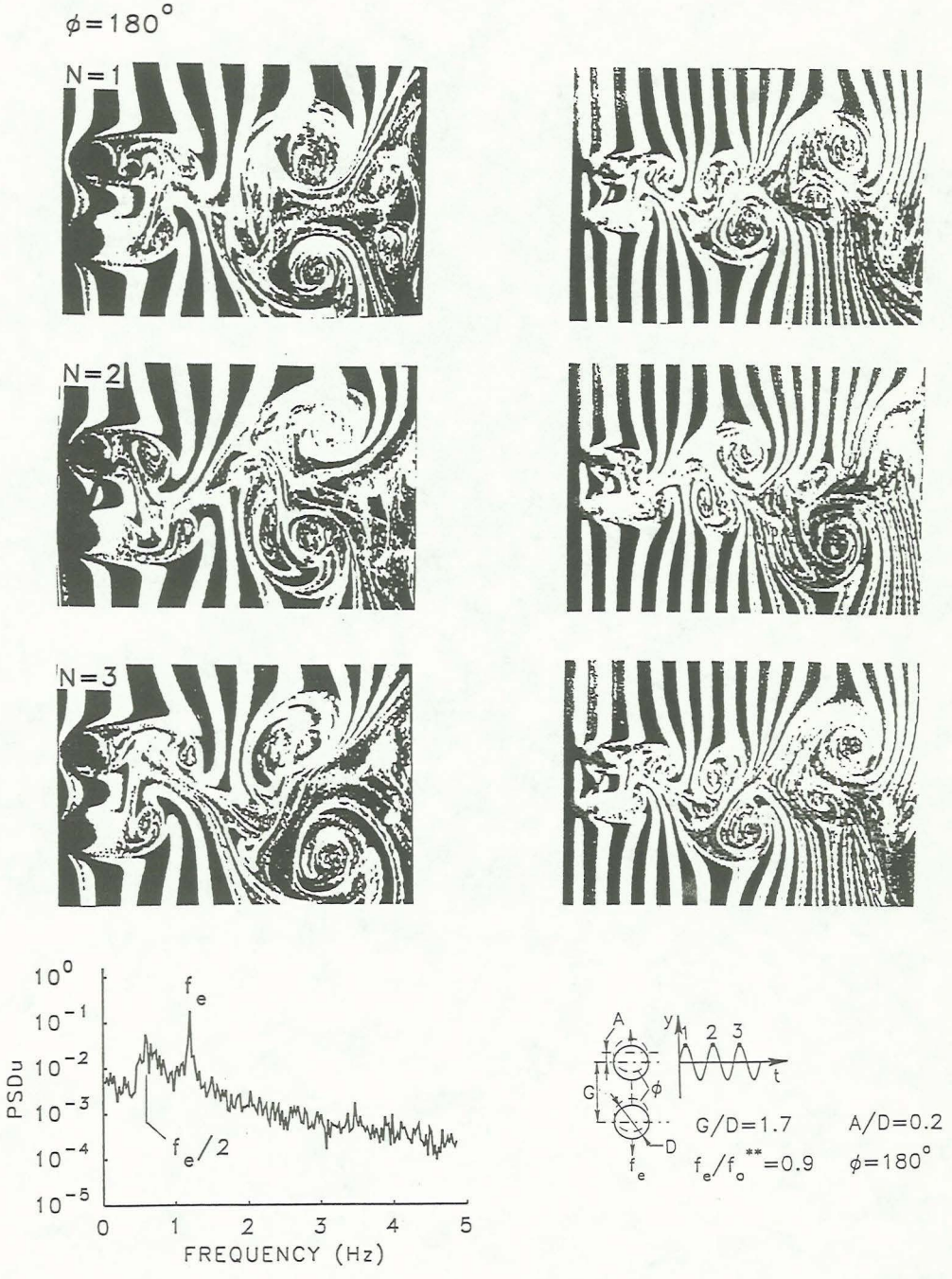

Figure 37b: Flow structure and spectra of velocity fluctuation in near-wake region of two cylinders representing transition to organized vortex formation via changes in phase angle. Spacing of cylinders G/D = 1.85; excitation amplitude A/D = 0.2; excitation frequency f_e/f_o^{**} = 0.9; and phase angle ϕ = 180°. Spectra acquired at location ξ_a.

APPENDIX

Dimensionless excitation amplitude (A/D)	Dimensionless excitation frequency (f_e/f_o^*)	Peaks in response spectrum	General type of response
0.08	0.95	f_e, f_o^*	Non-locked-in
	1.05	f_o^*	Non-locked-in
0.1	0.85	f_e, f_o^*	Non-locked-in
	0.9	f_e	Locked-in
	0.95	f_e	Locked-in
	1.05	f_e	Locked-in
	1.1	f_e, f_o^*	Non-locked-in
0.2	0.1	f_o^*	Non-locked-in
	0.2	f_o^*	Non-locked-in
	0.3	f_o^*, f_m	Non-locked-in
	0.4	f_o^*, f_m	Non-locked-in
	0.5	f_o^*, f_m	Non-locked-in
	0.6	f_o^*	Non-locked-in
	0.7	f_o^*, f_e, f_m	Non-locked-in
	0.8	f_o^*, f_e, f_m	Non-locked-in
	0.85	f_e	Locked-in
	0.9	f_e	Locked-in
	1.0	f_e	Locked-in
	1.05	f_e	Locked-in
	1.1	f_e, f_o^*	Non-locked-in
0.3	0.7	f_m, f_o^*	Non-locked-in
	0.75	f_m, f_e	Non-locked-in
	0.8	f_e	Locked-in
	1	f_e	Non-locked-in
	1.05	f_e	Locked-in
	1.1	f_e, f_m, $(f_e - f_m)$	Non-locked-in
0.4	0.7	f_e, f_m	Non-locked-in
	0.75	f_e, f_m, $(f_e - f_m)$	Non-locked-in
	0.8	f_e	Locked-in
	1.05	f_e	Locked-in
	1.1	f_e, f_m, $(f_e - f_m)$	Non-locked-in
	1.15	f_o^*	Non-locked-in
0.5	0.1	f_o^*	Non-locked-in
	0.2	f_o^*, f_m	Non-locked-in

Table 1: Representative types of response and spectral peaks of velocity in wake of a single cylinder system.

Dimensionless excitation amplitude (A/D)	Dimensionless excitation frequency (f_e/f_o^*)	Peaks in response spectrum	General type of response
0.5	0.3	f_o^*, f_m	Non-locked-in
	0.4	f_o^*, f_m	Non-locked-in
	0.5	f_o^*, f_m	Non-locked-in
	0.6	f_o^*, f_m	Non-locked-in
	0.7	f_e	Locked-in
	0.75	f_e	Locked-in
	0.8	f_e	Locked-in
	0.9	f_e	Locked-in
	1.0	f_e	Locked-in
	1.05	f_e	Locked-in
	1.1	f_e	Locked-in
	1.15	f_o^*	Non-locked-in
0.6	0.65	f_e, f_m, (f_e+f_m)	Non-locked-in
	0.7	f_e	Locked-in
	1.05	f_e	Locked-in
	1.1	f_e, f_m, (f_e-f_m)	Non-locked-in
	1.15	f_o^*	Non-locked-in
0.7	0.65	f_e, f_m	Non-locked-in
	0.7	f_e, $2f_e$	Locked-in
	0.75	f_e	Locked-in
	1.05	f_e	Locked-in
	1.1	f_e	Locked-in
	1.15	f_e, f_m	Non-locked-in

Table 1: Representative types of response and spectral peaks of velocity in wake of a single cylinder system.

Dimensionless excitation amplitude (A/D)	Dimensionless excitation frequency (f_e/f_o^{**})	Peaks in response spectrum	General type of response
0.02	0.8	f_o^{**}	Non-locked-in
	0.9	f_o^{**}	Non-locked-in
	1.0	f_o^{**}	Non-locked-in
	1.1	f_o^{**}	Non-locked-in
	1.2	f_m	Non-locked-in
	1.3	f_o^{**}, f_m	Non-locked-in
0.05	0.8	f_o^{**}	Non-locked-in
	0.9	f_o^{**}, f_e	Non-locked-in
	0.95	f_o^{**}, f_e	Non-locked-in
	1.0	f_e	Locked-in
	1.1	f_e	Locked-in
	1.2	f_e	Locked-in
	1.25	f_e, f_m	Non-locked-in
	1.3	f_e, f_m	Non-ocked-in
0.1	0.8	f_e, f_o^{**}	Non-locked-in
	0.9	f_e	Locked-in
	0.95	f_e	Locked-in
	1.3	f_e	Locked-in
	1.35	f_e, f_m	Non-locked-in
	1.4	f_e, f_m	Non-locked-in
0.2	0.1	f_o^{**}	Non-locked-in
	0.2	f_o^{**}	Non-locked-in
	0.3	f_o^{**}, f_m	Non-locked-in
	0.4.	f_o^{**}, f_e	Non-locked-in
	0.5	f_e, f_o^{**}	Non-locked-in
	0.6	f_e, f_o^{**}, f_m	Non-locked-in
	0.7	f_e, f_o^{**}, f_m	Non-locked-in
	0.8	f_e, f_o^{**}, f_m	Non-locked-in
	0.85	f_m	Non-locked-in
	0.9	f_e	Locked-in
	1.3	f_e	Locked-in
	1.35	f_e	Locked-in
	1.4	f_e	Locked-in
	1.5	f_e, f_o^{**}, $(f_e - f_m)$	Non-locked-in

Table 2: Representative types of response and spectral peaks of velocity in wake of two cylinder system in tandem arrangement. Spacing of cylinders P/D = 2.5, phase angle $\phi = 0°$.

Dimensionless excitation amplitude (A/D)	Dimensionless excitation frequency (f_e/f_o^{**})	Peaks in response spectrum	General type of response
0.3	0.6	f_e, f_o^{**}, f_m	Non-locked-in
	0.7	f_e, f_o^{**}, f_m	Non-locked-in
	0.75	f_e, f_o^{**}, f_m	Non-locked-in
	0.8	f_e	Locked-in
	0.9	f_e	Locked-in
	1.2	f_e	Locked-in
	1.3	f_e	Locked-in
	1.4	f_e	Locked-in
	1.45	f_e, f_m	Non-locked-in
	1.5	f_m	Non-locked-in
	1.6	f_m	Non-locked-in
0.4	0.4	f_e, f_o^{**}, f_m	Non-locked-in
	0.5	f_e, f_o^{**}, f_m	Non-locked-in
	0.6	f_e, f_o^{**}, f_m	Non-locked-in
	0.65	f_e, f_o^{**}	Non-locked-in
	0.7	$f_e, 2f_e$	Locked-in
	0.8	$f_e, 2f_e$	Locked-in
	0.9	$f_e, 2f_e$	Locked-in
	1.3	f_e	Locked-in
	1.4	f_e	Locked-in
	1.45	f_m	Non-locked-in
	1.5	f_e, f_m	Non-locked-in
0.5	0.1	f_o^{**}	Non-locked-in
	0.2	f_o^{**}, f_m	Non-locked-in
	0.3	f_o^{**}, f_m	Non-locked-in
	0.4	f_e, f_o^{**}, f_m	Non-locked-in
	0.5	f_e, f_o^{**}, f_m	Non-locked-in
	0.55	f_e, f_o^{**}, f_m	Non-locked-in
	0.6	$f_e, 2f_e$	Locked-in
	0.7	f_e	Locked-in
	0.8	f_e	Locked-in
	0.9	f_e	Locked-in
	1.4	f_e	Locked-in
	1.45	f_e	Locked-in
	1.5	f_e, f_o^{**}	Non-locked-in

Table 2: Representative types of response and spectral peaks of velocity in wake of two cylinder system in tandem arrangement. Spacing of cylinders P/D = 2.5, phase angle $\phi = 0°$.

Dimensionless excitation amplitude (A/D)	Dimensionless excitation frequency (f_e/f_o^{**})	Peaks in response spectrum	General type of response
0.6	0.4	f_e, f_o^{**}	Non-locked-in
	0.45	f_e, f_o^{**}	Non-locked-in
	0.5	f_e, $2f_e$	Locked-in
	0.6	f_e, $2f_e$	Locked-in
	0.7	f_e, $2f_e$	Locked-in
	1.5	f_e, $2f_e$	Locked-in
	1.55	f_e, f_m	Locked-in
	1.6	f_e, f_m	Non-locked-in
0.7	0.3	fm, f_o^{**}	Non-locked-in
	0.35	fm, f_o^{**}	Non-locked-in
	0.4	f_e, $2f_e$	Locked-in
	0.5	f_e, $2f_e$	Locked-in
	0.6	f_e, $2f_e$, $3f_e$	Locked-in
	1.4	f_e	Locked-in
	1.5	f_e	Locked-in
	1.6	f_e	Locked-in
	1.7	f_e	Locked-in
	1.75	f_e	Locked-in
	1.8	f_e, f_m	Non-locked-in

Table 2: Representative types of response and spectral peaks of velocity in wake of two cylinder system in tandem arrangement. Spacing of cylinders P/D = 2.5, phase angle $\phi = 0°$.